MECHANISMS OF LOCAL SYNAPTIC EFFECTS OF INTRACORTICAL MICROSTIMULATION IN SOMATOSENSORY CORTEX OF MICE AND RATS

Dissertation
zur Erlangung des Grades eines Doktors
der Naturwissenschaften der Fakultät für Biologie
und
der Medizinischen Fakultät
der Eberhard-Karls-Universität Tübingen
vorgelegt von

Sergejus Butovas

aus Vilnius, Litauen

Tübingen, December 2006

Date of defense: 22 May, 2007

Dean Faculty of Biology:	Prof. Dr. rer. nat. Friedrich Schöffl
Dean Faculty of Medicine:	Prof. Dr. Ingo B. Autenrieth
First Reviewer:	PD Dr. rer. nat. Cornelius Schwarz
Second Reviewer:	Prof. Dr. rer. nat. Hanspeter Mallot
Examination Committee:	PD Dr. rer. nat. Cornelius Schwarz
	Prof. Dr. rer. nat. Peter Thier
	Prof. Dr. rer. nat. Hanspeter Mallot
	Prof. Dr. rer. nat. Bernd Antkowiak
	PD Dr. Dipl.-Psych. Marina Pavlova

I hereby declare that I have produced the work entitled: "Mechanisms of local synaptic effects of intracortical microstimulation in somatosensory cortex of mice and rats", submitted for the award of a doctorate, on my own (without external help), have used only the sources and aids indicated and have marked passages included from other works, whether verbatim or in content, as such. I swear upon oath that these statements are true and that I have not concealed anything. I am aware that making a false declaration under oath is punishable by a term of imprisonment of up to three years or by a fine. I also declare that this version of the work does not differ in form or contents from the one submitted to the evaluation committee for review purposes.

Sergejus Butovas

Tübingen, December 2006.

Dedicatory

This work is dedicated to

my mother, Svetlana Butova, who has been infinite source of love for me, to my family, wife Natalie and son Patrick, who have been always with me, and who have been supporting me over these years.

Contents

List of Figures

"The most exciting phrase to hear in science, the one that heralds new discoveries, is not 'Eureka!' but 'That is funny'..."

Isaac Asimov, writer

"The important thing in science is not so much to obtain new facts as to discover new ways of thinking about them."

William Bragg, scientist

Foreword

The idea to stimulate neural tissue to restore impaired sensory functions originates from inspiring studies of Brindley and Lewin, who have found that electrical stimulation of human occipital cortex produces simple visual percept (Brindley and Lewin, 1968). Today's most successful application of electrical stimulation is the cochlear implant, a device that stimulates auditory nerve to treat deafness. However patients with lesions at higher stations of central nervous system cannot benefit from stimulation of peripheral nerves, leaving only opportunity to use neocortex for sensory signal introduction. As a result, the feasibility to use direct cortical stimulation to overcome injured pathways has acquired much of scientific attention. The main difficulty in this approach is to encode relevant percepts by using electrically induced neocortical activity. Despite recent evidence that cortical microstimulation is able to provide the substrate for a sensory percept, lack of knowledge about neuronal mechanisms underlying the "artificial" percepts delays clinical application of intracortical stimulation in neurologic patients. In this light, studies introduced in present thesis are focused on characterizing the neuronal and perceptual effects of intracortical stimulation. They are an attempt to relate percept to detailed spatio-temporal features of electrically evoked activity.

Introduction

One major group of neuroprostheses consists of technical devices that transfer data from a computer to the brain by means of electrical pulse sequences via chronically implanted electrodes. Early systematic studies on neural tissue stimulation that finally led to routine medical application were performed on the auditory nerve of deaf patients (House and Urban, 1973; Clark et al., 1977). The neuroprosthetic device, eventually called cochlear implant, allowed the patients to hear various sounds and recover speech understanding, thus essentially improving their life quality. However, the approach to stimulate peripheral nerves is not applicable in patients with lesions at higher stations of the central nervous system, and therefore requires a different solution. In this light, one of the structures that appear to be potentially useful for sensory signal introduction is neocortex. First, because it has well defined topographic representation of sensory modalities; and second, because it offers uncomplicated access to the target stimulated area. There have been earlier attempts to exploit direct cortical stimulation in blind patients to restore vision (Brindley and Lewin, 1968; Dobelle and Mladejovsky, 1974; Dobelle et al. 1976). In these experiments epicortical multielectrode stimulation was able to elicit a simple percept, termed "phosphene", which by spatiotemporal patterning of the pulses could be combined to simple visual patterns. However, medical application of such implants was highly limited due to large currents used ($>$ 100 mA) and the poor spatial resolution yielded.

The basic difficulty to reproduce meaningful percepts by electrical stimulation is the complexity of neural code that is used in different parts of nervous system. In general, the degree of complexity increases on the path

from periphery to neocortex, where signal processing involves inter-modal integration and is integrated with internal behaviorally relevant contextual information. These aspects significantly impede clinical application of cortical neuroprostheses and therefore require further experimentation.

To reproduce a sensory percept by means of electric impulse sequence in the neocortex, firstly, factors that determine the volume of electrically induced activity should be assessed. It is generally accepted that the current amplitude required to excite cortico-spinal neurons in primates and cats is a function of squared distance between electrode tip and the neuron (Asanuma and Sakata, 1962; Stoney et al., 1968; Andersen, 1975). Particularly, according to Stoney et al. (1968), current pulse at 10 μA amplitude applied for 200 μsec activates volume of 0.029 mm^3 of cats' motor cortex, exciting approximately 2000 neurons. The effective current, however, is dependent on electrode geometry, which determines density of electric field: the smaller the electrically exposed surface - the less current is required to activate neurons in the direct vicinity of the electrode (Yeomans et al. 1985). Also, it is known that different parts of neurons (e.i., soma, dendrite and axon) do not equally contribute to electrically driven activation. The most sensitive sites to microstimulation are located at initial segment and Ranvier nodes (Gustafsson and Jankowska 1976; McIntyre and Grill 2000; Nowak and Bullier 1998a, b; Porter, 1963; Ranck, Jr. 1975; Rattay 1999; Swadlow, 1992). Such excitability is due to the high density of sodium channels at these segments (Nowak and Bullier 1998a, b; Catterall, 1981; Waxman and Quick, 1978). This, in turn, introduces the problem of activity spread by means of action potentials traveling in both ortho- and antidromic way along axons that pass the stimulus site, followed by polysynaptic activation, the extent of which remains unclear.

Second, the link between electrically induced activity and percept must be established. There is growing evidence that electrical stimulation is able to generate a percept of its own, or to modulate a percept. Romo and colleagues trained monkeys to discriminate between flutter stimuli, applied to the fingertips, replaced later by trains of electrical pulses delivered to primary somatosensory cortex (Romo et al, 1998 and 2000). Psychophysical per-

formance with pure mechanical and electrical stimulations matched closely, demonstrating that tactile discrimination could be purposefully substituted by intracortical microstimulation. Stimulation of direction-selective neurons in visual cortex of primates (area MT) effectively biased the judgment of perceived motion (Murasugi et al. 1993; Salzman et al. 1990). However, the exact relation between stimuli, electrically induced activity, and percept remains generally unresolved.

Toward the goal to establish an optimal stimulation strategy for future neuroprostheses, the present thesis work probed the effects of electrical stimulation using rats' whisker representation in primary somatosensory cortex. An outstanding feature of rats' whisker system is highly resolved topographical one-to-one representation of the whiskers on several stations of the somatosensory pathway, including primary somatosensory cortex, which makes it a perfect model system to study somatosensory processing mechanisms (Zucker and Welker 1969; Woolsey and Van der Loos 1970; Welker 1971).

Study 1. Local synaptic effects of microstimulation in rat barrel cortex

Butovas S. and Schwarz C. (2003). Spatiotemporal effects of microstimulation in rat neocortex: A Parametric Study Using Multielectrode Recordings. *J Neurophysiol 90*: 3024-3039.

The very first step towards establishing cortical neuroprostheses is to explore effects of simple electrical stimulus on neuronal circuits. Towards this end, threshold and spatial spread of neuronal activation in barrel cortex has been measured in ketamine anesthetized rats (Figure 1).

Single pulse electrical stimulation evoked a complex neuronal response consisting of a short excitation followed by a long lasting suppression of the firing rate. Electrically induced neuronal activity was continuously spread around the stimulation site and did not reflect the patchiness of cortical horizontal connections (Kim and Ebner, 1999). In particular, the inhibition showed salient features. While higher stimulation currents led to enhancement of the inhibitory pattern and extension of its horizontal spatial spread, its duration was fixed. It was neither susceptible to higher stimulation currents nor to pulse duplets.

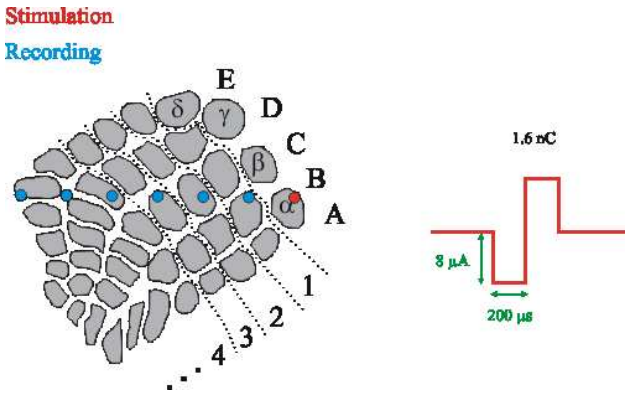

Figure 1. Position of the multielectrode array in barrel cortex of rat. The array was placed rostro-caudally under 90° angle relative to the surface of the cortex. Stimulation electrode (red dot) was always at the end of the array. Distance between electrodes was 450 μm. For stimulation biphasic pulses were used at fixed amplitude of 8 μA, only phase duration was varied. As measure of stimulation intensity charge in nC (multitude of pulse amplitude with phase duration) was used, see diagram on right.

There are two basic mechanisms that could underlie this inhibition: a withdrawal of excitation or an activation of the inhibitory network. The first class of mechanisms includes afterhyperpolarization (AHP) of pyramidal neurons and depression of intracortical excitatory synapses. Decisively, the double pulse experiments demonstrated that the inhibitory response could not be elongated and short excitation after each of pulses remained intact. If reduction of firing rates would be based on AHP, the second pulse should have reinforced the ongoing AHP because it is known that repetitive spiking elongates and strengthens the AHP. Similar reasoning applies to synaptic depression.

The conclusion therefore is that characteristics of inhibitory processes themselves most likely contribute to the non-linear summation of the duration of inhibition. One possibility emerges form the fact that the sub-linear integration of inhibitory duration found in the present study closely resembles characteristics of $GABA_B$-based slow inhibitory postsynaptic potentials (IPSP) (Thomson and Destexhe, 1999). The depression of firing rate, thus, could be based on the action of the inhibitory system via postsynaptic $GABA_B$ receptors, a hypothesis that was subsequently investigated in Study 2.

Study 2. Responses to microstimulation are determined by electrical synapses.

Butovas S., Hormuzdi S.G., Monyer H. and Schwarz C. (2006). Effects of electrically coupled inhibitory networks on local neuronal responses to intracortical microstimulation. *J Neurophysiol 96*: 1227-1236.

In Study 1 long-lasting reduction of firing rates induced by electrical stimulation of neocortex has been described. Amongst most possible mechanisms underlying this inhibition, including decreased network excitability, activation of GABA-ergic networks seems most likely. Such landmarks of the inhibition as duration of 150 ms and the inability of a second pulse delivered at different time during the inhibitory period to extend it resemble typical temporal properties of slow IPSP's based on activation of $GABA_B$ receptors. It is commonly known that activity in neocortex is strongly determined by heterogeneous populations of inhibitory interneurons, albeit they comprise only one fifth of the total neuronal population (Peters 1987; Szentagothai 1978). A remarkable feature of the inhibitory network is that certain classes of interneurons form a syncytium by means of coupling via gap junctions, shown in Figure 2 (Beierlein et al. 2000; Blatow et al. 2003; Galarreta and Hestrin 1999; Gibson et al. 1999; Hormuzdi et al. 2001).

The basic molecular component of neuronal gap junctions is connexin 36, which is expressed exclusively in the brain and retina (Condorelli et al., 2000; Belluardo et al., 2000). Communication via gap junctions ensures highly syn-

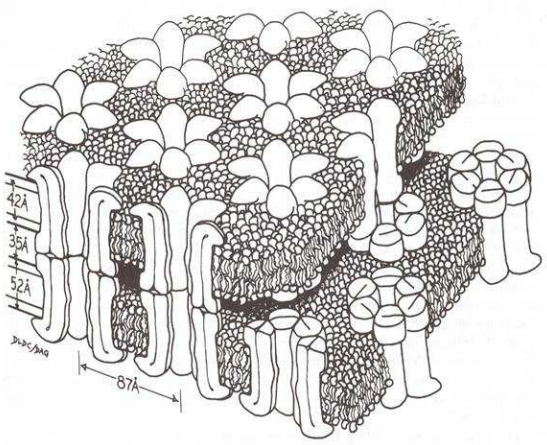

Figure 2. Electrical gap junction is an array of channels embedded in plasma membrane that allow passage of small molecules and propagation of electrical signals between two cells in both directions. The channel consists of two hexagonal tubes, called "connexon", which is in turn built of six connexin molecules. (From Makowski et al., 1977).

chronous firing, not only between coupled neurons, but also in neurons that receive the syncytium's synchronized output via chemical synapses (Connors and Long 2004; Galarreta and Hestrin 2001). This feature is thought to play a critical role in generating synchronous activities in the brain, see Figure 3 (Buhl et al. 2003; Whittington et al. 1995). The present study investigated in how far gap junction coupled inhibitory networks may play a role in suppressing firing rates following electrical stimulation.

The participation of the inhibitory network was shown using two approaches. First, GABAergic transmission was directly altered using the systemic administration of the selective $GABA_B$ receptor blocker CGP 46381. This drug led to a reduction of the inhibitory responses and in some cases even completely abolished it. It also resulted in significant increase of background firing rates, pointing directly to failure of slow IPSPs to regulate spontaneous firing rate. The second approach was more indirect. Connexin 36 knockout (KO) mice that are completely devoid of the gap junction protein responsible for gap junctions between neurons (Hormuzdi et al., 2001) were compared with wild type mice. It turned out that the inhibitory response in KO was markedly longer, weaker and often delayed by 50 ms. In addition ultra fast oscillations in the field potentials (200-300 Hz) (Barth et

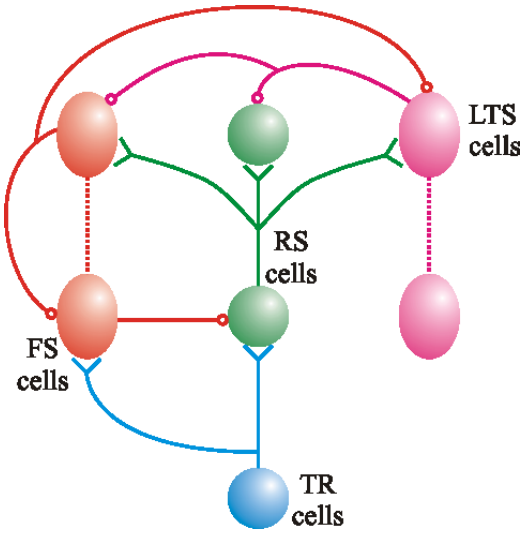

Figure 3. Activity of cortical interneurons is synchronized via gap junctions. FS - fast spiking cells, LTS - low threshold spiking cells, RS - regular spiking cells, TR - thalamic relay cells. Two classes of interneurons, FS and LTS cells, make inhibitory synapses (round terminals) mainly on RS neurons. Principal excitatory neurons, RS cells, make excitatory synapses (Y-like terminals). Gap junctions (broken lines) connect inhibitory neurons of the same class. (From Beierlein et. al., 2000).

al., 2003) were longer and spatially more spread out in infragranular layers of KO. Together these findings are compatible with the idea that missing synchronization of inhibitory networks in mutant mice result in weaker temporal precision of IPSPs, and thus, lead to lowered strength of inhibition. The experiments support the notion that electrically coupled inhibitory networks play a major role in shaping responses to electrical stimulation in neocortex.

Study 3. Intrapontine communication mediated by the cerebellum

Möck M., **Butovas S.** and Schwarz C. (2006). Functional unity of the ponto-cerebellum: evidence that intrapontine communication is mediated by a reciprocal loop with the cerebellar nuclei. *J Neurophysiol 95*: 3414-3425.

Another important issue that requires attention is the possible contribution of neuronal architecture of the stimulated structure to the spatial spread of electrically induced activity. As has been demonstrated in Study 1, intracortical stimulation evokes a continuous blur of activity at a radius of almost 3 mm away from stimulation electrode. Such spatial activity pattern is predicted by horizontal connections, which are very pronounced in neocortex. The universality of this response pattern has been tested by stimulation of a structure with very different neuronal architecture, the pontine nuclei (PN). Unlike neocortex, PN, a structure located in brain stem, has compartmentalized architecture. Being part of cerebro-cerebellar pathway, PN integrates cortical sensory-motor information (see Figures 4 and 5), where each cortical site is represented in several separate non-overlapping compartments with well defined borders (Schwarz and Möck, 2001).

This study presented evidence for the absence of intercompartmental communication in PN: intracellular dye fillings showed that most of the axons do not branch outside parental compartment, and double patch-clamp recordings demonstrated no indication of synaptic connections between proximate

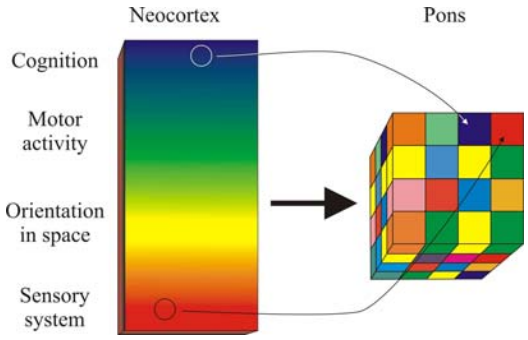

Figure 4. Pontine nuclei receive multiple projections from different cortices and generate a compartmentalized 3-dimentional map by reshuffling cortical representations.

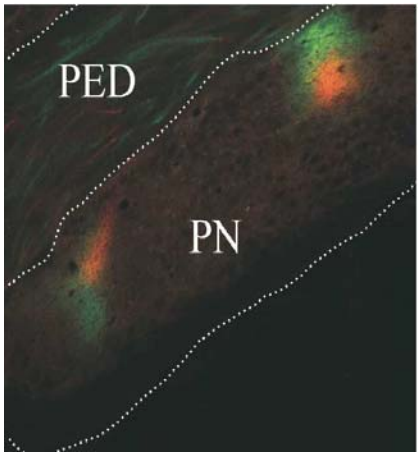

Figure 5. Spatial distribution of anterogradely labeled terminals in PN by cortical injections of yellow (DiI) and green (DiAsp) fluorescent tracers. PED, cerebral peduncle; PN, pontine nuclei. (From Schwarz and Möck, 2001).

neurons. The stimulation parameters used in current study were identical with those in the Study 1. As expected from this local separation of networks, electrical stimulation of PN evoked responses very different to those observed in neocortex. The first decisive difference found was a spatially discontinuous, patch-like response pattern, where responses of neurons at a distant recording site did not predict the response of neurons located closer to the stimulation electrode. Second, in contrast to neocortex, intrapontine stimulation did not elicit reduction of firing rates, as expected from the absence of intrinsic GABA-ergic neurons in rat PN (Möck et al 1999).

The difference of stimulation effects in PN and neocortex demonstrates

the importance of local neuronal architecture, albeit as mentioned in the discussion of Study 1, microcircuitry is not faithfully reflected by stimulation effects (e.g. the continuity of horizontal spread in neocortex despite the presence of patchy horizontal connections, Kim and Ebner, 1999).

Study 4. Intracortical microstimulation of barrel cortex in awake, head-restraint rats: assessment of detection threshold.

Butovas S. and Schwarz C. (2007). Detection psychophysics of intracortical Microstimulation in rat primary somatosensory cortex. *Eur J Neurosci 25(7)*: 2161 - 9.

The evidence that electrically evoked cortical activity could provide the basis for sensory percepts or modulate it in specific ways, led electrical stimulation to appear as a useful approach to imprint sensory information directly to neocortex. To make use of intracortical stimulation in this sense, the link between electrically induced activity and the evoked percept must be established. Of particular interest is the impact of interactions of neuronal activity on the percept, which takes place in spatial (i.e. using dense multielectrode stimulation) and temporal (i.e. using repetitive stimulation) domains, as shown in Studies 1 and 2. Two questions were posed in the present study. First, it was asked whether psychophysical and neuronal thresholds are compatible, and second, whether electrically evoked inhibition affects the detection of repetitive stimulation.

A set of stimuli that varied stimulus intensity (charge transfer), pulse number and pulse frequency were presented to head-restraint chronically implanted rats, trained to respond to the stimulation by emitting lick in order to get a water reward (Figure 6).

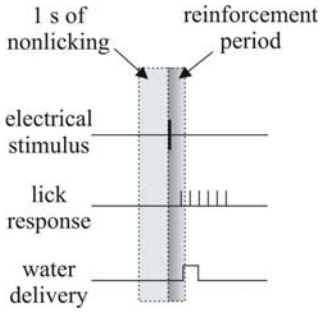

Figure 6. Schematic of experimental design. Licking during 1 second of nonlicking interval delayed stimulus presentation by 1 second. The animals were required to respond within 500 ms after stimulus onset ("reinforcement period") to obtain a reward.

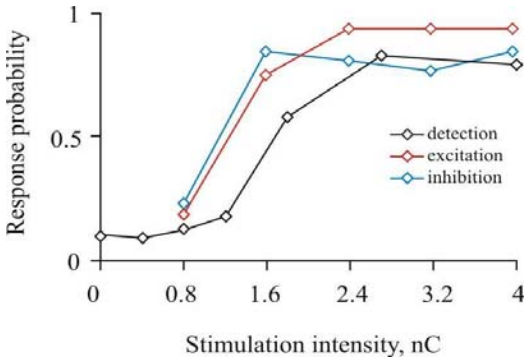

Figure 7. Neurometric and psychometric functions to single pulse stimulation. Probability to evoke excitatory (in red) and inhibitory (in blue) responses were obtained from neurons recorded 450 μm away from stimulation electrode in ketamine anesthetized rats (Study 1). Black trace shows population average of psychophysical detection of single pulse.

The animals readily reported the detection of single pulse stimulation at intensities close to threshold for the neuronal responses observed in anesthetized rats (Study 1). Figure 7 visualizes this statement by assembling neurometric data (Study 1) with psychometric data (Study 4). The match of neurometric data for excitation and inhibition with the psychophysical results prompt the question whether the animals make use of additional spikes during the fast excitation or missing spikes during the long lasting inhibition to detect the presence of the stimulus. Considerations of the response time typically observed in the present experiments argue in favor of the fast excitation as source of the percept. The animals emitted the first lick at an average latency of 200 ms, which, assuming a minimal reaction time of ~100 ms and tongue movement time of ~70 ms, renders the contribution of the inhibitory response less likely than the excitatory response. The second important finding of the present study was that addition of pulses decreased the detection threshold. In Study 1 it was found that the second pulse delivered at > 10 Hz frequency (< 100 ms interpulse interval) failed to extend the inhibition, but it elicited the same number of excess spikes (see Fig. 11 in Butovas and Schwarz, 2003). Repetitive stimulation with more than 2 pulses at > 10 Hz frequency evoked a constant number of excess spikes and led to the integration of inhibitory periods into one continuous inhibitory response against which the evoked spikes stand out.

Thus, the improved detection of repetitive stimulation vs. single pulse could be based on the better signal-to-noise ratio of excess spikes due to the continuous reduction of background activity during the repetitive stimulation. Consequently, the detectability of repetitive stimulation should exceed the detectability of the same number of pulses with independent effects i.e. the combinatorial probability to detect at least one out of n pulses. The analysis presented in Study 4 showed that only the detection of pulse duplets matched this expectation. Five and fifteen pulses in series were detected at the same probability as the same number of independent pulses would have been detected. So the benefit of the enhanced signal to noise ratio seems to be exploited only with small series of pulses. Longer series probably activate unknown additional mechanisms that tend to suppress the percept. Such

mechanisms could be related to the total fading of the perceived phosphene with long stimulation trains in primary visual cortex as seen in a patient that received intracortical electrodes in primary visual cortex (Schmidt et al., 1996).

Summary and conclusions

Introduction of sensory information directly to neocortex by means of multi-electrode stimulation is considered a promising approach for neuroprosthetic devices. The studies conducted for the present thesis yielded a number of considerations regarding the effects of intracortical stimulation onto neuronal activity and its relation to perception. Electrical stimulation evoked spatially extended neuronal response in neocortex, consisting of a fast excitation followed by long-lasting reduction of firing rates (Study 1).

Such spatial propagation of electrically induced activity in neocortex, probably based partly on horizontal intracortical connections, pose a potential source of problems for high density multielectrode stimulation in future neuroprosthetic devices. Spots of activity introduced by adjacent electrodes may overlap, causing unwanted interactions, which could potentially limit the spatial resolution of the evoked percept. Investigation of PN, a subcortical structure that does not show local interactions, showed that the spread of activation critically depends on the neuronal architecture (Study 3).

Activation of inhibitory networks (Study 2) by intracortical stimulation introduces another potential problem for artificial sensory signal transfer. Lasting nearly 100 - 200 ms reduction of firing rates may theoretically affect psychophysical detection of stimuli delivered with frequencies higher than 5 Hz in future neuroprostheses. However, psychophysical experiments using pulse duplets of different intensity to assess the impact of temporal interaction of inhibitory effects found no evidence that electrically evoked inhibition reduces detectability (Study 4). On the contrary, improvement of the animals' performance was observed with stimulation trains that used less than five repetitive pulses. Thus, the presence of inhibition did not deteri-

orate the percept as one might have assumed. Rather, the opposite is true. The presence of inhibition seems to be helpful to generate the percept at least with small series of pulses. It is likely that inhibition provides for low background firing letting the evoked spikes following each pulse stand out at a higher signal-to-noise ratio. This finding becomes relevant when trying to find stimulation patterns that would maximize perceptual effect while minimizing deleterious effects on the neuronal tissue. Many neurobiological studies that evoked motor or sensory responses used high stimulation currents (see for review Tehovnik, 1996). For neuroprosthetic application these stimulus intensities are potentially not applicable because already currents above 40 μA applied for 200 μs have been shown to have damaging effects on neuronal tissue (Asanuma and Arnold, 1975).

Therefore, future clinical application of intracortical stimulation must trade to minimize low stimulation intensities with the quality of the evoked percept. Study1 and Study 4 have shown very low currents are able to elicit neuronal activity as well as a percept. Study 4 has shown that, in addition, the perceptual effect was maximized by double pulse stimulation at short interpulse intervals. When compared to stimulation with single pulses and long repetitive stimulus trains. Therefore, one prospect emerging from the present thesis work is that stimulating with pulse duplets might be a beneficial strategy for future neuroprosthetic devices.

Reference list

Asanuma H, Arnold AP. (1975) Noxious effects of excessive currents used for intracortical microstimulation. *Brain Res 96(1)*: 103-7.

Barth DS. Submillisecond synchronization of fast electrical oscillations in neocortex. (2003) *J Neurosci 23(6)*: 2502-10.

Beierlein M, Gibson JR, and Connors BW. (2000) A network of electrically coupled interneurons drives synchronized inhibition in neocortex. *Nat Neurosci 3*: 904-910.

Belluardo N, Mudo´ G, Trovato-Salinaro A, Le Gurun S, Charollais A, Serre-Beinier V, Amato G, Haefliger JA, Meda P, and Condorelli DF. (2000) Expression of connexin36 in the adult and developing rat brain. *Brain Res 865*: 121-138.

Blatow M, Rozov A, Katona I, Hormuzdi SG, Meyer AH, Whittington MA, Caputi A, and Monyer H. (2003) A novel network of multipolar bursting interneurons generates theta frequency oscillations in neocortex. *Neuron 38*: 805-817.

Brindley GS, Lewin WS. (1968) The sensations produced by electrical stimulation of the visual cortex. *J Physiol 196(2)*: 479-93.

Buhl DL, Harris KD, Hormuzdi SG, Monyer H, and Buzsaki G. (2003) Selective impairment of hippocampal gamma oscillations in connexin-36 knock-

out mouse in vivo. *J Neurosci 23*: 1013-1018.

Butovas S and Schwarz C. (2003) Spatiotemporal effects of microstimulation in rat neocortex: a parametric study using multielectrode recordings. *J Neurophysiol 90*: 3024-3039.

Clark GM, Black R, Dewhurst DJ, Forster IC, Patrick JF, and Tong YC. (1977) A multiple-electrode hearing prosthesis for cochlea implantation in deaf patients. *Med Prog Technol 5*: 127-140.

Condorelli DF, Belluardo N, Trovato-Salinaro A, Mudo G. (2000) Expression of Cx36 in mammalian neurons. *Brain Res Brain Res Rev 32(1)*: 72-85.

Connors BW and Long MA. (2004) Electrical synapses in the mammalian brain. *Annu Rev Neurosci 27*: 393-418.

Dobelle WH and Mladejovsky MG. (1974) Phosphenes produced by electrical stimulation of human occipital cortex, and their application to the development of a prosthesis for the blind. *J Physiol 243*: 553-576.

Dobelle WH, Mladejovsky MG, Evans JR, Roberts TS, and Girvin JP. (1976) "Braille" reading by a blind volunteer by visual cortex stimulation. *Nature 259*: 111-112.

Galarreta M and Hestrin S. (1999) A network of fast-spiking cells in the neocortex connected by electrical synapses. *Nature 402*: 72-75.

Galarreta M and Hestrin S. (2001a) Electrical synapses between GABA-releasing interneurons. *Nat Rev Neurosci 2*: 425-433.

Gustafsson B. and Jankowska E. (1976)Direct and indirect activation of nerve cells by electrical pulses applied extracellularly. *J Physiol 258*: 33-61.

Gibson JR, Beierlein M, and Connors BW. (1999) Two networks of electrically coupled inhibitory neurons in neocortex. *Nature 402*: 75-79.

Hormuzdi SG, Pais I, LeBeau FE, Towers SK, Rozov A, Buhl EH, Whittington MA, and Monyer H. (2001) Impaired electrical signaling disrupts gamma frequency oscillations in connexin 36-deficient mice. *Neuron 31*: 487-495.

House WF and Urban J. (1973) Long term results of electrode implantation and electronic stimulation of the cochlea in man. *Ann Otol Rhinol Laryngol 82*:504-517.

Kim U, Ebner FF. (1999) Barrels and septa: separate circuits in rat barrels field cortex. *J Comp Neurol 408(4)*:489-505.

Makowski L, Caspar DL, Phillips WC, Goodenough DA. (1977) Gap junction structures. II. Analysis of the x-ray diffraction data. *J Cell Biol 74(2)*:629-45.

McIntyre CC and Grill WM. (2000) Selective microstimulation of central nervous system neurons. *Ann.Biomed.Eng 28*: 219-233.

Möck M, Schwarz C, Wahle P, Thier P. (1999) GABAergic inhibition in the rat pontine nuclei is exclusively extrinsic: evidence from an in situ hybridization study for GAD67 mRNA. *Exp Brain Res 124(4)*:529-32.

Murasugi CM, Salzman CD, and Newsome WT. (1993) Microstimulation in visual area MT: effects of varying pulse amplitude and frequency. *J Neurosci 13*: 1719-1729.

Nowak LG and Bullier J. (1998a) Axons, but not cell bodies, are activated by electrical stimulation in cortical gray matter. I. Evidence from chronaxie measurements. *Exp Brain Res 118*: 477-488.

Nowak LG and Bullier J. (1998b) Axons, but not cell bodies, are activated by electrical stimulation in cortical gray matter. II. Evidence from selective inactivation of cell bodies and axon initial segments. *Exp Brain Res 118*: 489-500.

Peters A. Synaptic specifity in the cerebral cortex. (1987) In: Synaptic Function, edited by Edelman GM, Gall WE, and Cowan WM. New York: Wiley, p. 373-397.

Ranck JB, Jr. (1975) Which elements are excited in electrical stimulation of mammalian central nervous system: a review. *Brain Research 98*: 417-440.

Rattay F. (1999) The basic mechanism for the electrical stimulation of the nervous system. *Neuroscience 89*: 335-346.

Romo R, Hernandez A, Zainos A, Brody CD, and Lemus L. (2000). Sensing without touching: psychophysical performance based on cortical microstimulation [In Process Citation]. *Neuron 26*: 273-278.

Romo R, Hernandez A, Zainos A, and Salinas E. (1998). Somatosensory discrimination based on cortical microstimulation. *Nature 392*: 387-390.

Salzman CD, Britten KH, and Newsome, WT. (1990). Cortical microstimulation influences perceptual judgements of motion direction. *Nature 346*: 174-177.

Schmidt, E. M., Bak, M. J., Hambrecht, F. T., Kufta, C. V., O'Rourke, D. K., & Vallabhanath, P. (1996). Feasibility of a visual prosthesis for the blind based on intracortical microstimulation of the visual cortex. *Brain 119 (Pt 2)*: 507-522.

Schwarz C and Möck M. Spatial arrangement of cerebro-pontine termi-

nals. *J Comp Neurol 435*: 418-432, 2001.

Stoney, SD Jr., Thompson, WD, and Asanuma, H. (1968). Excitation of pyramidal tract cells by intracortical microstimulation: effective extent of stimulating current. *J Neurophysiol 31*: 659-669.

Szentagothai J. The neuron network of the cerebral cortex: a functional interpretation. *Proc R Soc Lond B Biol Sci 201*: 219-248, 1978.

Tehovnik, EJ (1996). Electrical stimulation of neural tissue to evoke behavioral responses. *J Neurosci Methods 65*: 1-17.

Thomson AM, Destexhe A. (1999). Dual intracellular recordings and computational models of slow inhibitory postsynaptic potentials in rat neocortical and hippocampal slices. *Neuroscience 92*: 1193-1215.

Welker C. (1971). Microelectrode delineation of fine grain somatotopic organization of (SmI) cerebral neocortex in albino rat. *Brain Res 26*: 259-275.

Whittington MA, Traub RD, and Jefferys JG. (1995) Synchronized oscillations in interneuron networks driven by metabotropic glutamate receptor activation. *Nature 373*: 612-615.

Woolsey TA and Van der Loos H. (1970). The structural organization of layer IV in the somatosensory region (SI) of mouse cerebral cortex. The description of a cortical field composed of discrete cytoarchitectonic units. *Brain Res 17*: 205-242.

Yeomans J, Mercouris N, and Ellard C. (1985). Behaviorally measured refractory periods are lengthened by reducing electrode tip exposure or raising current. *Behav Neurosci 99*: 913-928.

Zucker E and Welker WI. (1969). Coding of somatic sensory input by vibrissae neurons in the rat's trigeminal ganglion. *Brain Res 12*: 138-156.

Appendix A1: Animal care statement

The studies included in present dissertation performed to investigate consequences of intracortical microstimulation for purposes of central neuroprostheses. The experiments described here required the use of laboratory animals, such as mice (*Muscus Domesticus*) and rats (*Rattus Rattus*).

All procedures within each of experiments were performed to impose minimum suffering and provide maximum comfort to preserve animals' health and well being by the allowed methods available to date. All experimental protocols were approved by responsible regulatory institution (Regierungspräsidium Tübingen) and carried out in accordance with the policy on the use of animals in neuroscience research of the Society for Neuroscience and German national law.

Appendix A2: Statement of authorship contribution

The publications listed below in this Appendix do relate to the work presented in the dissertation. I declare that I did actively contribute to each of the studies in the indicated stage of the work.

Publications 1, 2, 3 and 4:

1. Study design
2. Conduction of experiments and data collection
3. Data analysis
4. Draft and revision of final Manuscript

Original publication list:

1. **Butovas S**, Schwarz C. (2003). Spatiotemporal effects of microstimulation in rat neocortex: a parametric study using multielectrode recordings. *J Neurophysiol 90(5)*: 3024-39.

2. **Butovas S**, Hormuzdi SG, Monyer H, Schwarz C. (2006). Effects of electrically coupled inhibitory networks on local neuronal responses to intracortical microstimulation. *J Neurophysiol 96*: 1227-1236.

3. Möck M, **Butovas S**[1], Schwarz C. (2006). Functional unity of pontine and cerebellar signal processing: intrapontine communication is mediated by a reciprocal loop with the cerebellar nuclei. *J Neurophysiol 95(6)*: 3414-25.

4. **Butovas S**, Schwarz C. (2007). Intracortical microstimulation of barrel cortex in awake, headrestraint rats: assessment of detection threshold. *Eur J Neurosci 25(7)*: 2161-9.

[1]Note: indicates shared first autorship

Appendix A3

I would like to express my gratitude to many people, whom I worked with and who made my entire life and work in Germany experience that I will never forget.

First of all, I would like to thank my present supervisor, Dr. Cornelius Schwarz for giving me chance. Your infinite patience, care, compromise, excellent supervising and wise advising made this work possible.

Second, I would like to shake hands of my colleagues, Harald Hentschke, Florent Haiss and Maik Stüttgen for their discussions, support, friendship, great working atmosphere and many nice minutes that we spent together.

Next, I'm extremely grateful to Ute Grosshenning. Without your help, my first days in Germany would become horror.

I would also like to thank Susanne Kramer, Gudrun Sessler and Ursula Pascht for their significant contribution to my work.

I will always be indebted to Dr. Horst Herbert and Dr. Katja Deiss, for helping me to get over the bureaucratic obstacles.

Finally, I'm obliged to all my friends in Germany and in Lithuania for being with me during these years.

This page left blank intentionally

J Neurophysiol 90: 3024–3039, 2003.
First published July 23, 2003; 10.1152/jn.00245.2003.

Spatiotemporal Effects of Microstimulation in Rat Neocortex: A Parametric Study Using Multielectrode Recordings

Sergejus Butovas and Cornelius Schwarz
Abteilung Kognitive Neurologie, Neurologische Universitätsklinik Tübingen, 72076 Tübingen, Germany

Submitted 14 March 2003; accepted in final form 22 July 2003

Butovas, Sergejus and Cornelius Schwarz. Spatiotemporal effects of microstimulation in rat neocortex: a parametric study using multielectrode recordings. *J Neurophysiol* 90: 3024–3039, 2003. First published July 23, 2003; 10.1152/jn.00245.2003. Using microstimulation to imprint meaningful activity patterns into intrinsically highly interconnected neuronal substrates is hampered by activation of fibers of passage leading to a spatiotemporal "blur" of activity. The focus of the present study was to characterize the shape of this blur in the neocortex to arrive at an estimate of the resolution with which signals can be transmitted by multielectrode stimulation. The horizontal spread of significant unit activity evoked by near-threshold focal electrical stimulation (charge transfer 0.8–4.8 nC) and multielectrode recording in the face representation of the primary somatosensory cortex of ketamine anesthetized rats was determined to be about 1,350 μm. The evoked activity inside this range consisted in a sequence of fast excitatory response followed by an inhibition lasting >100 ms. These 2 responses could not be separated by varying the intensity of stimulation while a slow excitatory rebound after the inhibitory response was restricted to higher stimulus intensities (>2.4 nC). Stimulation frequencies of 20 and 40 Hz evoked repetitive excitatory response standing out against a continuous background of inhibition. At 5- and 10-Hz stimulation, the inhibitory response showed a complex interaction pattern attributed to highly sublinear superposition of individual inhibitory responses. The present data help to elucidate the neuronal underpinnings of behavioral effects of microstimulation. Furthermore, they provide essential information to determine spatiotemporal constraints for purposeful multielectrode stimulation in the neocortex.

INTRODUCTION

Electrical stimulation of nervous tissue has been a tool used extensively in experimental neuroscience to elicit neuronal or behavioral responses in a large variety of preparations (Ranck 1975; Tehovnik 1996). Recently, a new interest for stimulation of neuronal tissue has arisen from the prospect that signals from machines may be transferred directly to neuronal tissue by electrical stimulation to circumvent damaged afferent pathways. Although there is considerable progress in stimulating peripheral sensory structures for this purpose (Loeb 1990; Zrenner 2002), the prospect of using electrical stimulation also in central brain regions like the neocortex are far from being routinely applicable (see pioneering work by Dobelle et al. 2000; Luethje et al. 1992; McCreery et al. 1998). One reason for this is that the manner in which extracellular current activates complexly organized neural tissues is only partly understood.

Basically, 3 interdependent problems have to be solved to be able to feed defined activity patterns into complexly organized CNS structures. First, the exact extent and shape of the "directly" activated brain area has to be known. It may be substantially different from area to area because it is dependent on electrode geometry and the cellular composition of the neural tissue. In cat motor cortex Asanuma and colleagues showed that the current needed to evoke an action potential in corticospinal projection neurons is proportional to the square of the distance between a microelectrode and the soma (Asanuma et al. 1976; Stoney et al. 1968). In particular, it has been shown that the population of corticospinal projection neurons directly activated by a small current pulse (e.g., <20 μA and 0.2 ms) is grouped around the electrode at a distance of about 100 μm (Stoney et al. 1968) and thus excites a few thousand cortical cells directly (Tehovnik 1996). The second problem to be solved is the relative contribution of different neuronal elements, like dendrites, somata, and axons to the direct activation of neurons. There is substantial evidence from experimental work as well as from computer simulations that electrically evoked activity in gray matter is attributed mainly to the excitability of axonal elements and only to a small degree to somata and dendrites (Gustafsson and Jankowska 1976; McIntyre and Grill 2000; Nowak and Bullier 1998a,b; Ranck 1975; Rattay 1999). This insight represents the third problem to be solved: that the direct neuronal activation of somata must be expected to be masked by intense axonal excitation carrying the activation by ortho- and antidromic conveyance of spikes to areas, the spatial layout of which depends much on the interconnectivity of the structure ("indirect" effects). Because intrinsic axonal elements are abundant in neocortex and most other gray matter in the CNS, local antidromic and/or synaptic effects must be expected to carry the major part of the stimulation effect even though only a small number of neuronal somata have been stimulated directly.

The present study focuses on the "indirect" effects of intracortical electrical stimulation, which we refer to as the spatiotemporal "blur" of evoked activity. The neocortex is an important future candidate for CNS stimulation aimed at restoring brain function because important functions are localized on the neocortical surface in an easily accessible way and in many cases are functionally separated and organized in well-charac-

Address for reprint requests and other correspondence: C. Schwarz, Abteilung Kognitive Neurologie, Neurologische Universitätsklinik Tübingen, Auf der Morgenstelle 15, 72076 Tübingen, Germany (E-mail: cornelius.schwarz@uni-tuebingen.de)

The costs of publication of this article were defrayed in part by the payment of page charges. The article must therefore be hereby marked "*advertisement*" in accordance with 18 U.S.C. Section 1734 solely to indicate this fact.

terized cortical maps. On the other hand, the prototypic neocortical architecture contains several excitatory and inhibitory cell types that are complexly interconnected locally as well as over larger distances (see reviews in Braitenberg and Schüz 1991 and Peters and Jones 1984). Neocortical connectivity is strongest within cortical columns spanning the depth of the neocortex (Hubel and Wiesel 1977; Mountcastle 1957) but it is pronounced as well along the axes spanning its surface. Long horizontal fibers present in all layers (with a preponderance in layers 2/3 and 5) transmit excitatory signals over distances of up to several millimeters and contacts mainly excitatory but also to inhibitory neurons (Dalva et al. 1997; Hirsch and Gilbert 1991; Kim and Ebner 1999; McGuire et al. 1991; Schubert et al. 2001). Inhibitory signals show horizontal spread as well. Long horizontal inhibitory axons are shorter on average than the excitatory ones (about 1 mm; for review see Kisvárday 1992), but in addition, inhibition can be transmitted by electrically (and synaptically) interconnected networks of interneurons and thereby potentially may spread over a large range of neocortex as well (Galarreta and Hestrin 1999; Gibson et al. 1999). As alluded to in the previous paragraph, the high interconnectivity of the neocortex predicts that indirectly evoked activity—by retrograde, synaptic, or electrical transmission—must play an important role in determining the effect of electrical stimulation of neocortex (Nowak and Bullier 1998a). This spatiotemporal extent of indirect effects determines whether and how interaction of stimulus applied at different points in space and time occurs and will be critical for future applications because it is clear from the distributed representation of signals on the surface of the neocortex that multielectrode techniques have to be employed to reach the spatiotemporal resolution needed to evoke functional activity patterns (Nicolelis 2001). To use multielectrode stimulation in the neocortex, a mandatory step must be to gain detailed knowledge on how a single electrical pulse affects the activity of the surrounding neuronal circuit. What are the changes of neuronal activity evoked by a certain stimulation intensity in space and time and what follows from these characteristics for the interaction of two stimuli in the temporal (pulse intervals) and spatial (cross electrode) domain? As a first step, we measured these parameters using dense microelectrode arrays in primary somatosensory cortex of ketamine anesthetized rats. Responses of single unit and multiunit spike trains were recorded varying electrical (charge transfer), spatial (electrode location), and temporal (pulse intervals) parameters of electrical stimulation.

METHODS

Surgery

Twenty-one Sprague–Dawley rats of both sexes (body weight 300 to 400 g) were used in the present study. All experimental and surgical procedures were performed in accordance with the policy on the use of animals in neuroscience research of the Society for Neuroscience and German Law. The rats were anesthetized with a mixture of ketamine (100 mg/kg) and xylacine (10 mg/kg) administered intraperitoneally. The depth of anesthesia was maintained with additional doses of ketamine as required to keep the hind-limb withdrawal reflex to a painful stimulus below threshold. The animal's rectal temperature and heart rate were constantly monitored. The temperature was adjusted to 37.0°C using a controlled heating pad (Fine Science Tools, Heidelberg, Germany). For recordings from the neocortex, animals were placed in a stereotaxic apparatus and craniotomy was performed to open the primary somatosensory cortex. After removal of the dura mater a multielectrode array consisting of a row of 7 electrodes was lowered into the neocortex at a 90° angle with respect to its surface using a hydraulic micropositioner (Kopf 650; David Kopf Instruments, Tujunga, CA). After placement of the electrode array the cortex was covered with mineral oil to prevent drying. The receptive field of the recording sites was coarsely assessed using either an air puff (originating from a plastic tube; diameter about 0.5 mm) directed against the whiskers (duration 20 ms, distance to whisker pad 2–3 cm) and/or a cotton swap lightly touching parts of the body. In preliminary experiments the placement and orientation of the electrode array were varied. Stimulation of areas representing whiskers, snout, and forelimb yielded qualitatively the same results. For the recordings presented here locations were analyzed for which an air puff against the whisker pad on the contralateral side to the recorded hemisphere elicited a clear response in at least part of the electrodes. The data of the present study were thus recorded in whisker and neighboring snout representations. At the end of the experiment the recording sites were marked with electrolytic lesions. The animal was deeply anesthetized with barbiturates and perfused through the aorta using phosphate buffer (0.1 M) followed by paraformaldehyde (4% in phosphate buffer). The brain was processed using standard histological procedures. The layer of recording was assessed by investigating lesions in Nissl-stained sections oriented orthogonally to the surface of the neocortex.

Electrodes

Multielectrode arrays were custom made in our laboratory. Seven standard etched and lacquered tungsten electrodes (shaft diameter 100 μm; tip size about 10 μm; impedance >2 MΩ) were mounted inside a linear array of polyimide tubing (HV Technologies, Trenton, GA) and crimp connected on their back ends to a microplug (Bürklin, München, Germany). The tip distance was 450 μm. The electrode at one end of the row was used for electrical stimulation and was placed inside a stainless steel tube that was connected to ground during the recording sessions. This shielding reduced the stimulus artifact such that minimal latencies of 2 ms could be safely determined (see next section).

Electrophysiology

The electrophysiological recordings of extracellular signals were performed using a multichannel extracellular amplifier (MultiChannel Systems, Reutlingen, Germany; gain 5000; sampling rate 20 kHz; band-pass filter with cutoff frequencies of 200 and 5000 Hz). Action potentials were extracted from the voltage traces off-line by a threshold and stored as cutouts of 2 ms length on the hard drive of a PC. Spike sorting was performed with PCA clustering using a MATLAB-based program (Egert et al. 2002; the software is available on the internet at http://www.brainworks.uni-freiburg.de/). Through the first electrode in the row of electrodes rectangular biphasic current pulses (cathodal first) were delivered at a rate of 1 Hz using a programmable stimulator (STG 1008; MultiChannel Systems). To avoid the need to apply very low current amplitudes, the stimulus amplitude was fixed to 8 μA and the intensity was changed by varying the pulse duration between 100 to 600 μs in steps of 100 μs (charge transfer of 0.8 to 4.8 nC, varied from pulse to pulse in a pseudo-random fashion). The intervals chosen cover the range of pulse durations for which the most significant change of direct excitability of pyramidal cells was observed by Stoney et al. (1968; see their Fig. 6: the chronaxie of neocortical pyramidal cells is just above the lowest intervals used here). In double-pulse experiments the intensity of the first ("conditioning") pulse was adjusted to a charge transfer that was just subthreshold (i.e., it did not elicit a response), or to a suprathreshold

charge transfer showing a clear response. The second ("test") stimulus was then varied as described for the single-pulse experiments. The interpulse interval was 75 ms. In a second set of double-pulse experiments the intensities of both pulses were set to the same suprathreshold charge transfer and the interval between the pulses was varied in a pseudo-random fashion (25, 50, 100, and 200 ms).

Data analysis

The calculation of response parameters for the short latency response was hampered by the stimulus artifact and thus had to be restricted to single units with a good signal-to-noise ratio. Figure 1, *A* and *B* demonstrates the assessment of latencies of single units that could be performed accurately to within a minimum of 2 ms. The stimulus artifact consisted of a fast phase in which its amplitude was very high, driving the amplifiers into saturation lasting for <2 ms and followed by a slow positive wave ending at around 5 ms. Short-latency spikes residing on the slow phase of the artifact typically could not be detected using a voltage threshold (Fig. 1*A*). This, however, could be commonly achieved by blanking the high-amplitude phase of the stimulus artifact (0 to 2 ms after onset of the stimulus; gray area in Fig. 1, *A* and *B*), subsequent differentiation, and the usage of a threshold of voltage slope (μV/ms). Spike extraction was realized by a semiautomatic MATLAB program (MathWorks, Natick, MA). Voltage traces of all spike trains thus extracted were visually inspected by the experimenter to exclude errors.

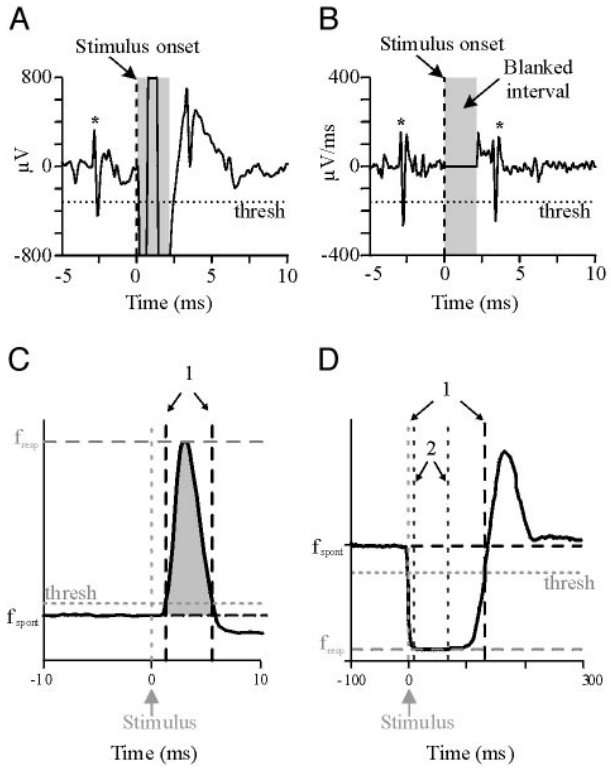

FIG. 1. *A* and *B*: isolation of short latency single-unit action potentials from stimulus artifact. *A*: *voltage trace* showing spontaneous (about 2.5 ms before stimulation) and an evoked (about 3 ms after stimulation) action potential. As shown in this example, evoked action potentials at short latencies were riding on slow component of electrical artifact and therefore could not be detected by threshold (denoted thresh; successfully detected spikes are marked by asterisk in *A* and *B*). *B*: after blanking of the stimulus artifact (0–2 ms, gray area) and differentiation of signal, action potentials at latencies >2 ms were detected by negative threshold. *C* and *D*: schematic showing quantification of fast excitatory (*C*) and inhibitory (*D*) responses using low-pass filtered peristimulus time histograms (PSTHs). Spontaneous frequency: f_{spont}, horizontal black broken line. Response frequency: f_{resp}, horizontal gray broken line. Threshold to detect response [computed as $(f_{spont} \pm f_{spont})0.25$; horizontal gray dotted line]. *Interval 1* in both figures depicts duration of response (vertical black broken lines; in *D* only end of response is depicted for clarity). *C*: strength of excitatory response is represented by area under the PSTH (gray area). Latency was estimated as interval from stimulus onset to beginning of *interval 1*. *D*: firing rate during inhibition (f_{resp}) was estimated as average rate within *interval 2* (12–80 ms). Strength of inhibitory response was calculated as $1 - f_{resp}/f_{spont}$. Note that fast excitatory response was blanked for clarity in *D*. Rebound response is visible after end of inhibitory response. Its quantification was performed in an analogous way to fast excitatory response shown in *C*.

Peristimulus time histograms (PSTHs) were computed as spike renewal densities (Abeles 1982) at a resolution of 0.1 ms (for fast excitation) and 1 ms (for inhibition and rebound response) to estimate firing rates at different points in time around the stimulation. They were used to quantify excitatory bursts and inhibitory responses after electrical stimulation. The spontaneous frequency (f_{spont}) was the average rate before the application of an electrical stimulus (horizontal black broken line in Fig. 1, *C* and *D*). For the analysis of fast excitatory responses, the PSTH was low-pass filtered by passing a Gaussian (kernel length 5 bins) over it. The unit was counted as generating a response if the firing rate increased by $1.25f_{spont}$ (denoted "thresh" in Fig. 1*C*) in an interval of 2 to 10 ms after stimulation. The rebound response after the inhibitory response was quantified the same way. The duration of excitatory responses was taken as the time the firing frequency stayed above threshold (*interval 1* in Fig. 1*C*). The strength of the response was defined as the integral of the response above the spontaneous firing rate yielding the number of excess spikes per trial (gray area in Fig. 1*C*). For the analysis of inhibitory responses, the PSTH was low-pass filtered by passing a Gaussian (kernel length 50 bins) over it. A unit was classified as responding if the firing rate undershot $0.75f_{spont}$ (denoted "thresh" in Fig. 1*D*). The duration of the inhibitory response was measured from the stimulation to the point in time where the firing rate crossed the threshold again (*interval 1* in Fig. 1*D*). The strategy to calculate the response frequency f_{resp} and the strength of the response deviated from that used for excitation. The reason was that the minimal frequency during the inhibition in many cases was zero but the slope back to the spontaneous firing rate varied from case to case. We thus took the average frequency within the interval 12 to 80 ms after stimulus onset as f_{resp} (see *interval 2* in Fig. 1*D*). The strength of the inhibitory response was computed as $1 - (f_{resp}/f_{spont})$.

Test for antidromic invasion

Testing for antidromic invasion was realized by applying spike-triggered stimulation and comparing the response strength and latencies of single units in a "collision" situation with those obtained in a "no collision" situation. The "collision" experiment was realized by triggering the stimulation (4.8 nC) on the occurrence of a single-unit action potential at a delay of 1 ms. The "no collision" experiment differed from this by a longer delay that exceeded the response latency by ≥ 2 ms (we used typically about 10 ms) to ensure that the axons contributing to an eventual antidromic response recovered from the refractory period before the onset of stimulation. The duration of the command pulse that triggered the stimulator was set to 1 s, thus defining a lower limit for possible interstimulus intervals. As a control for possible introduction of features of temporal patterns in spike trains by the spike-triggered nature of the recordings (i.e., features of the autocorrelogram), we performed control recordings that were identical to the "collision" and "no collision" tests in that they were recorded in a spike-triggered way but the stimulator was deactivated. The response strength and latency apparent in "collision" and "no collision" experiments was calculated after subtraction of the control histograms (Fig. 4, *A* and *B*).

RESULTS

In a preliminary set of experiments, the range of stimulus intensities that would evoke cortical responses in units at distances ≤2.25 mm was qualitatively explored. In these experiments, stimulation of 0.1 to 0.4 nC (1 to 4 μA at 0.1 ms) never induced visible neuronal responses (80 out of 80 units; Fig. 2*A*). Higher stimulus intensity of 0.8 nC (8 μA at 0.1 ms) evoked excitatory and/or inhibitory responses in 4 of these cases, a fraction that could be increased to 33 out of 80 cases at the highest intensity tested (4.8 nC equivalent to 8 μA at 0.1 ms; Fig. 2*A*). Guided by these results we set the range of stimulus intensities to be used for the quantitative analyses from 0.8 to 4.8 nC. It should be noted that this range of intensities is lower than typical intensities used in earlier studies to evoke behavioral responses in rat, cat, and monkeys by a factor of 10 to 2,000 (Tehovnik 1996; see his Fig. 10 and references therein). However, studies that deliberately sought to minimize stimulation currents showed that stimulation intensities comparable to those used here readily modulated behavior [Salzman et al. (1990) used repetitive stimulation at 2

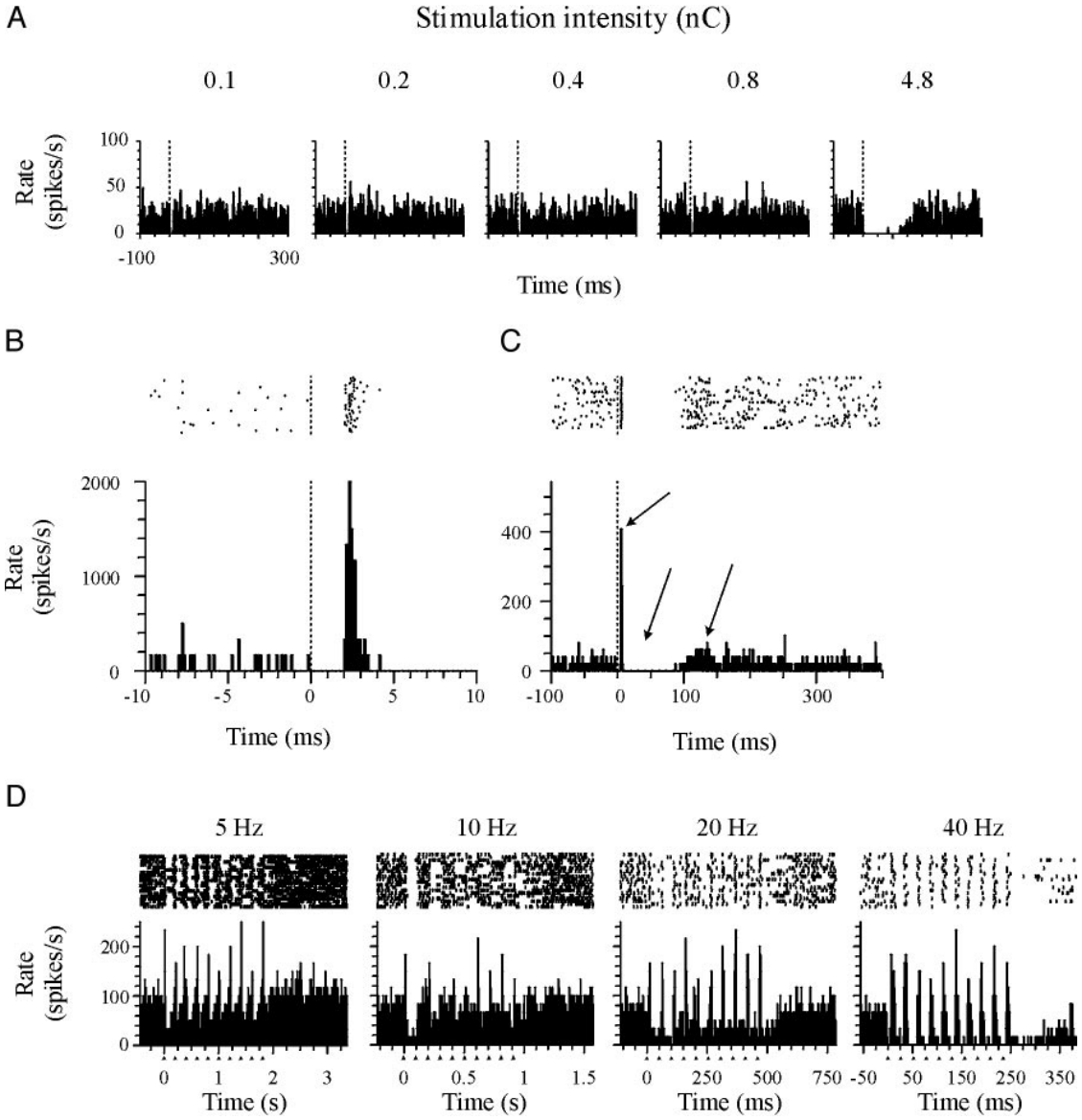

FIG. 2. Typical responses to microstimulation. Raster plots and PSTHs (recorded 450 μm away from stimulation electrode) are plotted on different time scales. *A*: range of effective stimulation intensity demonstrated by typical multiunit recording (scales of leftmost histogram apply to all; bin size, 1 ms). In a set of preliminary experiments, intensities < 0.8 nC evoked neuronal responses in 4 of 80 cases. At intensities of 4.8 nC responses could be evoked in 33 of 80 cases. Based on these results range of stimulation intensities used for quantitative analyses (see Figs. 3 and 6 and Tables 1–3) was restricted from 0.8 to 4.8 nA. *B*: excitatory response (single-unit recording; bin size, 0.1 ms). Stimulation (4.0 nC) occurred at *time 0*. *C*: full sequence of responses consisting of fast excitatory, long-lasting inhibitory and rebound response (indicated by arrows) (multiunit recording; bin size, 1 ms). Stimulation (4.0 nC) occurred at *time 0*. *D*: fast excitatory response followed stimulation frequencies of ≤40 Hz (occurrence of stimulus pulses are marked with triangles along time axis). Long-lasting inhibition shows complex interaction pattern best visible with stimulation at intervals of 100 ms (10 Hz), corresponding roughly to its duration. Inhibitory responses to individual pulses merged at stimulation frequencies of 20 and 40 Hz. Last pulse in these trains readily evoked inhibitory response.

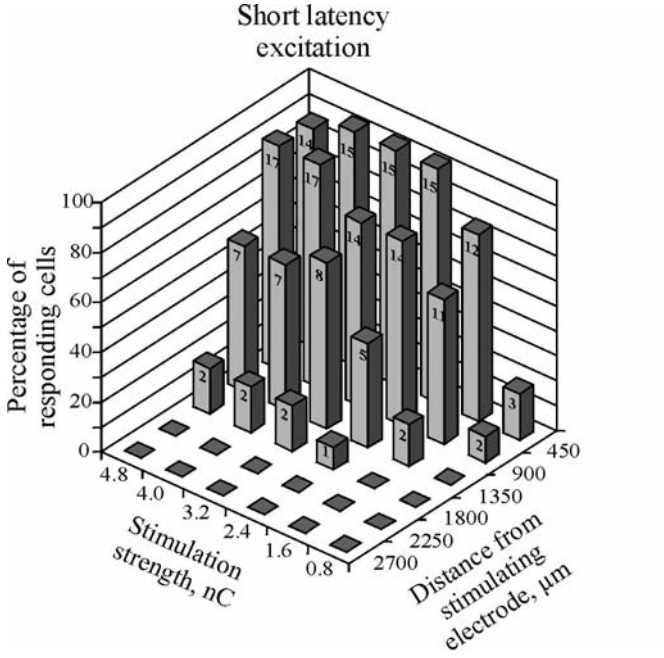

FIG. 3. Excitatory response. Percentage of single units at different distances from recording electrode responding to varying intensity of stimulation. Units recorded at all cortical depths were pooled. Absolute number of responding cells is indicated on columns. See also Table 1.

nC in monkey area MT to bias direction estimation of the animal; Tehovnik et al. (2003) found a minimum of 0.6 nC applied repetitively to evoke saccades in monkey area V1].

Typically, suprathreshold electrical microstimulation at all cortical depths induced a short latency excitatory[1] response containing a single spike or doublet of spikes (Fig. 2*B*), followed by a conspicuous inhibition, which lasted for 100 to 150 ms after the stimulation (Fig. 2*C*). In some cases stronger stimulus intensity (>2.4 nC) evoked a variable rebound excitation after the long inhibition that lasted for several hundreds of milliseconds (Fig. 2*C*). In 10 out of 11 cases tested the short-term excitatory spikes followed stimulus trains delivered at frequencies of 5, 10, 20, and 40 Hz (Fig. 2*D*). The spatial pattern of neuronal responses was surprisingly similar from case to case. In particular, the orientation of the electrode array on the cortical surface had no visible effect and there was no sign of patchiness of the responses obtained in the major responsive area (≤1,350 μm) (Fig. 5 shows a representative example of an inhibitory response with a complete set of recordings from all electrodes). We thus did not try to correlate response patterns to the location of electrodes within the rat's somatosensory body map. Also the neuronal responses at different depths corresponding to layer 2 to layer 6 (130 to 1,467 μm below the pia) were uniform, confirming earlier results in association cortex (Contreras et al. 1997) and were thus pooled for the analysis. Quantitative analysis was performed on 72 single-unit spike trains with signal-to-noise ratio >3 (see METHODS) for excitation and 126 spike trains for inhibition (multiunit: $n = 84$; single unit: $n = 42$). All spike trains used for the quantitative analysis were recorded under pseudo-random presentation of stimulus intensities. An additional 351 units were not analyzed quantitatively because the stimulus intensity was not ordered in a pseudo-random fashion; however, they qualitatively supported the main results reported in the following sections. Multiunit and single-unit spike trains were pooled for the quantitative analysis of the inhibition because they did not show obvious differences in response properties. In a first step we assessed the percentage of units that responded to the stimulus for the 2 factors *stimulus intensity* and *distance from the stimulating electrode*. From the responding units, we assessed 3 response variables: *strength*, *latency*, and *duration*. To assess statistically significant effects of the 2 factors on the response variables MANOVA was employed.

[1] To use consistent terminology throughout this report we chose to call the responses in firing rates observed here "excitatory" and "inhibitory." This choice reflects our conclusion (see DISCUSSION) that these responses are based mainly on synaptic excitation and inhibition but it does not exclude possible contributions from other mechanisms (i.e. changes in synaptic efficacy and/or intrinsic membrane properties).

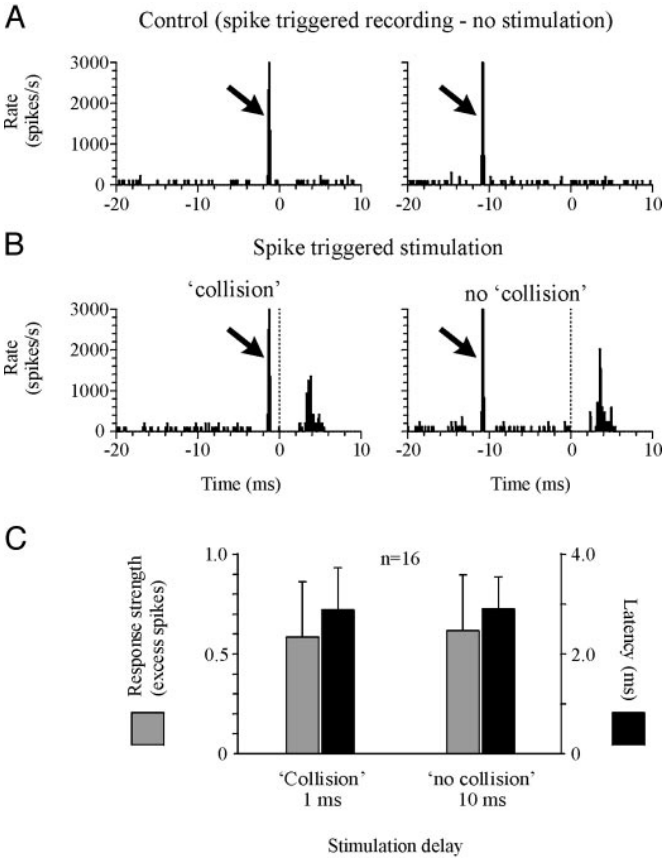

FIG. 4. Excitatory response, collision test for antidromic invasion. *A*: control recordings. Firing with respect to spontaneously occurring action potentials (arrows) of a single unit is shown. Minimal interval between action potentials that triggered recording was 1 s. Resulting histogram reflects features of autocorrelogram function introduced by these conditions of spike-triggered recording. *B*: spike-triggered stimulation at delay of 1 ms ("collision") and 10 ms ("no collision"). Cell and recording conditions were identical to those shown in *A* with exception that stimulation device was activated (stimulation occurred at *time 0*). If antidromic invasion played a role in generation of response, it should lead to extinction of spikes by collision in case of short delay but not in case of long delay. This was not the case. *C*: response strength of 16 single units recorded under conditions shown in *A* and *B*. Measurement was taken as area under peak in test situation (*B*) minus that found in control (*A*). No statistical difference in response strength and latency was found (paired *t*-test for both parameters, $P > 0.05$).

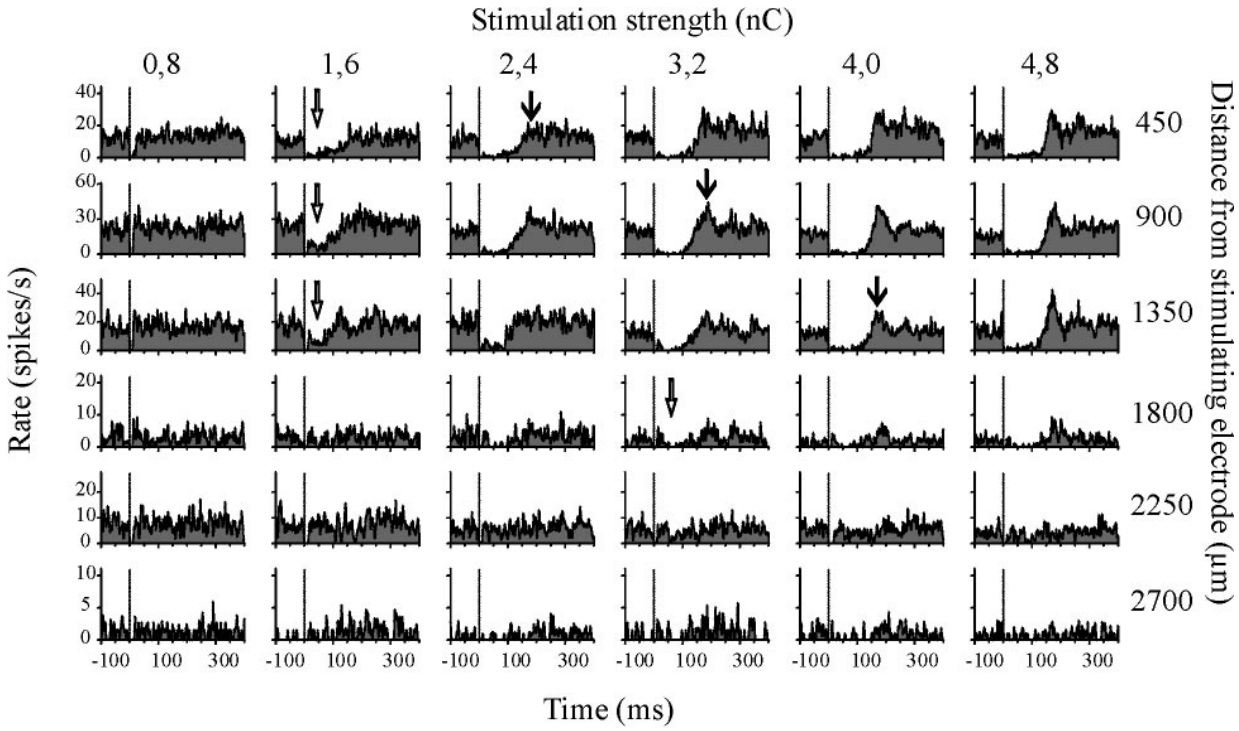

FIG. 5. Inhibitory response. Example of multielectrode recording at depth of 1,150 μm. PSTHs for each stimulus intensity are depicted (columns). Rows depict PSTHs computed from one multiunit spike train recorded from each of 6 electrodes. Occurrence of inhibitory response and subsequent rebound excitation depended on stimulus intensity and distance from recording site to stimulation electrode. Thresholds for inhibitory response (empty arrows) and subsequent rebound response (filled arrow) found by our quantitative analysis are marked. Dotted lines indicate occurrence of stimulus. Note that short latency excitatory response has been blanked.

Excitatory response

Figure 3 depicts the percentage of single units that showed a short excitatory response for all distances from the stimulation site and for all stimulation intensities. The probability of obtaining an excitatory response was close to one (>90%) in the higher range of stimulus intensities and the shortest distance to the stimulation site (450 μm). The percentage then fell rapidly with distance and decreasing stimulus intensity. Within a range of 1,350 μm and a charge transfer of more than 1.6 nC, about 50% of the cells responded. Farther away only 2 responding cells were found (out of 25).

Table 1 shows the response properties of the cells that were classified as responding. The strength of the fast excitatory response was most conspicuously related to the distance of the cell to the stimulation site. It was strongest at 450 μm with up to a mean of 0.65 excess spikes/trial (maximum 0.9 excess spikes/trial in an individual case) and declined to about half this value at 1,350 μm. Latency was related to the distance as well. The latency at 450 μm was on average 2.39 ms and increased to 2.73 ms at 1,350 μm. The average progression of activity across the first 3 electrodes occurred therefore at a velocity of 2.6 m/s. In the 2 cases observed farther away than 1,350 μm the latency was unusually long (about 6 ms). The duration of the response was between 1.3 and 2.8 ms, indicating that the response showed a high temporal precision. The highest precision (i.e., shortest response) was found in cells that were recorded close to the stimulation site. Significance testing was performed on the part of the data matrix that satisfied the complete design criterion of MANOVA (entries of $n > 1$). The range, thus tested, was 1.6–4.8 nC and 450–1350 μm and contained numbers of cells as given in the first section of Table 1. It should be noted that the 2 sole cells located farther away than 1,350 μm showed outlying values for all 3

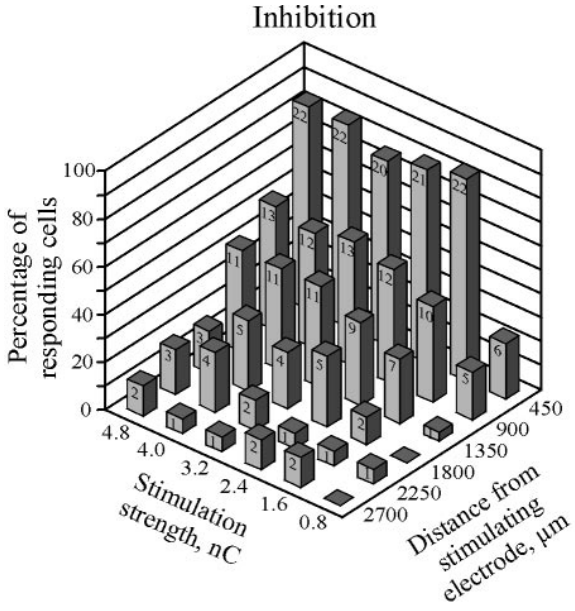

FIG. 6. Inhibitory response. Percentage of units at different distances from recording electrode responding to varying intensity of stimulation. Single and multiunits recorded at all cortical depths were pooled. Absolute number of responding units is indicated on columns. See also Table 2.

TABLE 1. *Properties of the fast excitatory response with respect to stimulation intensity and distance from stimulation electrode*

	Excitation					
	0.8 nC	1.6 nC	2.4 nC	3.2 nC	4.0 nC	4.8 nC
Number of units						
450 μm (n = 16)	3	12	15	15	15	14
900 μm (n = 19)	2	11	14	14	17	17
1,350 μm (n = 12)	—	2	5	8	7	7
1,800 μm (n = 11)	—	—	1	2	2	2
2,250 μm (n = 6)	—	—	—	—	—	—
2,700 μm (n = 8)	—	—	—	—	—	—
Strength (spikes)						
450 μm	0.15 ± 0.05	0.52 ± 0.50	0.56 ± 0.45	0.63 ± 0.45	0.63 ± 0.58	0.65 ± 0.66
900 μm	0.11 ± 0.05	0.35 ± 0.53	0.49 ± 0.49	0.53 ± 0.53	0.53 ± 0.60	0.52 ± 0.65
1,350 μm	—	0.12 ± 0.00	0.28 ± 0.17	0.21 ± 0.22	0.23 ± 0.19	0.32 ± 0.19
1,800 μm	—	—	0.64	0.60 ± 0.08	0.72 ± 0.12	0.68 ± 0.03
2,250 μm	—	—	—	—	—	—
2,700 μm	—	—	—	—	—	—
Latency (ms)						
450 μm	2.10 ± 0.14	2.16 ± 0.27	2.36 ± 0.61	2.30 ± 0.32	2.41 ± 0.31	2.72 ± 0.60
900 μm	2.05 ± 0.05	2.18 ± 0.30	2.26 ± 0.35	2.67 ± 1.02	2.93 ± 1.11	3.18 ± 1.01
1,350 μm	—	2.55 ± 0.25	2.56 ± 0.22	3.03 ± 0.60	2.64 ± 0.26	2.87 ± 0.29
1,800 μm	—	—	6.2	6.05 ± 0.15	5.65 ± 0.25	5.75 ± 0.15
2,250 μm	—	—	—	—	—	—
2,700 μm	—	—	—	—	—	—
Duration (ms)						
450 μm[1]	1.30 ± 0.41	1.44 ± 0.59	1.57 ± 0.70	1.60 ± 0.61	1.51 ± 0.45	1.81 ± 0.91
900 μm[2]	1.50 ± 0.30	1.39 ± 0.48	1.72 ± 0.69	1.71 ± 0.52	1.96 ± 0.57	1.64 ± 0.36
1,350 μm[3]	—	2.20 ± 0.60	1.98 ± 0.59	1.63 ± 0.47	1.76 ± 0.43	2.54 ± 1.08
1,800 μm[4]	—	—	2.80	2.35 ± 0.05	2.60 ± 0.30	2.30 ± 0.10
2,250 μm	—	—	—	—	—	—
2,700 μm	—	—	—	—	—	—

Values are means ± SD. All statistical analysis using MANOVA was done on the section of the matrix indicated by the broken frame (satisfying the complete design requirement). Compare to Fig. 3.

variables tested. They showed a strong response at a long latency of over 5 ms. Because the factors for the 2 cells fell outside the testable range they did not enter the statistical analysis. A significant dependency was determined for all 3 variables on the distance to the stimulation site (response strength: $P = 0.003$; latency: $P = 0.018$; duration: $P = 0.01$). There was a certain trend in the data also for the second factor, the intensity of stimulation. The strength of the response tended to be larger with higher stimulation intensity. This was most obvious for the 5 cells close to the stimulation site (450 and 900 μm) that responded to the weakest stimulation intensity of 0.8 nC. They barely reached the criterion for a response and displayed weak strengths of around 0.1 excess spikes per trial. The duration of the response tended to grow longer with increasing stimulus intensity, indicating that with stronger stimulation some cells fired doublets of spikes. The latency showed a slight tendency to increase by around 0.2 ms from low to high stimulation intensity. None of these trends, however, reached significance ($P > 0.05$).

To test for antidromic activation, stimulation pulses triggered by a spontaneous action potential of a responding cell were applied ("collision experiment"). The underlying (sometimes tacit) assumption for the classic version of this test (Lipski 1981) was that there is a clear dichotomy between antidromic and orthodromic conductance (i.e., the origin of the evoked spike was expected to be *either* antidromic *or* orthodromic conductance, but never both at the same time). The classic interpretation of spike-triggered stimulation is then simple: the evoked response is entirely blocked in case of antidromic invasion but it is left untouched if the conveyance is orthodromic. In the present experimental situation, however, such a dichotomy did not exist because stimulation as well as recording sites were located nearby in the cortical gray matter with rich interconnections between them running both ways. We thus resorted to a quantitative version of the collision test to detect a possible contribution of antidromic invasion. Triggering the stimulation by a spontaneously occurring action potential created a situation of possible "collision" of the spontaneous spike and an antidromically conveyed one if the delay between spike and stimulation was below the response latency. A "no collision" situation was created by increasing the spike-stimulation delay to values exceeding the response latency plus a presumed axonal refractory period (typical value used here was 10 ms; Fig. 4*B*). We corrected for firing rate modulations arising from temporal patterning of spikes (i.e., features of the autocorrelogram introduced by the spike-triggered nature of the recording) using a control recording obtained under spike-triggered conditions but without stimulation. These controls were subtracted from the test histograms after aligning the histograms to the spike times that served as trigger (Fig. 4*A*). Figure 4*B* shows a typical example of the data obtained. The latency as well as the strength of response were not substantially changed. Reduced response strength was observed in 10 out of 16 single units tested (maximum reduction 0.11 excess spikes), whereas it was slightly increased in 6 of them (maximum increment 0.10 excess spikes). Statistically, the response strengths and latencies obtained from our sample were indistinguishable between the two experimental conditions ("collision": response strength 0.60 ± 0.27 excess spikes; latency 2.89 ± 0.63; "no collision": response strength 0.62 ±

TABLE 2. *Properties of the inhibitory response with respect to stimulation intensity and distance from stimulation electrode*

	Inhibition					
	0.8 nC	1.6 nC	2.4 nC	3.2 nC	4.0 nC	4.8 nC
Number of units						
450 μm (n = 26)	6	22	21	20	22	22
900 μm (n = 25)	5	10	12	13	12	13
1,350 μm (n = 26)	—	7	9	11	11	11
1,800 μm (n = 17)	—	2	5	4	5	3
2,250 μm (n = 16)	1	1	1	2	4	3
2,700 μm (n = 16)	—	2	2	1	1	2
Strength						
450 μm	0.66 ± 0.22	0.64 ± 0.15	0.72 ± 0.15	0.79 ± 0.11	0.78 ± 0.13	0.85 ± 0.09
900 μm	0.71 ± 0.27	0.60 ± 0.18	0.63 ± 0.22	0.74 ± 0.16	0.75 ± 0.20	0.72 ± 0.18
1,350 μm	0.59	0.52 ± 0.08	0.57 ± 0.20	0.56 ± 0.19	0.58 ± 0.20	0.65 ± 0.19
1,800 μm	—	0.35 ± 0.03	0.49 ± 0.10	0.44 ± 0.14	0.41 ± 0.09	0.43 ± 0.09
2,250 μm	0.63	1.00	0.28	0.35 ± 0.07	0.53 ± 0.22	0.66 ± 0.15
2,700 μm	—	0.37 ± 0.02	0.48 ± 0.16	0.47	0.77	0.34 ± 0.02
Duration (ms)						
450 μm	76 ± 22	107 ± 33	102 ± 39	127 ± 26	122 ± 37	133 ± 32
900 μm	57 ± 13	109 ± 33	129 ± 33	117 ± 49	133 ± 49	150 ± 82
1,350 μm	123	128 ± 60	125 ± 47	138 ± 51	117 ± 62	96 ± 55
1,800 μm	—	102 ± 0.5	110 ± 10	111 ± 60	124 ± 30	148 ± 22
2,250 μm	85	21	130	167 ± 30	155 ± 19	161 ± 37
2,700 μm	—	81 ± 8	121 ± 4	120	86	152 ± 18

Values are means ± SD. All statistical analysis using MANOVA was done on the section of the matrix indicated by the broken frame (satisfying the complete design requirement). Compare to Fig. 6.

0.27 excess spikes, latency 2.87 ± 0.84, n = 16, t-test for paired samples, $P > 0.05$ for both parameters; Fig. 4*C*). These results do not point to a major role of antidromic invasion for the generation of the short latency excitatory response.

Inhibitory response

The short latency excitatory response was typically followed by a widespread and long-lasting depression of firing rates. A representative multielectrode recording is shown in Fig. 5. PSTHs for multiunit spike trains recorded at all distances and for all stimulation intensities are depicted. The threshold to evoke the inhibitory response in this example was 1.6 nC and the response was detected up to a distance of 1,800 μm from the stimulation electrode. The stimulus intensity required to evoke the inhibitory response was higher for greater distances from the stimulation electrode (marked with hollow arrows in Fig. 5). A remarkable finding was that the duration of the inhibitory response was almost constant for the whole range of stimulus intensities applied. Whenever an inhibitory response was evoked, it had a fixed duration that could not be changed by higher stimulus intensities and was the same at different locations with respect to the stimulus electrode. After the end of the inhibition a rebound excitation was visible at thresholds higher than that evoking inhibition alone (marked with filled arrows in Fig. 5).

The characteristics demonstrated by the example in Fig. 5 match those observed in the population of recorded spike trains (Fig. 6). The overall distribution of units showing an inhibitory response was similar to that seen with fast excitation. At the lowest charge transfer applied (0.8 nC) 23% of the units closest to the stimulation electrode (450 μm) showed a long-lasting inhibitory response. The probability to detect it increased with increasing stimulus intensity to a maximum of 85% and decayed to very low values at 1,800 μm from the stimulation size but was observed in 2 cases even at the greatest distance (2.7 mm).

Table 2 shows the response variables of the units that were classified as generating an inhibitory response. The duration was fixed, irrespective of location and stimulation intensities, as seen in the example of Fig. 5. The part of the data matrix that contained at least $n > 1$ spike trains to satisfy the complete design criterion of MANOVA (distance from 450 to 1,800 μm; charge transfer from 1.6 to 4.8 nC; see Table 2) confirmed this impression: no statistical significance was obtained ($P > 0.05$). The strength of the inhibitory response, on the other hand, was significantly dependent on intensity of stimulation as well as distance from the recording site. It was highest (0.85) in units recorded at 450 μm distance and stimulated with the highest charge transfer. The strength fell to around 0.3 in the responding cells farther away than 1,800 μm. The dependency of the response strength on both factors was statistically significant in the range of factors tested (MANOVA, stimulation intensity: $P < 0.04$, distance: $P < 10^{-6}$; see Table 2).

Rebound response

The rebound response was not a common observation at the stimulus intensities used in this study. The rebound response after the inhibition could be avoided (except in one case) by keeping the stimulation intensity below 2.4 nC (Table 3). The highest percentage of cells generating a rebound response (between 15 and 19%) was observed at a stimulation intensity of 4.8 nC and distances ≤1,350 μm. The rebound response showed variable shapes from unit to unit. For instance, the duration was on average 262 ms and ranged in individual cases from 86 to 520 ms. There was a slight tendency to obtain stronger and longer rebound responses at sites close to the stimulation electrode. The effect, however, did not reach significance within the part of the matrix (distance from 450 to

TABLE 3. *Properties of the rebound response with respect to stimulation intensity and distance from stimulation electrode*

	Rebound					
	0.8 nC	1.6 nC	2.4 nC	3.2 nC	4.0 nC	4.8 nC
Number of units						
450 μm (n = 26)	—	1	3	3	4	4
900 μm (n = 25)	—	1	3	4	4	4
1,350 μm (n = 26)	—	—	2	3	4	5
1,800 μm (n = 17)	—	—	2	2	2	2
2,250 μm (n = 16)	—	—	—	—	1	1
2,700 μm (n = 16)	—	—	—	—	1	3
Strength (spikes)						
450 μm	—	0.58	0.43 ± 0.19	0.50 ± 0.17	0.46 ± 0.19	0.45 ± 0.19
900 μm	—	0.43	0.3 ± 0.15	0.39 ± 0.20	0.51 ± 0.17	0.52 ± 0.14
1,350 μm	—	—	0.42 ± 0.04	0.43 ± 0.14	0.37 ± 0.18	0.43 ± 0.14
1,800 μm	—	—	0.28 ± 0.09	0.37 ± 0.02	0.39 ± 0.05	0.38 ± 0.05
2,250 μm	—	—	—	—	0.22	0.44
2,700 μm	—	—	—	—	0.34	0.31 ± 0.09
Duration (ms)						
450 μm	—	296	183 ± 80	295 ± 83	300 ± 96	294 ± 149
900 μm	—	414	289 ± 166	200 ± 116	307 ± 191	308 ± 194
1,350 μm	—	—	255 ± 161	129 ± 16	334 ± 135	292 ± 175
1,800 μm	—	—	234 ± 25	168 ± 59	192 ± 77	127 ± 34
2,250 μm	—	—	—	—	138	126
2,700 μm	—	—	—	—	139	164 ± 28

Values are means ± SD. All statistical analysis using MANOVA was done on the section of the matrix indicated by the broken frame (satisfying the complete design requirement).

1,800 μm; charge transfer from 2.4 to 4.8 nC) that allowed statistical testing using MANOVA ($P > 0.05$; see Table 3).

Temporal interaction of inhibitory response

The duration of the inhibitory response of more than 100 ms must have a critical impact on the local effect of repetitive neocortical stimulation at rates higher than about 10 Hz. This was demonstrated by the complex interaction patterns of the inhibitory response observed at a stimulation frequency of 10 Hz (Fig. 2*D*). To test the temporal interaction more quantitatively, we employed double pulses given by the stimulation electrode at an interval of 75 ms such that the second pulse would fall halfway into the ongoing inhibitory response evoked by the first pulse. The *test* pulse (the single pulse in control trials or 2nd pulse in the double-pulse trials) was varied across the whole range of intensities (0.8 to 4.8 nC; Fig. 7*A*). The *conditioning* (1st) pulse was chosen to be either subthreshold (i.e., not evoking an overt inhibitory response; Fig. 7*B*) or just suprathreshold (Fig. 7*C*). The single pulse and these 2 double-pulse conditions were applied in pseudo-random order. The effect of the conditioning pulse on the inhibition evoked by the test pulse was then compared with the effect of the single pulse alone. Figure 7 demonstrates PSTHs of a typical experiment (electrode distance 450 μm). The inhibition evoked by a test pulse after a subthreshold conditioning pulse (Fig. 7*B*) was undistinguishable from the one evoked by a single pulse alone (Fig. 7*A*; for purposes of comparison, the arrow depicts the duration of the inhibition evoked by a single pulse of 1.6 nC charge transfer and has the same length throughout the plot). In the second condition when the conditioning pulse evoked an inhibitory response itself, the test pulse elongated the ongoing inhibition by maximally 25 ms at the highest stimulus intensities of 4.0 and 4.8 nC (Fig. 7*C*). This elongation, however, was clearly less than would have been expected from a linear superposition (75 ms).

The results of the example shown in Fig. 7 are reflected in the population data. Figure 8*A* plots the duration of inhibition evoked by a single pulse and by the test pulse in the case of a subthreshold conditioning pulse. Measurements from spike trains recorded at different distances were pooled. For all stimulus intensities, the null hypothesis that the duration of the inhibition evoked by the test pulse was not different from the one evoked by the single pulse had to be accepted (Fig. 8*A*, *t*-test for paired samples, $P > 0.05$ for all stimulation intensities, 0.8 nC: $n = 4$; 1.6 nC: $n = 19$; 2.4 nC: $n = 25$; 3.2 nC: $n = 25$; 4.0 nC: $n = 28$; 4.8 nC: $n = 28$). The second graph (Fig. 8*B*) depicts the results from experiments in which the conditioning pulse was suprathreshold. It compares the duration of the inhibition as expected if the test pulse evoked an inhibition of normal length (duration of inhibition after a single pulse plus the interpulse interval) with the actual duration of the inhibition measured in the double-pulse experiments. For stimulus intensities higher than 1.6 nC, the observed inhibition was significantly shorter than expected by linear superposition (Fig. 8*B*, *t*-test for paired samples, $P < 0.05$ for stimulation intensities marked by an asterisk; 0.8 nC: $n = 19$; 1.6 nC: $n = 19$; 2.4 nC: $n = 20$; 3.2 nC: $n = 25$; 4.0 nC: $n = 21$; 4.8 nC: $n = 21$).

The double-pulse experiments described so far indicated that inhibitory responses evoked by electrical stimulation interact in a highly nonlinear way. Subthreshold conditioning pulses do not influence the characteristics of an inhibitory response, whereas, conversely, overt inhibitory responses can be modified by a second pulse only to a small degree. To investigate the temporal properties of this interaction pattern, we systematically varied the pulse interval with which a second pulse was applied after a suprathreshold conditioning pulse. The recording shown in Fig. 9 featured an inhibitory response after a single pulse lasting for somewhat longer than 100 ms (electrode distance 450 μm). The control trials (single pulse) and

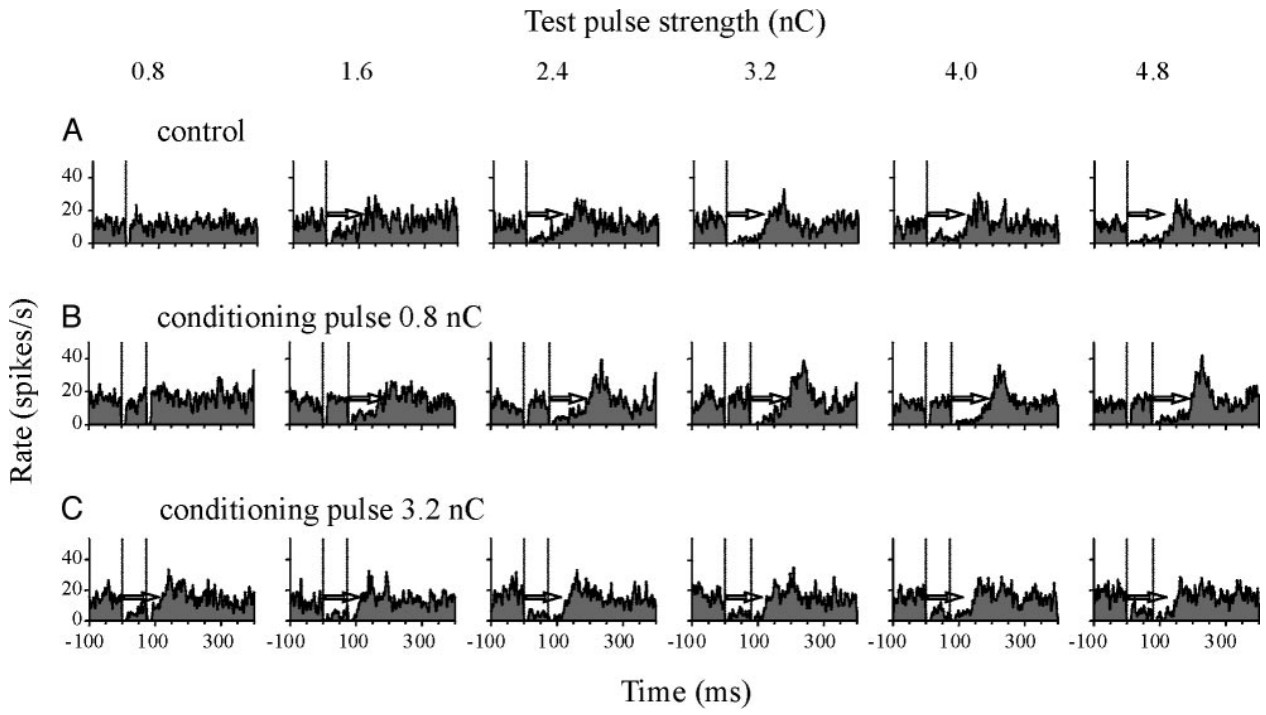

FIG. 7. Double-pulse stimulation. PSTHs computed from multiunit spike train recorded at distance of 450 μm from stimulation electrode. An interval of 10 ms after stimulus was blanked to exclude stimulus artifact. *A*: single pulse. PSTHs computed from trials applying different stimulus intensity show inhibitory response starting at 1.6 nC. *B*: double-pulse: conditioning with subthreshold stimulation. Conditioning pulse applied first was at 0.8 nC intensity. As seen in *A* (*leftmost PSTH*) it did not evoke an inhibitory response by itself. Test pulse followed at interval of 75 ms and was varied in strength like single pulse in *A*. Duration and strength of inhibition evoked by test pulse were comparable to those observed after single pulses in *A*. *C*: double pulse: conditioning with suprathreshold stimulation. Conditioning pulse transferred a charge of 3.2 nC and evoked a clear response by itself (see *PSTH 3rd from right* in *A*). Test pulses of different intensities elongated inhibitory response by about 25 ms, which is less than 75 ms expected from simple concatenation of effects. For purposes of comparison empty arrows are of same length in all plots.

double-pulse trials at intervals of 25, 50, 100, and 200 ms were presented in pseudo-random order. The general finding was that the second pulse, if it fell within the period of inhibition, elongated the inhibition by about 25 ms as seen before. This was true even for the trials in which the second pulse was given at a point in time just before the cessation of the inhibition (interval 100 ms). Pulses that occurred after the end of the inhibitory response (interpulse interval of 200 ms) evoked an inhibitory response of their own by interrupting the rebound excitation. The average effect on the duration of inhibition computed from all recording sites is shown in Fig. 10. Statistically, the duration of the compound inhibition of double pulses at all intervals smaller than 200 ms was indistinguishable (one-way ANOVA, $P > 0.05$, $n = 76$; unit recordings from all distances were pooled). At an interval of 200 ms the measured duration corresponded to the one observed after single pulses, given that the second pulse evoked a separate response of its own. We conclude from these experiments that the highly nonlinear mode of interaction is active throughout the entire duration of the inhibitory response.

One possibility to explain the inability of the second pulse to prolong the inhibitory response is the failure to activate fibers at the stimulation site after the second pulse. This possibility, however, was rendered unlikely by the finding that the excitatory response to the second pulse (or a train of pulses; see Fig. 2*D*) was largely intact. Figure 11*A* shows an example of a unit stimulated with a double pulse at different intervals (distance from stimulation site 900 μm). The stimulation intensity for both pulses (conditioning: gray histogram; test: black histograms) was identical and suprathreshold to evoke an inhibition (4.0 nC). Test pulses applied at interpulse intervals of 25, 50, and 100 ms fell within the inhibitory period and consistently evoked a short latency excitatory response at even a higher amplitude than that generated by the conditioning pulse. This tendency was observed also in the population average, although it did not reach statistical significance (Fig. 11*B*; one-way ANOVA, $P > 0.05$, $n = 8$; neurons recorded at different distances from the stimulation electrode were pooled for statistical analysis). The response after a test pulse at 200 ms occurred after the end of the inhibitory response and was more nearly comparable with the first response.

DISCUSSION

General considerations

The present study provides an estimate of the maximal resolution of signals that can be transferred to the neocortex by microstimulation. To this end the spatiotemporal blur of activity evoked at the stimulation site was measured. Although we consider the neocortex in many species and cortical areas to be built up according to a prototypic cortical architecture (for review, see Braitenberg and Schüz 1991), it has to be borne in mind that there are certain variations between different cortical areas in architecture and, particularly, in the layout of horizontal connections (Lund et al. 1993). Furthermore, at some sites

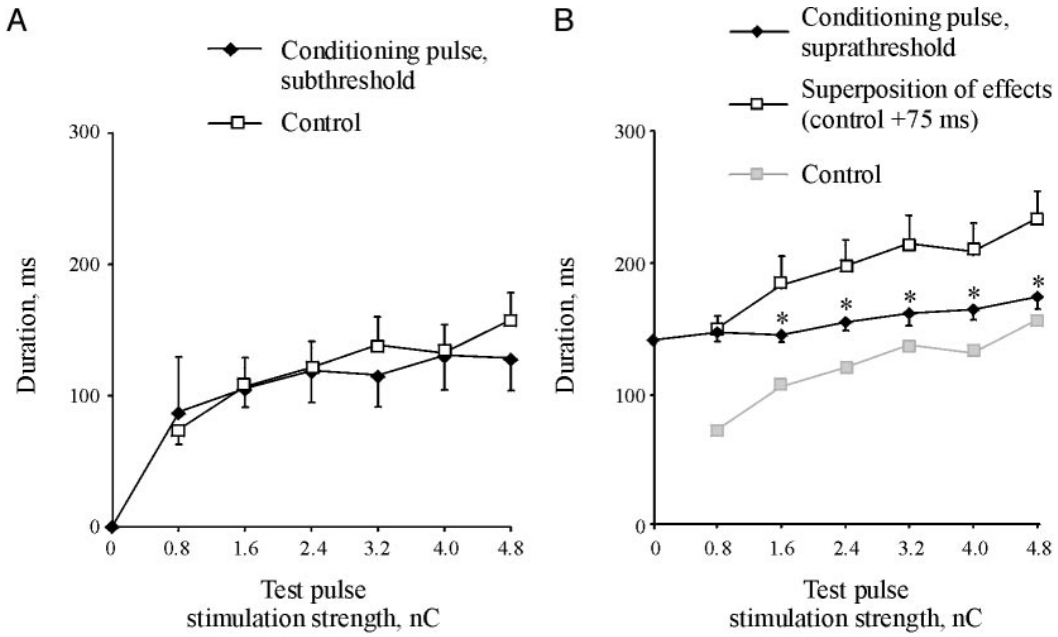

FIG. 8. Population data of double-pulse experiments. Duration of inhibitory response is plotted against intensity of test pulse. All spike trains featuring an inhibitory response were used for this analysis. Single and multiunits recorded at different distances to stimulation electrode were pooled. *A*: double pulse: conditioning at subthreshold stimulus intensity (compare Fig. 7*B*). Duration of inhibitory response evoked by test pulse (black diamonds) is not significantly different from that observed after single pulses (squares) of same intensity (*t*-test for dependent samples, $P > 0.05$ for all stimulus intensities). *B*: double pulse: conditioning at suprathreshold stimulus intensity (compare Fig. 7*C*). Inhibition (as measured from occurrence of conditioning pulse) shows small elongation at higher intensity of test pulse (black diamonds). Observed duration is significantly shorter than that expected from linear superposition of inhibitory responses (open squares, *t*-test for dependent samples, $P < 0.05$ when marked with asterisks). Mean duration observed after single pulses is plotted as well (gray).

on the cortical surface, within or between neighboring areas, distinct spatial discontinuities of horizontal connections exist (e.g., Manger et al. 1997). Such variability might affect the detailed profile of activity evoked by electrical stimulation and deserves attention in each case in which microstimulation is used. Nevertheless, in view of the prototypic architecture of neocortex we feel confident that the present results obtained in rat somatosensory cortex provide a correct description in general terms also for other cortical areas and/or species.

How much did the effects of ketamine anesthesia contribute to the patterns of evoked activity observed in the present study? Ketamine takes effect by selective blockade of NMDA receptors leaving fast transmission by AMPA and, notably, GABA receptors intact (Ebert et al. 1997; Sonner et al. 2003). In contrast to other anesthetics, the responsiveness of the neocortex is not reduced—spontaneous firing rate and sensory evoked cortical activity are actually enhanced (Kayama et al. 1972). The main statements of the present study are based on a sequence of fast excitation and inhibition evoked by electrical stimulation. As we discuss later in detail, both responses are presumably based on direct electrical activation of fibers around the stimulation electrode followed by antidromic and orthodromic monosynaptic conveyance. Because of this relatively direct link of these responses to the activating current we believe that their susceptibility to pharmacological effects of ketamine should be relatively small. Support for this notion comes, first, from the finding of very similar sequences of excitation and inhibition after peripheral sensory stimulation in the absence of general anesthesia (Simons 1978; Simons and Carvell 1989) as well as after electrical stimulation in vitro (Hirsch and Gilbert 1991). Second, we confirmed the existence of a comparable pattern of cortical excitation and long inhibi-

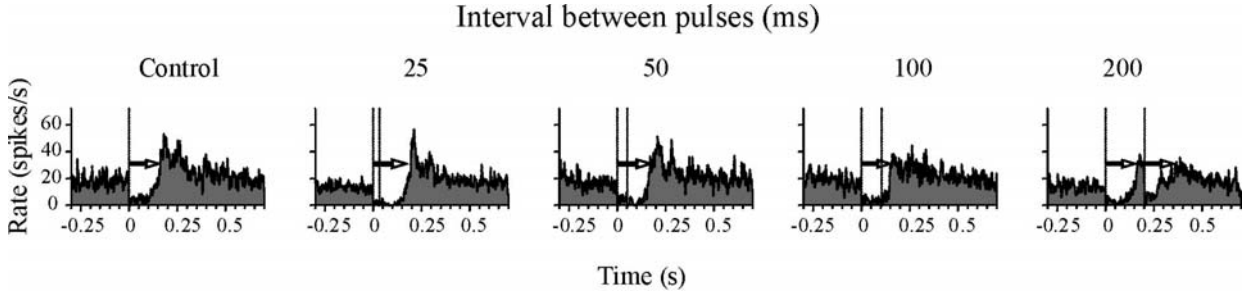

FIG. 9. Double-pulse stimulation: variation of interstimulus interval. Example was recorded at distance of 450 mm from stimulation electrode (stimulation intensity for both pulses: 4.0 nC). Up to an interval of 100 ms test pulse induced only a small change of about 25 ms in duration of inhibitory response. Note that fast excitation was blanked. For purposes of comparison empty arrows are of same length throughout figure.

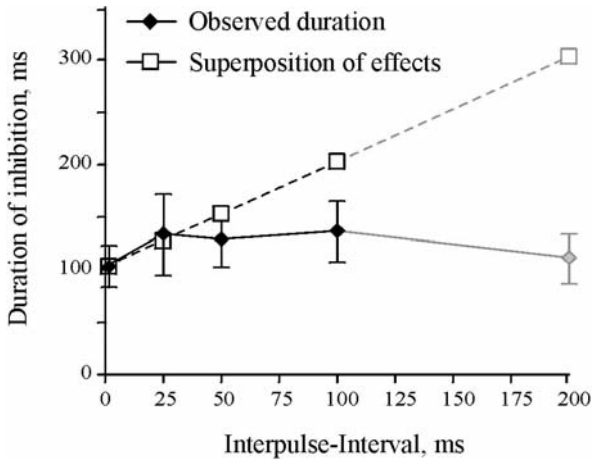

FIG. 10. Population data of double-pulse experiments varying interpulse interval. Mean duration of compound inhibitory response (black diamonds) using double-pulse stimulation is elongated by about 25 ms compared with that observed after single pulses (plotted at 0 ms). Expected values for linear superposition (response to single pulse plus interpulse interval) are plotted as empty squares. At 200-ms intervals duration corresponds to that observed with single pulses because second pulse occurred after end of inhibitory response (depicted in gray; compare Fig. 9).

tion after cortical microstimulation in preliminary experiments in awake animals (Butovas and Schwarz, unpublished results).

Origin of electrically evoked neuronal responses: the spatiotemporal blur

A decisive difference of electrically evoked to naturally occurring activation originates from the known bias of electrical stimulation to activate preferentially fibers of passage rather than somata (Gustafsson and Jankowska 1976; McIntyre and Grill 2000; Nowak and Bullier 1998a,b; Ranck 1975; Rattay 1999). A multitude of fibers pass by the stimulation site, many of which are not directly linked to the site of stimulation because their origin as well as their target reside at randomly distributed locations around the stimulated site. Once this—in functional terms—arbitrarily composed bundle of fibers gets excited, the activity carried along the horizontal axes must be expected to be composed of a complex mixture of antidromic and orthodromic conveyance of action potentials on excitatory and inhibitory fibers that we tag the "spatiotemporal blur." The present data reflect these expectations because the pattern of evoked activation indicated the contribution of both, excitation and inhibition. Direct antidromic evasion, however, did not play a major role in the generation of the excitatory responses, although it was reported using intracellular recordings (Contreras et al. 1997). It has to be emphasized that the collision experiment employed by us tests the contribution only of direct antidromic conveyance (i.e., on the axon of the cell under observation). Therefore the possibility remains that antidromic conveyance on axons of other, unobserved, neurons (which in turn are synaptically connected to the cell under observation) plays a role.

The notion that the spatiotemporal blur is based on activity in a conglomerate of fibers of different types rather than orderly conveyance on a homogeneous fiber tract may help to explain two unexpected findings of the present study. First, the horizontal progression of the fast excitatory response was about 5 times faster (about 2.6 m/s) than conduction velocities of horizontal axons measured in intracellular recordings (about 0.5 m/s; Nowak and Bullier 1998a). This feature is obviously incompatible with the idea that just one functionally defined type of fibers gets activated by the stimulation. To explain it, complex interactions of the functionally different parts of the activated conglomerate of fibers have to be assumed. It is noteworthy in this respect that at distances greater than 1,350 μm, excitatory responses did not match the characteristics of those typically found closer to the stimulation site. Such remote responses were rare, unusually strong, and showed latencies of more than 5 ms corresponding better to the range of conduction velocities found for individual horizontal fibers (Nowak and Bullier 1998b). It is entirely possible that these responses originated from individual fibers/somata or homogeneous fiber tracts activated at the stimulation site. The second unexpected result was that the extent of horizontal spatiotemporal blur was similar at all cortical depths tested and that it did not reflect the patchiness of horizontal connections as known from morphological studies (Kim and Ebner 1999). This finding may be easily explained by the notion that it is mainly fibers of passage (and not fibers that originate or terminate at the stimulation site) that contribute to the observed effects. The spatial specificity in the vertical (i.e., with respect to cortical layers) as well as the horizontal direction (i.e., with respect to other cortical columns), which undoubtedly exist in single neuron to neuron connections, must be expected to get skewed in the compound effect originating from the activation of fibers of passage.

The present results show that the extent of electrically evoked activity (even at intensities close to threshold) was large and seemed to surpass the known physiological spread of activity (e.g., assessed by the size of receptive fields and somatotopic maps) (Ghazanfar and Nicolelis 1999; Simons 1978). However, nonclassical properties of receptive fields in primary sensory areas have been shown to originate from an area several millimeters wide on the cortical surface (Bolz et al. 1989; Moore et al. 1999). Furthermore, a study using voltage-sensitive dye imaging in rat's somatosensory cortex has shown that sensory activity initially emerges at one cortical column but then is able to progress over large parts of the somatosensory cortex depending on the strength of input (Petersen et al. 2003). In summary then, the minimal extent of "physiological" types of activation may be in a similar range as observed here for electrically evoked activation. Additional evidence in favor of this notion comes from the fact that the overall horizontal spread observed in the present study is in general accordance with the extent of known presumptive anatomical substrates in rat's somatosensory cortex: intrinsic horizontal fibers ($\leq$2 mm: Gottlieb and Keller 1997; 2 to 3 barrels' distance: Kim and Ebner 1999) or horizontal branching of afferent thalamocortical fibers (1.3 mm: Arnold et al. 1997).

Neuronal bases for long-lasting inhibition.

The long-lasting inhibition may be attributed either to an activation of inhibitory synapses or to a decrement of the gain of excitatory synapses (or intrinsic membrane excitability) after the first volley of excitation. The contribution of synaptic inhibition is strongly supported by reports demonstrating horizontal spread of inhibitory fibers (Kisvarday 1992), polysyn-

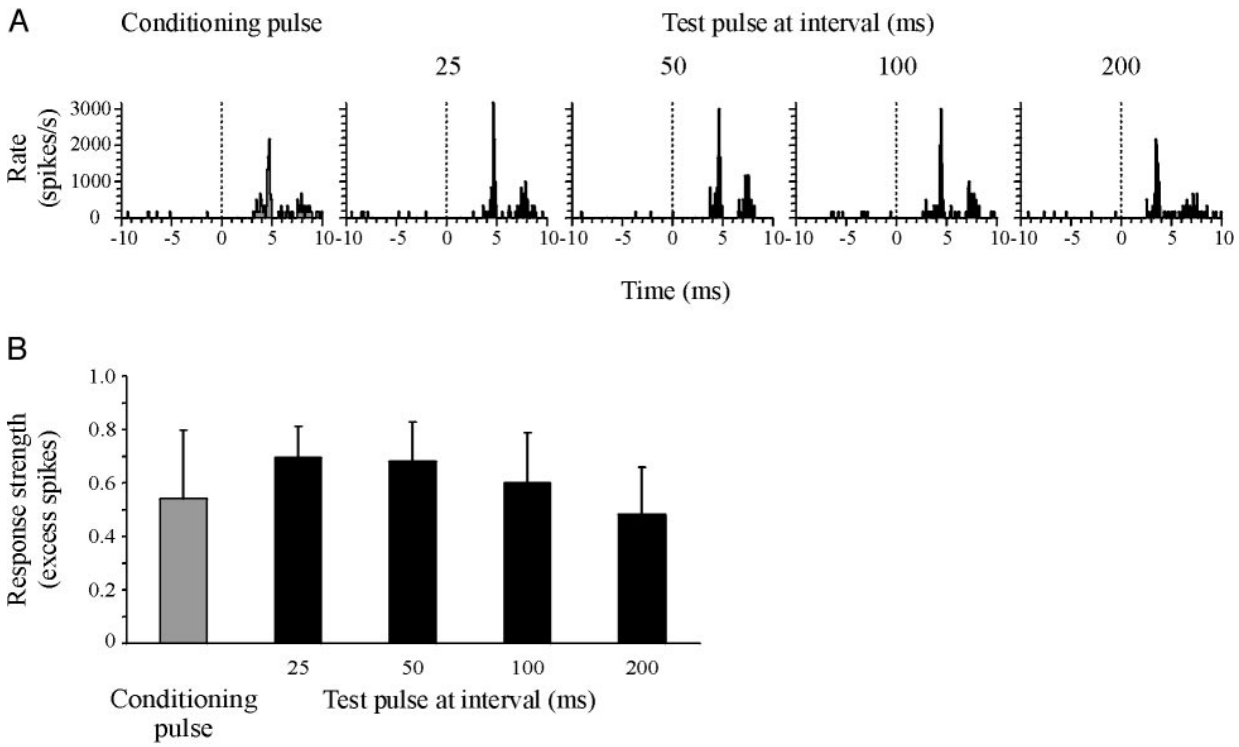

FIG. 11. Excitatory response evoked by double-pulse stimulation. *A*: PSTHs of one single unit spike train recorded at distance of 900 μm from stimulation electrode. PSTHs for conditioning (1st) pulse and test (2nd) pulses at intervals of 25, 50, 100, and 200 ms are shown. Conditioning and test pulse had same suprathreshold intensity (4.0 nC). Test pulse evoked an excitatory response of a somewhat higher amplitude at intervals of 25, 50, and 100 ms (intervals that placed test pulse within ongoing inhibitory response; compare Fig. 9). *B*: population data. Strength of excitation evoked by conditioning and test pulse (identical intensity suprathreshold for inhibition) is plotted for 4 interpulse intervals ($n = 8$). There was a tendency of responses evoked by test pulses at intervals 25, 50, and 100 ms to be stronger than that obtained with conditioning pulse. This tendency, however, did not reach significance (one-way ANOVA, $P > 0.05$).

aptic connection of long intrinsic excitatory fibers to inhibitory cells (McGuire et al. 1991), recruitment of inhibition by thalamocortical loops (Gil and Amitai 1996; Keller and White 1987; Swadlow 1995), and electrical coupling between inhibitory interneurons (Galaretta and Hestrin 1999; Gibson et al. 1999). A postsynaptic sequence of fast excitation and long-lasting inhibitory response of neocortex has been demonstrated by numerous intracellular recordings in vivo and in vitro from different mammals after electrical stimulation of afferents (in vivo: Berman et al. 1991; Li et al. 1956; in vitro: Chagnac-Amitai and Connors 1989; Connors et al. 1982, 1988; Porter et al. 2001; Shao and Burkhalter 1996, 1999), epicortical stimulation (Creutzfeld et al. 1966), intracortical microstimulation (in vivo: Asanuma and Rosen 1973; Chung and Ferster 1998; Contreras et al. 1997; in vitro: Hirsch and Gilbert 1991; Murakoshi et al. 1993; Salin and Prince 1996; Shao and Burkhalter 1996, 1999), and focal liberation of glutamate (Dalva et al. 1997; Schubert et al. 2001). Similar patterns have been observed also after short peripheral sensory stimulation (rat barrel cortex: Carvell and Simons 1988; Moore and Nelson 1998; Zhu and Connors 1999; cat visual cortex: Hirsch et al. 1998).

The alternative process—a reduction of excitation in the network—could in principle be carried by 2 different mechanisms. First, intrinsic membrane currents could be triggered by the first wave of excitation and lead to a long-lasting depression of firing rate. Prominent candidates for such a mechanism are long-lasting afterhyperpolarizations (AHPs) in pyramidal neurons based on calcium- or sodium-dependent potassium currents (Schwindt and Crill 1989; Schwindt et al. 1988). Second, a decrement of network excitability could be based on short-term depression of excitatory intracortical synapses (Abbott et al. 1997; Thomson et al. 1993; Tsodyks and Markram 1997). Both mechanisms, AHPs and lowered synaptic efficacy, would reduce excitatory drive from cortical neurons by suppressing firing rates in the population of postsynaptic neurons. The decisive argument against a significant contribution of these possible mechanisms comes from our double-pulse experiments: We show that the long inhibitory response cannot be elongated, although the arrival of fast excitation at the postsynaptic neuron was undisturbed. If the inhibition were based on slow AHPs, the second pulse should have elongated an ongoing AHP because postsynaptic spikes with concomitant additional influx of calcium/sodium were readily elicited. Supporting this argument, slow AHPs have been shown to be strengthened and elongated by repetitive spiking (Schwindt and Crill 1989; Schwindt et al. 1988). Synaptic depression should be strengthened by a successful second activation of the excitatory synapses as well. In conclusion, both mechanisms, AHPs and synaptic depression, most likely would elongate the inhibitory response to a greater extent and in a more graded way than observed in our experiments.

Our finding that the duration of inhibition is virtually fixed at the low stimulation intensities studied here (see, however, effects of high-intensity stimulation in Krnjevic et al. 1966) is

reminiscent of characteristics of $GABA_B$ receptor-mediated responses that have been found to underlie slow inhibitory postsynaptic potentials in the neocortex (Connors et al. 1988; Hirsch and Gilbert 1991; Shao and Burkhalter 1999; van Brederode and Spain 1995). Repetitive stimulation of individual GABAergic neocortical cells acting by postsynaptic $GABA_B$ receptors has revealed a highly sublinear relationship between the number and frequency of presynaptic action potentials on one side and the duration of the $GABA_B$ response on the other (Thomson and Destexhe 1999), akin to the relative inability of a second electrical pulse to elongate the inhibitory response observed by us.

Consequences for electrical stimulation of neocortex

At first glance the temporal properties of the evoked activity seem not be favorable for reliable signal transfer. The inhibitory response is very slow and leads to a complex interaction pattern at around 10 Hz determined by the nonlinear superposition, whereas it fuses at higher frequencies to form an almost uniform inhibitory background (Fig. 2*D*; see also Chung and Ferster 1998; Kara et al. 2002). The interaction pattern at frequencies around 10 Hz most likely does not correspond to any type of naturally occurring activity and its effect on the ability of the brain to use these frequencies deserves close attention in future behavioral experiments. Nonetheless, electrical stimulation seems to be able to transmit temporal information faithfully to the cortical substrate by the reliable fast excitatory response. At frequencies >10 Hz the continuous inhibition may even help to make the excitatory responses stand out at a favorable signal-to-noise ratio. The fact that awake behaving monkeys, indeed, were able to extract the rate of electrical stimulation >10 Hz and use it for a frequency discrimination task (Romo et al. 1998, 2000) supports this statement.

The spatial aspects of evoked activity have to be compared with the width of cortical columns that are believed to represent functional units of cortical processing. In sensory cortices, one set of columns typically separates cells in layer 4 with nonoverlapping sets of receptive fields and shows diameters of 0.5 to 1.5 mm (somatosensory cortex: slowly/quickly adapting neurons: Dykes et al. 1980; Sur at al., 1984; barrels in whisker representation in rodents: Simons 1978; visual cortex: ocular dominance: Hubel and Wiesel 1977; auditory cortex: tonotopy/areas of different spectral integration: Schreiner et al. 2000). Our finding of significant amounts of evoked activity in a range of about 2.7 mm (1.35 mm to each side) around the stimulation site—even at stimulus intensities close to the threshold—suggests that evoked excitation followed by strong inhibition supersedes the ongoing activity in an area of cortex that consists of several sets of columns. This prediction applies even better for subordinate types of cortical parcellation (e.g., orientation in primary visual cortex) (Grinvald et al. 1986), clusters of directionally selective neurons in visual area MT (Albright et al. 1984), or septum columns in barrel cortex of rodents (Kim and Ebner 1999), all of which are maximally a few hundred micrometers wide.

Despite this insight, column-specific effects of microstimulation have been reported to exist on the behavioral level in monkey's primary somatosensory cortex (Romo et al. 2000) and visual area MT (Salzman et al. 1990; see for review Nichols and Newsome 2002). Monkeys were able to extract the frequency of repetitive microstimulation if the electrode was placed within a column of quickly adapting neurons in the somatosensory cortex, whereas the animal's performance was impaired once the electrode was moved to a neighboring column of slowly adapting neurons (Romo et al. 2000). In the experiments of Salzman et al. (1990) the perception of the direction of a moving stimulus could be biased by microstimulation toward the preferred direction of MT cells at the stimulation site.

Our present results strongly suggest that the spatial spread of local activity must have been much higher than assumed in the studies cited above and challenges the view that the specific modulation of behavior was a consequence of the limitation of evoked activity to one column (Murasugi et al. 1993; Nichols and Newsome 2002). To account for column-specific behavioral responses to microstimulation the restriction of evoked activity to one column is not imperative. It is sufficient to assume that the geometrical center of the responding area can be estimated by integrating the activity of a distributed population of cells. Algorithms that perform such readout of population codes have been proposed to exist in different systems (e.g., Deneve et al. 1999) and appear to be well suited to focus and specify the blurred activity on the next stage of cortical processing as a basis for column-specific behavioral effects. The present finding that the percentage of responding cells as well as strength of neuronal responses fall at a monotonic slope over distance from the stimulation site, together with topographic mapping of features on the cortical surface, might be helpful for this task.

In summary, the optimal spatial resolution of multisite stimulation (i.e., electrode tip distances)—at least in some neocortical areas—may eventually be much higher than indicated by the extent of the spatial blur measured here. However, our data implicate that dense microelectrode arrays with tip distances in the order of the width of cortical columns will surely face the problem of spatial interaction of evoked activity. Also, nonlinear temporal interaction of inhibitory responses at low stimulation frequencies have to be taken into account. Future experiments must address the question of how the profile and multisite spatiotemporal interaction of electrically evoked activity and their arrangement on a cortical columnar map affect behavioral responses.

We thank C. M. Pedroarena and H. Hentschke for discussion and useful comments on an earlier draft of the manuscript and we thank S. Kramer and G. Sessler for excellent technical assistance.

DISCLOSURES

This work was supported by the German Ministry for Education and Research (BMBF 311858).

REFERENCES

Abbott LF, Varela JA, Sen K, and Nelson SB. Synaptic depression and cortical gain control. *Science* 275: 220–224, 1997.

Abeles M. Quantification, smoothing, and confidence limits for single-units' histograms. *J Neurosci Methods* 5: 317–325, 1982.

Albright TD, Desimone R, and Gross CG. Columnar organization of directionally selective cells in visual area MT of the macaque. *J Neurophysiol* 51: 16–31, 1984.

Arnold PB, Li CX, and Waters RS. Thalamocortical arbors extend beyond single cortical barrels: an in vivo intracellular tracing study in rat. *Exp Brain Res* 136: 152–168, 2001.

Asanuma H, Arnold A, and Zarzecki P. Further study on the excitation of pyramidal tract cells by intracortical microstimulation. *Exp Brain Res* 26: 443–461, 1976.

Asanuma H and Rosen I. Spread of mono- and polysynaptic connections within cat's motor cortex. *Exp Brain Res* 16: 507–520, 1973.

Berman NJ, Douglas RJ, Martin KA, and Whitteridge D. Mechanisms of inhibition in cat visual cortex. *J Physiol* 440: 697–722, 1991.

Bolz J, Gilbert CD, and Wiesel TN. Pharmacological analysis of cortical circuitry. *Trends Neurosci* 12: 292–296, 1989.

Braitenberg V and Schüz A. *Anatomy of the Cortex.* New York: Springer-Verlag, 1991.

Carvell GE and Simons DJ. Membrane potential changes in rat SmI cortical neurons evoked by controlled stimulation of mystacial vibrissae. *Brain Res* 448: 186–191, 1988.

Chagnac-Amitai Y and Connors BW. Synchronized excitation and inhibition driven by intrinsically bursting neurons in neocortex. *J Neurophysiol* 62: 1149–1162, 1989.

Chung S and Ferster D. Strength and orientation tuning of the thalamic input to simple cells revealed by electrically evoked cortical suppression. *Neuron* 20: 1177–1189, 1998.

Connors BW, Gutnick MJ, and Prince DA. Electrophysiological properties of neocortical neurons in vitro. *J Neurophysiol* 48: 1302–1320, 1982.

Connors BW, Malenka RC, and Silva LR. Two inhibitory postsynaptic potentials, and $GABA_A$ and $GABA_B$ receptor-mediated responses in neocortex of rat and cat. *J Physiol* 406: 443–468, 1988.

Contreras D, Dürmüller N, and Steriade M. Absence of a prevalent laminar distribution of IPSPs in association cortical neurons of cat. *J Neurophysiol* 78: 2742–2753, 1997.

Creutzfeldt OD, Watanabe S, and Lux HD. Relations between EEG phenomena and potentials of single cortical cells. I. Evoked responses after thalamic and erpicortical stimulation. *Electroencephalogr Clin Neurophysiol* 20: 1–18, 1966.

Dalva MB, Weliky M, and Katz LC. Relationships between local synaptic connections and orientation domains in primary visual cortex. *Neuron* 19: 871–880, 1997.

Deneve S, Latham PE, and Pouget A. Reading population codes: a neural implementation of ideal observers. *Nat Neurosci* 2: 740–745, 1999.

Dobelle WH. Artificial vision for the blind by connecting a television camera to the visual cortex. *ASAIO J* 46: 3–9, 2000.

Dykes RW, Rasmusson DD, and Hoeltzell PB. Organization of primary somatosensory cortex in the cat. *J Neurophysiol* 43: 1527–1546, 1980.

Ebert B, Mikkelsen S, Thorkildsen C, and Borgbjerg FM. Norketamine, the main metabolite of ketamine, is a non-competitive NMDA receptor antagonist in the rat cortex and spinal cord. *Eur J Pharmacol* 333: 99–104, 1997.

Egert U, Knott T, Schwarz C, Nawrot M, Brandt A, Rotter S, and Diesmann M. MEA-Tools: an open source toolbox for the analysis of multi-electrode data with MATLAB. *J Neurosci Methods* 117: 33–42, 2002.

Galarreta M and Hestrin S. A network of fast-spiking cells in the neocortex connected by electrical synapses. *Nature* 402: 72–75, 1999.

Ghazanfar AA and Nicolelis MA. Spatiotemporal properties of layer V neurons of the rat primary somatosensory cortex. *Cereb Cortex* 9: 348–361, 1999.

Gibson JR, Beierlein M, and Connors BW. Two networks of electrically coupled inhibitory neurons in neocortex. *Nature* 402: 75–79, 1999.

Gil Z and Amitai Y. Properties of convergent thalamocortical and intracortical synaptic potentials in single neurons of neocortex. *J Neurosci* 16: 6567–6578, 1996.

Gottlieb JP and Keller A. Intrinsic circuitry and physiological properties of pyramidal neurons in rat barrel cortex. *Exp Brain Res* 115: 47–60, 1997.

Grinvald A, Lieke E, Frostig RD, Gilbert CD, and Wiesel TN. Functional architecture of cortex revealed by optical imaging of intrinsic signals. *Nature* 324: 361–364, 1986.

Gustafsson B and Jankowska E. Direct and indirect activation of nerve cells by electrical pulses applied extracellularly. *J Physiol* 258: 33–61, 1976.

Hirsch JA, Gallagher CA, Alonso JM, and Martinez LM. Ascending projections of simple and complex cells in layer 6 of the cat striate cortex. *J Neurosci* 18: 8086–8094, 1998.

Hirsch JA and Gilbert CD. Synaptic physiology of horizontal connections in the cat's visual cortex. *J Neurosci* 11: 1800–1809, 1991.

Hubel DH and Wiesel TN. Functional architecture of macaque monkey visual cortex. *Proc R Soc Lond B Biol Sci* 198: 1–59, 1977.

Kara P, Pezaris JS, Yurgenson S, and Reid RC. The spatial receptive field of thalamic inputs to single cortical simple cells revealed by the interaction of visual and electrical stimulation. *Proc Natl Acad Sci USA* 99: 16261–16266, 2002.

Kayama Y and Iwama MD. The EEG, evoked potentials, and single-unit activity during ketamine anesthesia in cats. *Anesthesiology* 36: 316–328, 1972.

Keller A and White EL. Synaptic organization of GABAergic neurons in the mouse SmI cortex. *J Comp Neurol* 262: 1–12, 1987.

Kim U and Ebner FE. Barrels and septa: separate circuits in rat barrels field cortex. *J Comp Neurol* 408: 489–505, 1999.

Kisvárday ZF. GABAergic networks of basket cells in the visual cortex. In: *Progress in Brain Research: Mechanisms of GABA in the Visual System*, edited by Mize RR, Marc RE, and Sillito AM. Amsterdam: Elsevier Science Publishers B.V., 1992, vol. 90, p. 385–405.

Krnjevic K, Randic M, and Straughan DW. An inhibitory process in the cerebral cortex. *J Physiol* 184: 16–48, 1966.

Li CL. The inhibitory effect of stimulation of a thalamic nucleus on neuronal activity in the motor cortex. *J Physiol* 133: 40–53, 1956.

Lipski J. Antidromic activation of neurones as an analytic tool in the study of the central nervous system. *J Neurosci Methods* 4: 1–32, 1981.

Loeb GE. Cochlear prosthetics. *Annu Rev Neurosci* 13: 357–371, 1990.

Luetje CM, Whittaker CK, Geier L, Mediavilla SJ, and Shallop JK. Feasibility of multichannel human cochlear nucleus stimulation [see comments]. *Laryngoscope* 102: 23–25, 1992.

Lund JS, Yoshioka T, and Levitt JB. Comparison of intrinsic connectivity in different areas of macaque monkey cerebral cortex. *Cereb Cortex* 3: 148–162, 1993.

Manger PR, Woods TM, Munoz A, and Jones EG. Hand/face border as a limiting boundary in the body representation in monkey somatosensory cortex. *J Neurosci* 17: 6338–6351, 1997.

McCreery DB, Shannon RV, Moore JK, and Chatterjee M. Accessing the tonotopic organization of the ventral cochlear nucleus by intranuclear microstimulation. *IEEE Trans Rehabil Eng* 6: 391–399, 1998.

McGuire BA, Gilbert CD, Rivlin PK, and Wiesel TN. Targets of horizontal connections in macaque primary visual cortex. *J Comp Neurol* 305: 370–392, 1991.

McIntyre CC and Grill WM. Selective microstimulation of central nervous system neurons. *Ann Biomed Eng* 28: 219–233, 2000.

Moore CI and Nelson SB. Spatio-temporal subthreshold receptive fields in the vibrissa representation of rat primary somatosensory cortex. *J Neurophysiol* 80: 2882–2892, 1998.

Moore CI, Nelson SB, and Sur M. Dynamics of neuronal processing in rat somatosensory cortex. *Trends Neurosci* 22: 513–520, 1999.

Mountcastle VB. Modality and topographic properties of single neurons of cat's somatic sensory cortex. *J Neurophysiol* 20: 408–434, 1957.

Murakoshi T, Guo J-Z, and Ichinose T. Electrophysiological identification of horizontal synaptic connections in rat visual cortex in vitro. *Neurosci Lett* 163: 211–214, 1993.

Murasugi CM, Salzman CD, and Newsome WT. Microstimulation in visual area MT: effects of varying pulse amplitude and frequency. *J Neurosci* 13: 1719–1729, 1993.

Nichols MJ and Newsome WT. Middle temporal visual area microstimulation influences veridical judgments of motion direction. *J Neurosci* 22: 9530–9540, 2002.

Nicolelis MA. Actions from thoughts. *Nature Suppl* 409: 403–407, 2001.

Nowak LG and Bullier J. Axons, but not cell bodies, are activated by electrical stimulation in cortical gray matter. I. Evidence from chronaxie measurements. *Exp Brain Res* 118: 477–488, 1998a.

Nowak LG and Bullier J. Axons, but not cell bodies, are activated by electrical stimulation in cortical gray matter. II. Evidence from selective inactivation of cell bodies and axon initial segments. *Exp Brain Res* 118: 489–500, 1998b.

Peters A and Jones EG. Classification of cortical neurons. In: *Cerebral Cortex*, edited by Peters A and Jones EG. New York: Plenum Press, 1984, vol. 1, p. 107–121.

Petersen CC, Grinvald A, and Sakmann B. Spatiotemporal dynamics of sensory responses in layer 2/3 of rat barrel cortex measured in vivo by voltage-sensitive dye imaging combined with whole-cell voltage recordings and neuron reconstructions. *J Neurosci* 23: 1298–1309, 2003.

Porter JT, Johnson CK, and Agmon A. Diverse types of interneurons generate thalamus-evoked feedforward inhibition in the mouse barrel cortex. *J Neurosci* 21: 2699–2710, 2001.

Ranck JB Jr. Which elements are excited in electrical stimulation of mammalian central nervous system: a review. *Brain Res* 98: 417–440, 1975.

Rattay F. The basic mechanism for the electrical stimulation of the nervous system. *Neuroscience* 89: 335–346, 1999.

Romo R, Hernandez A, Zainos A, Brody CD, and Lemus L. Sensing without touching: psychophysical performance based on cortical microstimulation [In Process Citation]. *Neuron* 26: 273–278, 2000.

Romo R, Hernandez A, Zainos A, and Salinas E. Somatosensory discrimination based on cortical microstimulation. *Nature* 392: 387–390, 1998.

Salin PA and Prince DA. Electrophysiological mapping of $GABA_A$ receptor-mediated inhibition in adult rat somatosensory cortex. *J Neurophysiol* 75: 1589–1600, 1996.

Salzman CD, Britten KH, and Newsome WT. Cortical microstimulation influences perceptual judgements of motion direction. *Nature* 346: 174–177, 1990.

Schreiner CE, Read HL, and Sutter ML. Modular organization of frequency integration in primary auditory cortex. *Annu Rev Neurosci* 23: 501–529, 2000.

Schubert D, Staiger JF, Cho N, Kotter R, Zilles K, and Luhmann HJ. Layer-specific intracolumnar and transcolumnar functional connectivity of layer V pyramidal cells in rat barrel cortex. *J Neurosci* 21: 3580–3592, 2001.

Schwindt PC, Spain WJ, and Crill WE. Long-lasting reduction of excitability by a sodium-dependent potassium current in cat neocortical neurons. *J Neurophysiol* 61: 233–244, 1989.

Schwindt PC, Spain WJ, Foehring RC, Chubb MC, and Crill WE. Slow conductances in neurons from cat sensorimotor cortex in vitro and their role in slow excitability changes. *J Neurophysiol* 59: 450–467, 1988.

Shao Z and Burkhalter A. Different balance of excitation and inhibition in forward and feedback circuits of rat visual cortex. *J Neurosci* 16: 7353–7365, 1996.

Shao Z and Burkhalter A. Role of $GABA_B$ receptor-mediated inhibition in reciprocal interareal pathways of rat visual cortex. *J Neurophysiol* 81: 1014–1024, 1999.

Simons DJ. Response properties of vibrissa units in rat S1 somatosensory neocortex. *J Neurophysiol* 41: 798–820, 1978.

Simons DJ and Carvell GE. Thalamocortical response transformation in the rat vibrissa/barrel system. *J Neurophysiol* 61: 311–330, 1989.

Sonner JM, Zhang Y, Stabernack C, Abaigar W, Xing Y, and Laster MJ. GABA(A) receptor blockade antagonizes the immobilizing action of propofol but not ketamine or isoflurane in a dose-related manner. *Anesth Analg* 96: 706–712, 2003.

Stoney SD Jr, Thompson WD, and Asanuma H. Excitation of pyramidal tract cells by intracortical microstimulation: effective extent of stimulating current. *J Neurophysiol* 31: 659–669, 1968.

Sur M, Wall JT, and Kaas JH. Modular distribution of neurons with slowly adapting and rapidly adapting responses in area 3b of somatosensory cortex in monkeys. *J Neurophysiol* 51: 724–744, 1984.

Swadlow HA. Influence of VPM afferents on putative inhibitory interneurons in S1 of the awake rabbit: evidence from cross-correlation, microstimulation, and latencies to peripheral sensory stimulation. *J Neurophysiol* 73: 1584–1599, 1995.

Tehovnik EJ. Electrical stimulation of neural tissue to evoke behavioral responses. *J Neurosci Methods* 65: 1–17, 1996.

Thomson AM and Destexhe A. Dual intracellular recordings and computational models of slow inhibitory postsynaptic potentials in rat neocortical and hippocampal slices. *Neuroscience* 92: 1193–1215, 1999.

Thomson AM, Deuchars J, and West DC. Large, deep layer pyramid-pyramid single axon EPSPs in slices of rat motor cortex display paired pulse and frequency dependent depression, mediated presynaptically and self-facilitation, mediated postsynaptically. *J Neurophysiol* 70: 2354–2369, 1993.

Tsodyks MV and Markram H. The neural code between neocortical pyramidal neurons depends on neurotransmitter release probability. *Proc Natl Acad Sci USA* 94: 719–723, 1997.

van Brederode JF and Spain WJ. Differences in inhibitory synaptic input between layer II–III and layer V neurons of the cat neocortex. *J Neurophysiol* 74: 1149–1166, 1995.

Zhu JJ and Connors BW. Intrinsic firing patterns and whisker-evoked synaptic responses of neurons in the rat barrel cortex. *J Neurophysiol* 81: 1171–1183, 1999.

Zrenner E. Will retinal implants restore vision? *Science* 295: 1022–1025, 2002.

J Neurophysiol 96: 1227–1236, 2006;
doi:10.1152/jn.01170.2005.

Effects of Electrically Coupled Inhibitory Networks on Local Neuronal Responses to Intracortical Microstimulation

Sergejus Butovas,[1] Sheriar G. Hormuzdi,[2] Hannah Monyer,[2] and Cornelius Schwarz[1]
[1]*Hertie-Institute for Clinical Brain Research, Department of Cognitive Neurology, University Tübingen, Tübingen; and* [2]*Department of Clinical Neurobiology, University Hospital of Neurology, Heidelberg, Germany*

Submitted 4 November 2005; accepted in final form 15 May 2006

Butovas, Sergejus, Sheriar G. Hormuzdi, Hannah Monyer, and Cornelius Schwarz. Effects of electrically coupled inhibitory networks on local neuronal responses to intracortical microstimulation. *J Neurophysiol* 96: 1227–1236, 2006; doi:10.1152/jn.01170.2005. Using in vivo multielectrode electrophysiology in mice, we investigated the underpinnings of a local, long-lasting firing rate suppression evoked by intracortical microstimulation. Synaptic inhibition contributes to this suppression as it was reduced by pharmacological blockade of γ-aminobutyric acid type B ($GABA_B$) receptors. Blockade of $GABA_B$ receptors also abolished the known sublinear addition of inhibitory response duration after repetitive electrical stimulation. Furthermore, evoked inhibition was weaker and longer in connexin 36 knockout (KO) mice that feature decoupled cortical inhibitory networks. In supragranular layers of KO mice even an unusually long excitatory response (≤50 ms) appeared that was never observed in wild-type (WT) mice. Furthermore, the spread and duration of very fast oscillations (>200 Hz) evoked by microstimulation at a short latency were strongly enhanced in KO mice. In the spatial domain, lack of connexin 36 unmasked a strong anisotropy of inhibitory spread. Although its reach along layers was almost the same as that in WT mice, the spread across cortical depth was severely hampered. In summary, the present data suggest that connexin 36–coupled networks significantly shape the electrically evoked cortical inhibitory response. Electrical coupling renders evoked cortical inhibition more precise and strong and ensures a uniform spread along the two cardinal axes of neocortical geometry.

INTRODUCTION

Activity in neocortex is balanced by a heterogeneous population of inhibitory interneurons that constitute about a fifth of all cortical neurons (Peters 1987; Szentágothai 1978). Besides setting the level of depolarization and firing rate of cortical neurons (Hentschke et al. 2005), cortical inhibition plays an important role in shaping temporal (Blatow et al. 2003; Galarreta and Hestrin 2001b; Hormuzdi et al. 2001; Whittington et al. 1995) and spatial properties of cortical activity (Bolz and Gilbert 1986; Moore and Nelson 1998). Most, if not all, cortical inhibitory interneurons use γ-aminobutyric acid (GABA) as a transmitter and act by ionotropic $GABA_A$ receptors with fast and medium time course (Drexler et al. 2005; Fritschy and Brünig 2003), although slower kinetics of synaptic inhibitory responses are known to exist in subcortical structures (Banks et al. 1998; Huntsman et al. 1999). A second type of GABA receptor through which cortical interneurons affect other neurons is the metabotropic $GABA_B$ receptor, which shows very slow temporal properties with time constants >100 ms (Connors et al. 1988; Mott and Lewis 1994). The inhibitory network consists of distinct classes of interneurons characterized by histochemical staining, connectivity, expression of receptors, intrinsic membrane characteristics, and dendritic architecture (Kawaguchi and Kondo 2002; Markram et al. 2004). Remarkably, recent studies have indicated that coupling by connexin 36–containing electrical synapses organizes at least some of these interneuron subtypes into distinct syncytia (Beierlein et al. 2000; Blatow et al. 2003; Galarreta and Hestrin 1999; Gibson et al. 1999; Hormuzdi et al. 2001). Electrical coupling within inhibitory networks is important because it allows for tight synchronous firing—not only among the individual members of a syncytium but also of those neurons that communicate with the syncytium by chemical synapses (Connors and Long 2004; Galarreta and Hestrin 2001a). These features occasioned the notion that electrically coupled inhibitory networks may play a decisive role in generating and/or controlling rhythmic activity of the entire neocortical network (Buhl et al. 2003; Whittington et al. 1995).

In this study we investigated how electrical coupling within inhibitory networks affects spatiotemporal activation patterns evoked by intracortical microstimulation. Electrical stimulation has been of general importance for experimental neurobiology (Tehovnik 1996) and has recently gained new momentum in view of its prospective application in neuroprostheses (Nicolelis 2001; Rauschecker and Shannon 2002; Zrenner 2002). Indeed, a large body of work from intracellular and extracellular recordings in the neocortex in vitro and in vivo described a close correlation of both excitatory and inhibitory effects after electrical stimulation. Despite some variation across methods and preparations, the common finding was that excitation is evoked at short latencies and was always followed by a strong and long-lasting inhibitory response (see references in Butovas and Schwarz 2003). Assessing spatial and temporal parameters of the responses as well as electrical parameters of the stimulation indicated that the inhibition was remarkably static in its temporal characteristics and extended ≤1.35 mm from the stimulation site (Butovas and Schwarz 2003). Its duration was >100 ms and was almost unaffected by *1*) changes in near threshold stimulus intensity, *2*) the distance to the stimulation site, and *3*) double-pulse stimulation within the time span of its duration. The latter feature, in particular, suggested that it is synaptic inhibition that plays a major role in generating the inhibitory response because afterhyperpolariza-

Address for reprint requests and other correspondence: C. Schwarz, Hertie-Institute for Clinical Brain Research, Department of Cognitive Neurology, University Tübingen, Otfried Müller Str. 27, 72076 Tübingen, Germany (E-mail: cornelius.schwarz@uni-tuebingen.de).

The costs of publication of this article were defrayed in part by the payment of page charges. The article must therefore be hereby marked "*advertisement*" in accordance with 18 U.S.C. Section 1734 solely to indicate this fact.

tion or synaptic depression, the two major alternatives, would not be compatible with a virtual absence of prolonged inhibition after double-pulse stimulation (Butovas and Schwarz 2003). Its stereotyped and long-lasting characteristics can be well explained by a combination of the highly synchronized action of electrically coupled inhibitory networks and the usage of long-lasting inhibitory synaptic transmission. From the group of GABAergic synaptic mechanisms known to exist in neocortex, $GABA_B$-receptor–mediated inhibitory postsynaptic potentials (IPSPs) would best match the remarkable characteristics of evoked inhibition, that is, the long duration of $\leq$200 ms and the resistance to repetitive presynaptic action potentials (Thomson and Destexhe 1999). In the present work we found evidence for these conjectures using a combination of stimulation and multisite recording in genetically modified connexin 36 knockout mice (Hormuzdi et al. 2001) lacking electrical coupling between neocortical interneurons (Deans et al. 2001).

METHODS

Surgery

Nineteen mice (body weight 18.3–28.1 g) of both sexes and both genotypes [ten wild-type (WT) and nine connexin 36–deficient mice (KO) were used in the present study]. The generation of connexin 36 knockout mice is described elsewhere (Hormuzdi et al. 2001). All experimental and surgical procedures were performed in accordance with the policy and the use of animals in neuroscience research of the Society for Neuroscience and German Law. The mice were anesthetized with a mixture of ketamine (100 mg/kg) and xylacine, administered intraperitoneally (ip, 10 mg/kg). The depth of anesthesia was maintained with additional doses of ketamine to keep the hind-limb reflex to a painful stimulus below threshold. The animal's rectal temperature and heart rate were constantly monitored. The temperature was adjusted to 37°C using a controlled heating pad (Fine Science Tools, Heidelberg, Germany). For recordings from neocortex, animals were placed in a stereotaxic apparatus and a craniotomy was performed to expose the primary somatosensory cortex. After removal of the dura mater a multielectrode array, consisting of a row of seven electrodes, was lowered into the neocortex at an angle of 90° with respect to its surface using a hydraulic micropositioner (Kopf 650; David Kopf Instruments, Tujunga, CA). In some experiments we varied stimulation sites using a three-electrode array of individually movable electrodes (EPS, Alpha Omega Engineering, Nazareth, Israel). The middle one recorded from units in the supragranular or infragranular layers; the outer ones, used for stimulation, were moved during the experiment from infra- to supragranular sites. After placement of the electrode array the cortex was covered with mineral oil to prevent drying. The characteristic of recording sites was assessed using either an air puff, originating from a plastic tube (diameter $\approx$ 0.5 mm) and directed against the whiskers (duration of pulse: 20 ms; distance to whisker pad: 2–3 cm), and/or a cotton swab lightly touching parts of the body. All recordings presented here were performed at sites at which stimulation of the contralateral whisker pad elicited clear unit responses in at least a subset of electrodes. The data of the present study were thus recorded in whisker and neighboring snout representations. Recording sites were marked with electrolytic lesions after the experiment was completed. The animal was deeply anesthetized with barbiturates and perfused through the aorta using phosphate buffer (0.1 M) followed by paraformaldehyde (4% in phosphate buffer). The brain was processed using standard histological procedures. The recording layer was assessed by investigating lesions in Nissl-stained sections oriented orthogonally to the surface of the neocortex.

Electrodes

Multielectrode arrays were custom made in our laboratory. Seven pulled and ground glass–coated platinum tungsten electrodes (shank diameter: 80 μm; diameter of the metal core: 23 μm; free tip length: about 8 μm; impedance: >2 MΩ; Thomas Recording, Giessen, Germany) were mounted inside a 1 $\times$ 7 array of polyimide tubing, for which the distance between tips was set to 300 μm (HV Technologies, Trenton, GA). The free ends of the electrodes were soldered to Teflon-insulated silver wires (Science Products, Hofheim, Germany), which in turn connected to a microplug (Bürklin, Munich, Germany). The electrode at one end of the row was used for electrical stimulation and was placed inside a stainless steel tube that was connected to ground during the recording sessions. The same electrodes were used in the experiment in which three individual electrodes were manipulated.

Electrophysiology

The electrophysiological recordings of extracellular signals were performed using a multichannel extracellular amplifier (MultiChannelSystems, Reutlingen, Germany; gain 5,000; sampling rate 20 kHz; band-pass filter at cutoff frequencies of 200 and 5,000 Hz). Action potentials were extracted from the voltage traces off-line by a threshold and stored as cutouts of 2-ms length on the hard drive of a PC. Spike sorting was performed with PCA clustering using a MATLAB-based (The MathWorks, Natick, MA) program (Egert et al. 2002). Firing rates given in this report always pertain to units recorded with individual electrodes. Through the first electrode in the row of electrodes rectangular biphasic current pulses (cathodal first) were delivered at the rate of 1 Hz using a programmable stimulator (STG 1008; MultiChannelSystems). The electrical stimuli were identical to an earlier study and encompassed the threshold to elicit neuronal responses in rats (Butovas and Schwarz 2003). The stimulus amplitude was fixed to 8 μA and the intensity was changed by varying the pulse duration between 100 and 600 μs in 100-μs steps (charge transfer of 0.8 to 4.8 nC, respectively, varied from pulse to pulse in pseudorandom fashion).

Pharmacology

To investigate effects of $GABA_B$ blockade on electrically evoked inhibitory response pattern, CGP 46381 (Tocris Cookson, Ellisville, MO), dissolved in saline (150 mg/kg ip), was administered. The effect of this intervention was monitored by suprathreshold single electrical pulses (charge transfer 4.8 nC) applied at a frequency of 0.2 Hz for $\leq$120 min after injection.

Data analysis

Analysis of inhibitory responses was performed as described in a previous report (Butovas and Schwarz 2003; see their Fig. 5*D*). In short, the spike renewal density function [poststimulus time histogram (PSTH), 1-ms bin width; Abeles 1982] was low-pass filtered by passing a Gaussian (kernel length 50 bins) over it. A unit was classified as responding if the firing rate undershot three quarters of the spontaneous firing (f_{spont}). Duration of the inhibitory response was measured from the stimulation to the point in time where the firing rate crossed this value again. To calculate the response frequency f_{resp} and the strength of the response we took the average frequency within the interval 12 to 80 ms after stimulus onset as f_{resp}. The strength of the inhibitory response was computed as $1 - (f_{resp}/f_{spont})$.

Fast oscillations (FOs) in the field potential occurred at very small latencies. Therefore their frequency content could be determined only after eliminating the stimulus artifact and connecting the remaining parts of pre- and poststimulus voltage traces together in a smooth way. As a first step to this end the stimulus artifact was blanked from *time*

0 (stimulation) to the third zero crossing afterward. Then the signal was low-pass filtered at an edge frequency of 1,000 Hz, chosen to meet the dual goal *1*) to eliminate high-frequency noise needed to allow smooth interpolation in the next step and *2*) to avoid introduction of transients at the corners of the blanked interval. Cubic spline interpolation was applied to the signal from 100 ms before the stimulation to a point of the voltage trace with medium slope after the offset of the blanked period. This procedure ensured that no frequencies in the investigated range (>200 Hz) were introduced. Then a second low-pass filtering (edge frequency 600 Hz, Butterworth, <0.5 dB in ripple pass band, attenuation 30 dB/octave in stop band) was applied. This analysis completely abolished the stimulus artifact because resulting traces from recordings far away from the stimulus electrode (1,800 μm) in supragranular layers were consistently flat. In a final step the power spectrum density from an interval 0 to 40 ms after stimulation was calculated. For assessment of the duration of FO the root mean square (RMS) was computed from the extracted FO using a sliding window of 3-ms length. The interval from the point in time at which the RMS crossed a threshold (5 SD of the RMS during the first 150 ms of prestimulus time interval) until its relaxation back under the threshold was taken as duration of the FO. Trials in which the RMS did not surpass the threshold were counted as trials that did not evoke FO. Throughout this paper results are expressed as average ± SD for the data, assumed to be normally distributed, otherwise median [25th percentile 25–75th percentile].

RESULTS

Charge transfers equal or above 1.6 nC evoked a long-lasting inhibition in WT mice followed, in some cases, by rebound responses at higher stimulus intensities (Figs. 1 and 3*A*), similar to results obtained in an earlier study in rats (Butovas and Schwarz 2003). However, there were some quantitative differences with respect to rats. The average duration of the inhibition was significantly shorter (82.5 ± 19.2 ms, $n = 132$ in mice vs. 118 ± 20.6, $n = 186$ in rats; Mann–Whitney U test, $P < 0.01$). In addition, the responsiveness of neurons to local stimulation was lower than that in rats. Although inhibitory response frequency was significantly different from zero at a stimulus intensity of 1.6 nC (as in rats), the 50% mark of response frequency was reached at a stimulus intensity of only 3.2 nC in mice (compare Fig. 5*A* to Fig. 6 of Butovas and Schwarz 2003). Other features of the inhibitory response, however, closely matched those observed in rats. First, the duration was statistically independent of the distance

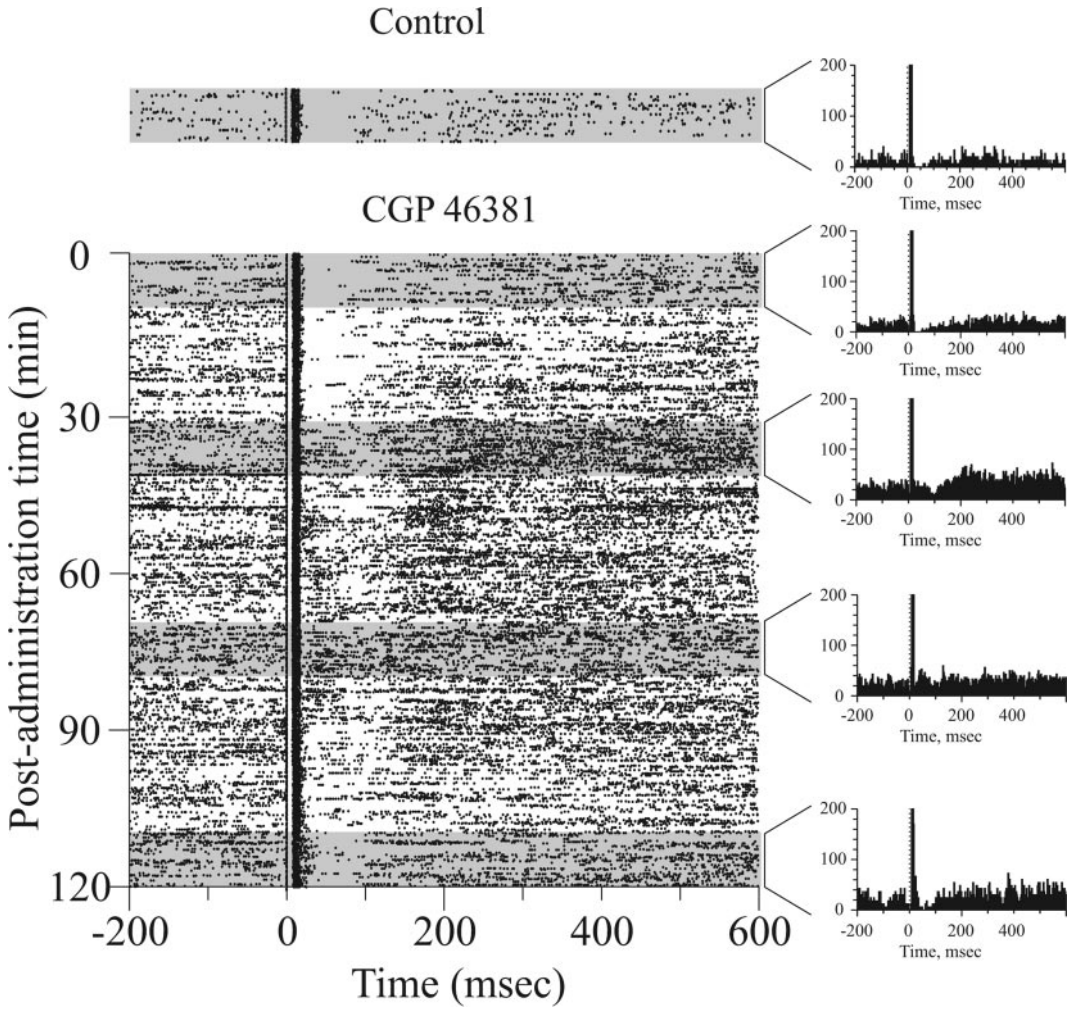

FIG. 1. Depression of firing rate is attributed to synaptic inhibition. γ-Aminobutyric acid type B ($GABA_B$)–receptor blockade reduces inhibitory response. Typical example of neuronal firing pattern (recorded at 824 μm depth, layer 5). Raster plot in *top left* denoted as "control" represents recording before CGP 46381 was administered. Poststimulus time histograms (PSTHs) computed from 10-min periods (gray fields in the raster plots) are shown on the *right*. By 30 min after the drug application inhibition was decreased (see corresponding PSTH on the *right*) and after 70 min it was nearly abolished. Recovery was observed 90 min after drug application.

from the stimulation electrode and the stimulation intensity (two-way ANOVA, $P > 0.05$, $n = 114$, Fig. 5*C*). Second, inhibitory response strength decreased with distance to the stimulation electrode (two-way ANOVA, $P < 0.05$, $n = 114$). Third, double-pulse stimulation within the inhibitory period did not elongate the inhibition (Fig. 2*A*).

Inhibition is based on GABAergic synaptic mechanisms

In principle, diminishing excitatory drive, hyperpolarizing transmembrane currents, and synaptic GABAergic transmission may be at the basis of the inhibitory response (Butovas and Schwarz 2003). Because we were interested in the third possibility—the contribution of the GABAergic system to the firing rate depression—we aimed at showing that it is amenable to the interference with postsynaptic GABA receptors. We chose to block $GABA_B$ receptors because, first, our working hypothesis entailed that $GABA_B$ receptors may play a role for the mediation of the long-lasting inhibitory response. A second reason was that the blockade of $GABA_B$ receptors is readily facilitated by the relatively benign effect of $GABA_B$ receptor blockade on gross cortical activity patterns (in sharp contrast to $GABA_A$ receptor blockers) and the availability of CGP 46381, a highly specific $GABA_B$ receptor blocker that can be administered systemically (Curtis and Lacey 1994; Hershman et al. 1995; Olpe et al. 1993). By using CGP 46381 we consistently found a reduction of the duration of the inhibitory period. In the example shown in Fig. 1 the inhibition was almost completely abolished starting about 30 min after drug application and the spontaneous firing rate increased from 15.3 to 68.4 Hz. This effect was reversed roughly 2 h after drug administration. The reduction in duration of the inhibitory period and the increase in spontaneous firing rate were found in three animals (from 146, 116, and 81 to 71, 43, and 0 ms, respectively; spontaneous firing rate changed from 38, 6.27, and 15.3 to 160, 11.7, and 68.4 Hz, respectively). Stimulating with double pulses showed a sublinear summation of the duration of inhibition in the three animals (Fig. 2*A*). In two animals that still showed some inhibition at the time of maximal $GABA_B$ receptor blockade, the opposite—a supralinear elongation of the remaining inhibitory response—was observed (Fig. 2*B*). These results strongly indicate a contribution of inhibitory synapses using $GABA_B$ receptors to the suppression of firing rate after intracortical stimulation. Furthermore, $GABA_B$ receptors seem to play a dominant role in determining the sublinearity of summation of response duration with repetitive stimuli.

Shape of inhibition is dependent on the presence of connexin 36–mediated electrical coupling

If the observed inhibition is at least partly of synaptic origin the question arises with respect to what impact the peculiar organization of inhibitory networks could have on the characteristics of the inhibitory response. Of particular interest is the syncytium-like organization of inhibitory networks by gap junctions containing connexin 36 (Hormuzdi et al. 2001). In studying KO mice, we could readily evoke inhibition. However, several features were distinct from those observed in WT mice (Fig. 3*A*). First, the duration of the response in KO mice was longer than that observed in WT mice (158.3 [131.4–200.1] ms; $n = 171$ in KO mice vs. 83.5 [71.0–90.8] $n = 170$ in WT mice;, Mann–Whitney *U* test, $P < 0.05$, Fig. 3*B*). Second, in some cases an excitatory response lasting for about 50 ms occurred (Fig. 3*C*), a feature that was never observed in WT mice. Interestingly, the occurrence of this prolonged excitation showed a clear pattern across cortical depth. Recording sites were histologically identified in all nine KO mice. Of the

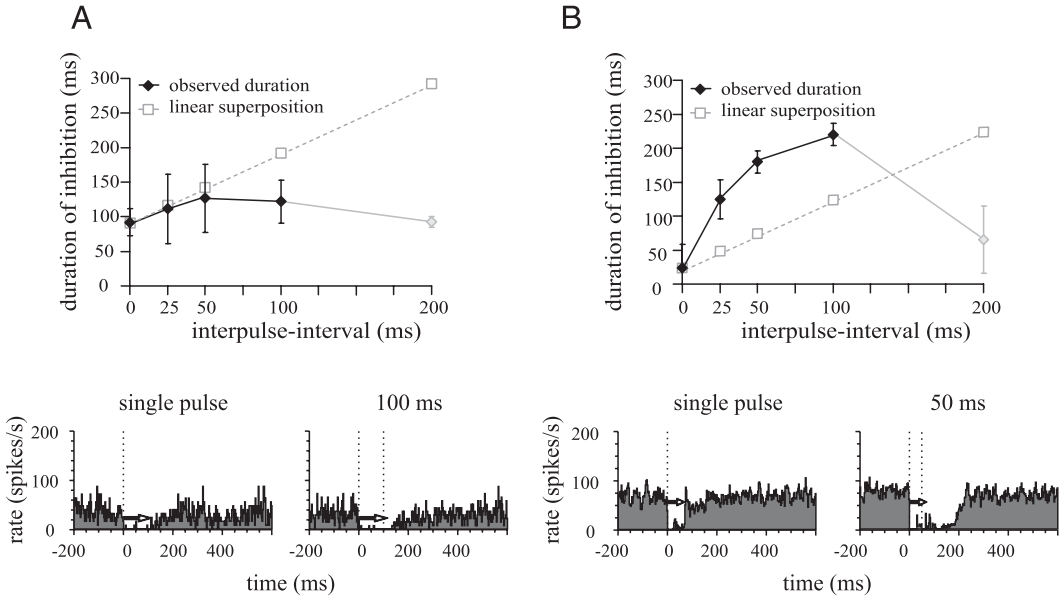

FIG. 2. Sublinear summation of inhibitory response duration evoked by a double-pulse protocol reverses to a supralinear relationship during $GABA_B$ receptor blockade. *A*: plot of observed response duration against the interval between double pulses (4.8 nC, $n = 3$). Expected values as predicted for linear superposition from responses to single pulse are plotted as open gray squares. At 200 ms, the duration of inhibitory response corresponds to the single pulse because the second pulse evoked a separated inhibitory response (gray diamond). PSTHs shown below demonstrate an example recorded at 801 μm, layer 5. Second pulse delivered at 100 ms elongates inhibition by 4 ms. For purposes of illustration the fast excitation was blanked and empty arrows indicate the same time interval. *B*: same conventions as in *A* but results from recordings during the maximum effect of CGP 46381. Only the 2 animals with measurable inhibitory duration were included. Two PSTHs depicted are computed from a recording taken at a subpial depth of 543 μm, layer 3.

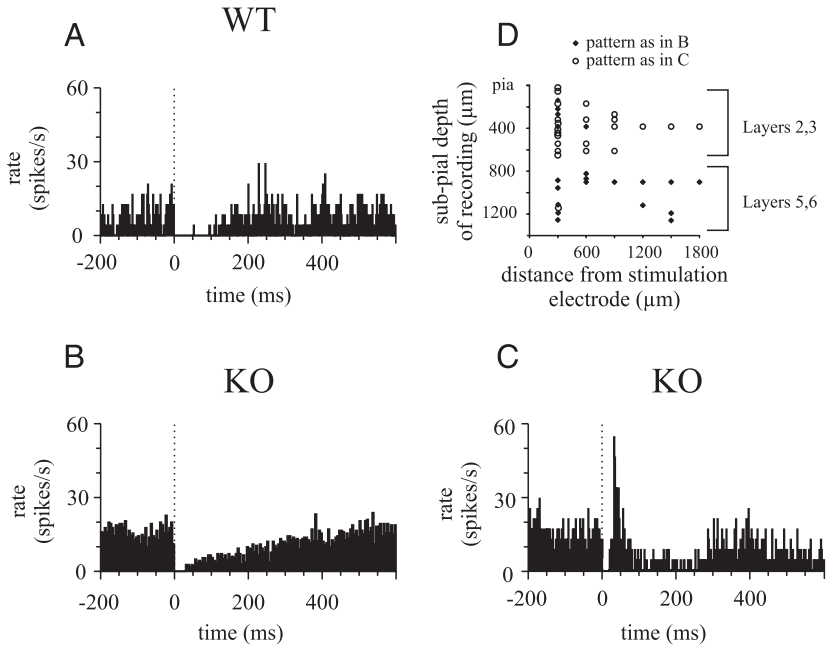

FIG. 3. Inhibitory response in connexin 36–deficient mice is weaker and elongated. *A*: typical PSTH as observed in wild-type (WT) mice. *B*: representative response pattern encountered in infragranular layers in connexin 36 deficient KO mice. *C*: in supragranular layers of KO mice, in addition a prolonged excitatory response is present. *D*: plot of type of response as depicted in *B* and *C* across cortical depth. Layers as reconstructed from histology are indicated.

identified recording sites, prolonged excitation was the predominant pattern in supragranular layers (it was absent only in some cases close to the stimulus electrode) but in infragranular layers was missing (with the exception of one case; Fig. 3*D*).

Next, we asked whether prolonged excitation could be attributable to fast oscillatory activity (FO), previously observed after sensory or electrical surface stimulation (Jones et al. 2000; Staba et al. 2003). Indeed our recordings demonstrated that FOs were evoked by electrical stimulation despite the absence of connexin 36 (Fig. 4) and displayed comparable peaks between 200 and 300 Hz in the power spectrum (data not shown). FOs of comparable amplitudes were never observed to occur spontaneously. In KO mice the FOs appeared extended and their duration was clearly increased. However, the spatial pattern was reversed with respect to that seen for the prolonged excitation. As exemplified in Fig. 4, *A–D*, FO duration was most conspicuously elongated in infragranular layers and less so in supragranular layers, as would have been expected from the distribution of the prolonged excitation. In infragranular layers the elongation of FOs measured 300 μm away from stimulation electrode at 4.8-nC stimulation intensity was 9.4 ms (KO: 23.1 [20.7–25.6] ms, $n = 9$, WT: 13.7 [12.7–15.7] ms, $n = 12$; Mann–Whitney U test, $P = 0.000$), whereas it reached only 2.4 ms in supragranular layers: KO: 14.9 [12.9–16.0] ms, $n = 15$, WT: 12.5 [9.9–13.8] ms, $n = 13$; Mann–Whitney U test, $P < 0.05$). Furthermore, close inspection of poststimulus voltage traces (Fig. 4*E*) clearly showed that extended FOs were not accompanied by action potentials. On the other hand, recordings in supragranular layers showed only a small FO content, which occurs before the action potentials that make up the elongated excitation (Fig. 4*F*). In summary, these results do not argue in favor of FOs being at the basis of the prolonged excitation that precedes the inhibition in supragranular layers of KO mice.

Spatial spread of inhibition shows marked anisotropy in the absence of connexin 36–mediated electrical coupling

We first investigated the spatial distribution of inhibitory responses in WT and KO mice with respect to horizontal cortical distance (Fig. 5, *A* and *B*). Surprisingly, the spread of inhibition along layers was very similar in WT and KO mice, although there was a certain tendency for inhibition in KO mice to be spread out more across the cortical surface at medium stimulus intensities (which reached significance at some parameter combinations: the bars with white top in Fig. 5, *A* and *B* are statistically different between WT and KO mice, χ^2 test, $P < 0.05$). In particular, near-threshold intensities of 1.6–2.4 nC evoked inhibitory responses at very distant sites ($\leq$1,800 μm), a feature absent in WT mice. Figure 5, *C* and *D* demonstrates that the typical elongation of inhibitory duration was seen irrespective of location and stimulus intensities. The distribution of durations across these parameters was flat in WT mice (two-way ANOVA, $P > 0.05$, $n = 114$), whereas in KO mice duration increased with higher charge transfer (two-way ANOVA, $P < 0.05$, $n = 149$).

Next, we investigated the spread of inhibition between supra- and infragranular layers through the cortical depth. Experiments in WT mice showed that horizontal spread of inhibition is the same, independent of the location of recording and stimulation electrodes in supra- or infragranular layers. The horizontal connections in supragranular (S-S) and infragranular (I-I) layers displayed inhibitory responses at an intensity close to threshold (7/10 at 3.2 nC) as did the connections that crossed the cortical depth (S-I and I-S; Fig. 6*C*). In KO mice the duration of inhibition in the horizontal direction was elongated as reported above and the threshold intensities were comparable to those in WT mice (2.4 nC). Upon observing the connections that traversed the cortical depth, however, the picture changed dramatically. No inhibitory response could be observed in the range of stimulus intensities applied (0.8–4.8 nC; S-I, $n = 5$; I-S, $n = 10$). Responses could be evoked only by unusually high stimulus intensities. In particular, the transmission S-I was virtually blocked, and in only two of five units shallow and long inhibitory responses at very long latencies about 300 ms were evoked by using exceedingly large stimulus intensities of 64 nC (Fig. 6*D*, gray PSTH). In I-S orientation 10 of 10 units could be driven by increasing the stimulus intensity

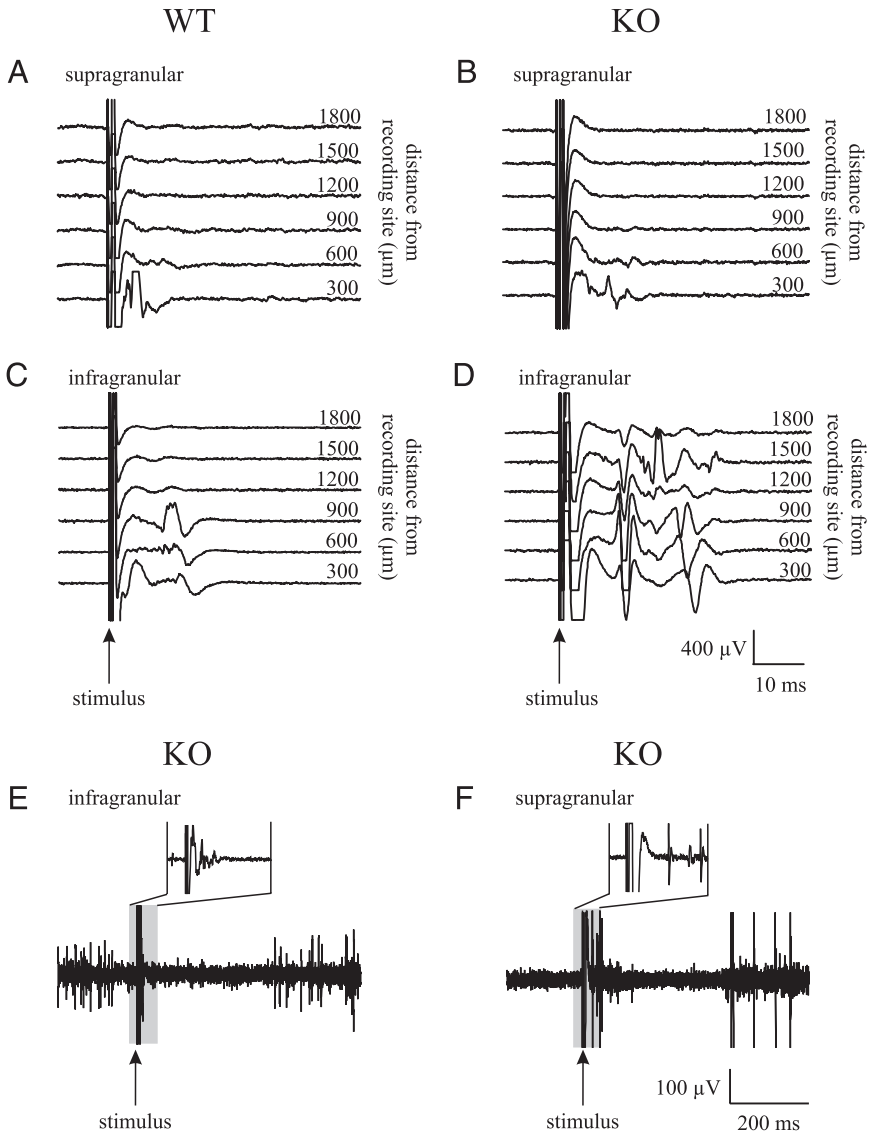

FIG. 4. Fast oscillations (FOs) evoked by intracortical microstimulation are elongated in the absence of connexin 36. *A* and *B*: FOs evoked in supragranular layers of KO mice are slightly longer and spread out across electrodes (recorded at depths of 220 μm and 279 μm, respectively). *C* and *D*: FOs evoked by intracortical microstimulation in KO mice were clearly longer and less spatially restricted than in WT mice (recorded 1,120 μm in WT and 1,191 μm in KO mice). *E* and *F*: elongated FOs and prolonged excitation in KO mice as shown in Fig. 3 are based on different neuronal mechanisms. *E*: typical situation at infragranular layers in KO mice. Raw signal as observed around electrical stimulation (same case as Fig. 3*B*). *Inset*: period after the stimulation at a higher temporal resolution. Prominent FOs are observed followed by a long inhibition. *F*: convention as in *E* but raw signal depicts typical recordings obtained from a supragranular layers (same case as shown in Fig. 3*C*). Here, a succession of rather unimposing FOs followed by prolonged spiking is observed.

to 12 nC (Fig. 6*B*, gray PSTH). The shape of this inhibitory response was comparable to that obtained with S-S direction (duration: Mann–Whitney *U* test, $P > 0.05$). Notably, the presence of elongated excitation depended on the location of the recording site. It was typically present in S-S and I-S situations but not in the other two. Therefore the prolonged excitatory responses revealed by lack of connexin 36 are determined by the recipient neural structures rather than the location of the electrical stimulation.

DISCUSSION

The present study provides evidence that inhibitory networks have a strong impact on local cortical responses after intracortical microstimulation. In particular, the long-lasting suppression of firing rate characteristically seen after microstimulation (Butovas and Schwarz 2003) is susceptible to pharmacological interference with GABAergic synaptic transmission. Furthermore, the presence of connexin 36, the constituent of gap junctions coupling intracortical inhibitory networks, shapes the spatial spread, strength, and duration of the response in complex ways.

Synaptic origin of inhibitory response

Intraperitoneal administration of CGP 46381 at a dose of 150 mg/kg in our study induced an increase of spontaneous firing rate and a reduction of electrically evoked inhibition. These findings can be attributed to the effect of $GABA_B$ receptors, given the well-established high specificity of CGP 46381 to $GABA_B$ receptors (Brucato et al. 1996; Froestl et al. 1996; Lingenhoehl and Olpe 1993). In particular, Olpe and colleagues (1993) demonstrated high specificity of CGP 46381 to $GABA_B$ receptors by showing that concentrations tenfold higher than needed to block late IPSPs were inactive in a battery of receptor assays including $GABA_A$. The dose used in the present study was fivefold higher than the reported threshold dose of 30 mg/kg (Olpe et al. 1993) and thus was well within the range of specific action to $GABA_B$ receptors. The pattern of interference—a reduction of evoked inhibition duration combined with an elevation of spontaneous firing—corresponds well to effects of $GABA_B$ blockers assessed in vitro by a wealth of studies (e.g., Connors et al. 1988). This close match suggests that receptors and inhibitory circuits located locally in the neocortex very likely contributed to it.

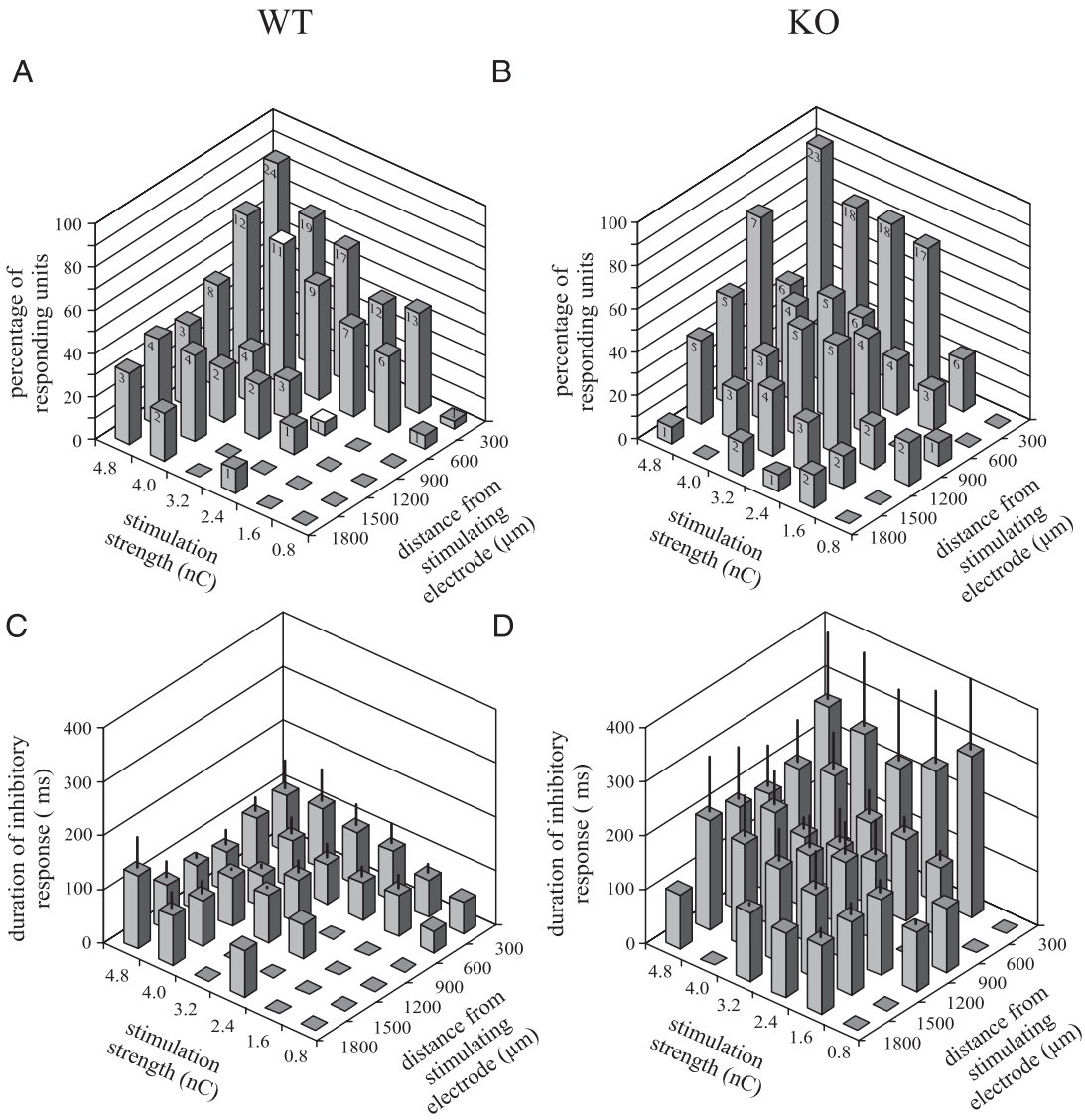

FIG. 5. Spatial spread of inhibitory responses in WT and KO mice in horizontal direction. *A* and *B*: frequency of units recorded in WT and KO mice that responded to varying stimulation intensity at different distances from stimulation electrode. Single units and multiunits recorded at all depths are pooled and analyzed together. Absolute number of recorded units for each parameter pair is indicated on the bars. Bars with a white top indicate significant differences between WT and KO mice (χ^2 test, $P < 0.05$). *C* and *D*: average duration and SD (vertical lines originating from top of bars) of inhibitory response as recorded in WT and KO mice.

Moreover, the short latency and quick succession of fast excitatory and inhibitory responses indicating monosynaptic conveyance (Butovas and Schwarz 2003) also speak in favor of this notion. Notwithstanding these arguments, possible contributions from subcortical $GABA_B$ receptors (e.g., those activated by reticular thalamic neurons in the thalamus) to the shortening of the inhibitory response by CGP 46381 cannot be excluded.

In a previous study (Butovas and Schwarz 2003) we proposed that the reduction of spontaneous firing rates elicited by microstimulation is not a result of afterhyperpolarization or decrement of network excitability. The main argument on which this statement was based was that double stimulation did not elongate the inhibitory response, a feature at odds with predictions from the notion that calcium-gated potassium channels (afterhyperpolarization) or synaptic depression is responsible. Our present finding that sublinear summation was abolished by $GABA_B$ receptor blockade adds supporting evidence to this view. Sublinear summation fits well with the widely accepted notion that repetitive or cooperative action of many GABAergic interneurons may be required to gate extrasynaptically located $GABA_B$ receptors (Isaacson et al. 1993; Mody et al. 1994; Thomson and Destexhe 1999; Thomson et al. 1996). Interestingly, $GABA_B$ receptor blockade reversed the summation from sublinear to supralinear summation, rather than simply making it linear. This raises questions about possible enhancement of $GABA_A$-based transmission under blockade of $GABA_B$ receptors. One possible mechanism—to be elucidated by future experimentation—is that blockade of *presynaptic* $GABA_B$ receptors leads to an enhancement of GABAergic transmission with accompanying adjustments in the dynamics of excitatory and inhibitory synaptic transmission (Deisz and Prince 1989; Howe et al. 1987).

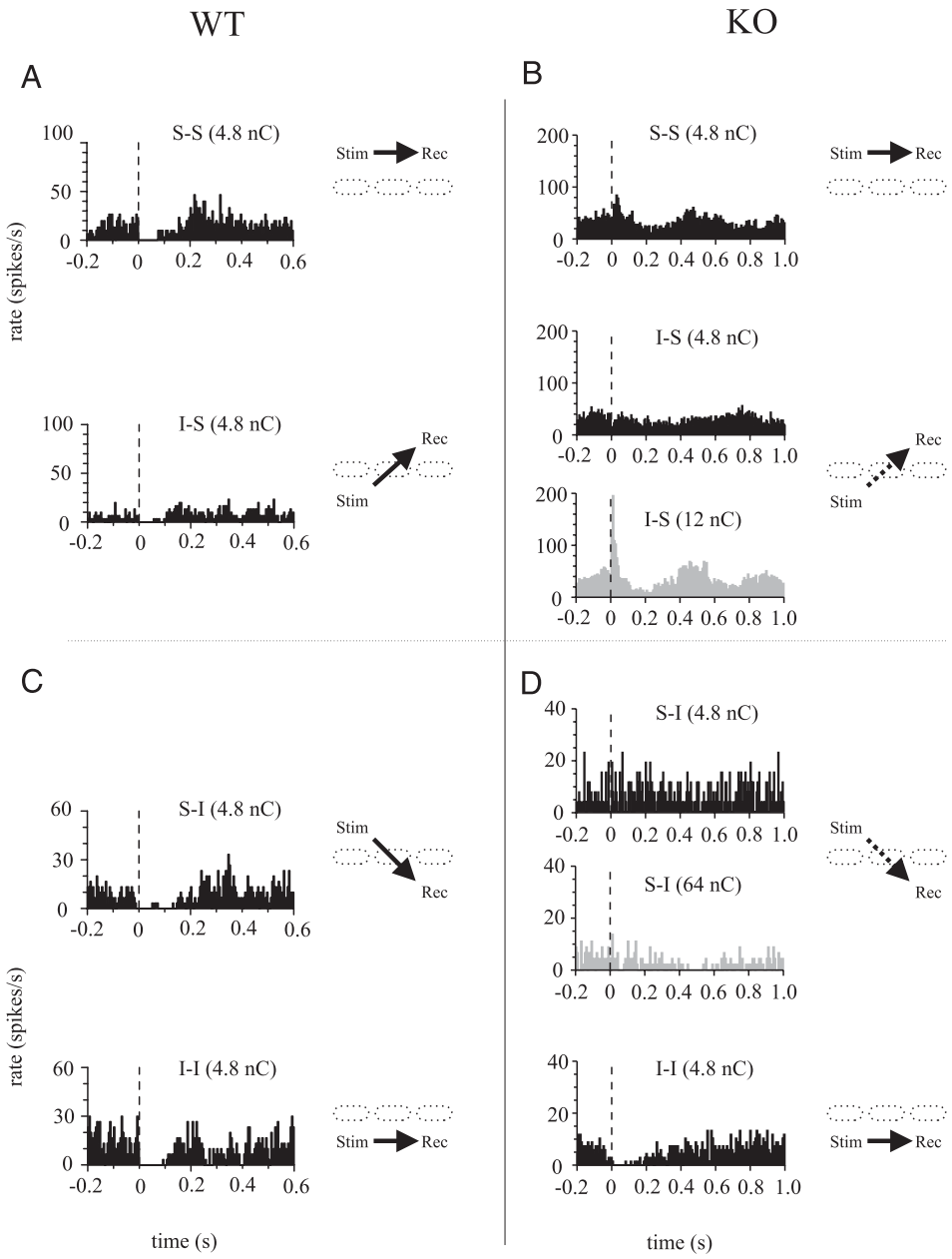

FIG. 6. Spatial spread of inhibitory responses in WT and KO mice in vertical direction. Typical PSTH as observed in WT (*left column*) and KO mice (*right column*) for all locations of stimulus and recording electrodes (e.g., I-S indicates stimulation infragranular–recording supragranular). Stimulus intensities used were 4.8 nC for all situations in WT and the horizontal directions of signal flow in KO mice (S-S and I-I). *B* and *D*: no responses were obtained in the stimulation intensity range from 0.8 to 4.8 nC in both S-I and I-S directions. In I-S direction, 12 nC evoked an inhibitory response similar to the one observed in the S-S situation (gray PSTH). In S-I direction virtually no inhibition could be evoked. Example shows a delayed (latency ≈ 300 ms) shallow inhibition evoked at 64 nC (gray PSTH). Schematics to the *right* of each PSTH depict the direction of signal flow studied on a cross section of the cortex (barrels in layer 4 are denoted; broken arrows signify the absence of inhibitory response at 4.8 nC).

Temporal coordination of electrically evoked cortical inhibition

We found that the inhibitory response to electrical stimulation in KO mice differed from that in WT mice because it lasted longer and gave rise to excitatory responses of duration ≤50 ms. This sluggishness of the long inhibitory response in KO mice speaks in favor of a certain weakness and temporal imprecision of the inhibitory response in the absence of connexin 36. It is in line with the view that the presence of gap junctions in cortical inhibitory networks plays a major role in temporally shaping firing patterns (Beierlein et al. 2000; Blatow et al. 2003; Hormuzdi et al. 2001). In view of the suggested contribution of $GABA_B$ receptors to the long inhibitory response, it should be recalled that many neurons cooperate in eliciting $GABA_B$-receptor–mediated responses. The need to activate extrasynaptic receptors implies that the temporal precision of such cooperation is determined by the speed of reuptake of GABA from the synaptic cleft, which has been reported to be faster than the time course of a miniature $GABA_A$ inhibitory postsynaptic current (Isaacson et al. 1993; Otis and Mody 1992; Solis and Nicoll 1992; Thompson and Gähwiler 1992). Functional gap junctions enable the inhibitory system to achieve high temporal precision in the millisecond (Beierlein et al. 2000; Galarreta and Hestrin 1999), and the lack of synchrony in KO mice (Blatow et al. 2003; Hormuzdi et al. 2001) is predicted to have a significant effect on the efficacy and precision with which $GABA_B$ receptors can be recruited. In conclusion, we interpret the sluggishness of the inhibition in KO mice as an expression of the impairment of temporal coordination (and concomitant inefficacy of $GABA_B$ receptor activation) within the inhibitory network when electrically decoupled.

Spatial coordination of electrically evoked cortical inhibition

We found that the horizontal spread of inhibition was principally intact in KO mice but its transmission across cortical

depth required connexin 36–containing electrical synapses. In WT mice, a stimulus intensity of 2.4–3.2 nC caused an inhibitory response that spread to the neighboring column. In the absence of connexin 36, inhibitory activity evoked by the same stimulus intensity was unable to straddle the granular layer and reached the neighboring column only at the same depth as the stimulation site. In principle, the diminished cross-layer inhibitory responses in the absence of connexin 36 may reflect properties of either inhibitory or excitatory axons straddling the granular layer (the latter giving rise to a polysynaptic response by local inhibitory neurons). It is a well-established fact that intrinsic cortical connections are highly specific (Kawaguchi and Kubota 1997): the likelihood of finding a connection between a given pair of neurons depends strongly on the location of the cells (i.e., layer) and their neuronal type (i.e., spiny, smooth, excitatory, inhibitory, etc.). Indeed, some known characteristics of specific connections, reported in visual cortex, tentatively match the present finding of weaker transmission of inhibition across the granular layer compared with horizontal directions and the asymmetry of I-S versus S-I signal transfer, and therefore may guide future attempts to elucidate the underlying mechanisms: Inhibitory axons generally show little tendency to straddle the granular layer in both directions (Watts and Thomson 2005). Furthermore, in the S-I direction, which is virtually blocked in the absence of connexin 36, layer 3 pyramids in visual cortex show a prominent excitatory connection to large layer 5 pyramidal neurons, but they do not target interneurons there. In the reverse direction (I-S, which shows existent but severed inhibitory transmission in KO mice), layer 5 pyramids do not target layer 3 pyramids, although connections to inhibitory interneurons in that layer have been found (Watts and Thomson 2005). In the horizontal direction, direct and indirect transmissions of inhibitory responses along layers have been well documented. Inhibitory basket cells extend axons as far as 1 mm in the horizontal direction (Kisvárday 1992) and about one fifth of the synaptic boutons on long horizontal axons of pyramidal cells have been reported to target putative inhibitory neurons (McGuire et al. 1991).

In line with our finding of unimpaired horizontal spread, synchronous oscillations of the membrane potential at 4 Hz (at which coupled pairs show a high coupling ratio (Galarreta and Hestrin 1999) fall off significantly within a horizontal distance of 600 μm within layer 4 (Beierlein et al. 2000)—a distance that is far smaller than the spatial spread of the inhibitory response in supra- and infragranular layers observed in the present study. Thus conductance through gap junctions between inhibitory interneurons in horizontal direction may be optimized to allow for temporal coordination but does not contribute much to the spatial spread of activity. However, the present finding of impaired spatial spread across cortical depth in KO mice does not fit this picture. Such an anisotropic pattern was not predicted from the fairly homogeneous distribution of connexin 36 across cortical layers (Belluardo et al. 2000). A possible explanation is that coupling ratios across layers are higher than those assessed in horizontal direction—a possibility that needs to be tested by future experiments using double recordings in vitro.

Further layer-specific characteristics of inhibition were unmasked by the absence of connexin 36 in KO mice. The prolonged elevation of firing rate was seen exclusively in supragranular layers and FOs were particularly affected in infragranular layers. These findings are in line with previous evidence that morphological and electrophysiological properties of the inhibitory system vary systematically between infra- and supragranular layers. Besides the above-mentioned layer-specific projection patterns, there is evidence that the impact of inhibition differs between infra- and supragranular layers: Counts of GABAergic neurons and terminals per cell have been found to be maximal in layer V in gerbil auditory cortex (Foeller et al. 2001), and the horizontal reach of inhibitory projections, as measured with electrical stimulation in rat somatosensory cortex, has been found to be maximal in infragranular layers (Salin and Prince 1996a). Furthermore, the frequency of spontaneous inhibitory input differs between supra- and infragranular layers (Jones and Woodhall 2005; Salin and Prince 1996b).

It is clear that more quantitative data about intracortical distribution of projections and their targets, as well as variation of electrical and pharmacological properties of inhibitory circuits, are needed, before the depth-specific effects observed in the present study can be fully understood. Furthermore, it must be borne in mind that the interpretation of our data with respect to cortical microcircuits rests on the assumption that the specificity of intrinsic connections in KO mice matches that in WT mice. Conversely, and most important, our findings highlight the predominance of gap junctions for shaping inhibitory responses to electrical stimulation in the neocortex: Electrical signaling is a decisive factor in establishing the cohesion of inhibitory response characteristics across cortical layers. The spread through cortical layers and both the timing and the precision of the inhibitory response depend on the presence of connexin 36.

REFERENCES

Abeles M. Quantification, smoothing, and confidence limits for single-units' histograms. *J Neurosci Methods* 5: 317–325, 1982.

Banks MI, Li TB, and Pearce RA. The synaptic basis of GABAA,slow. *J Neurosci* 18: 1305–1317, 1998.

Beierlein M, Gibson JR, and Connors BW. A network of electrically coupled interneurons drives synchronized inhibition in neocortex. *Nat Neurosci* 3: 904–910, 2000.

Belluardo N, Mudó G, Trovato-Salinaro A, Le Gurun S, Charollais A, Serre-Beinier V, Amato G, Haefliger JA, Meda P, and Condorelli DF. Expression of connexin36 in the adult and developing rat brain. *Brain Res* 865: 121–138, 2000.

Blatow M, Rozov A, Katona I, Hormuzdi SG, Meyer AH, Whittington MA, Caputi A, and Monyer H. A novel network of multipolar bursting interneurons generates theta frequency oscillations in neocortex. *Neuron* 38: 805–817, 2003.

Bolz J and Gilbert CD. Generation of end-inhibition in the visual cortex via interlaminar connections. *Nature* 320: 362–365, 1986.

Brucato FH, Levin ED, Mott DD, Lewis DV, Wilson WA, and Swartzwelder HS. Hippocampal long-term potentiation and spatial learning in the rat: effects of $GABA_B$ receptor blockade. *Neuroscience* 74: 331–339, 1996.

Buhl DL, Harris KD, Hormuzdi SG, Monyer H, and Buzsáki G. Selective impairment of hippocampal gamma oscillations in connexin-36 knock-out mouse in vivo. *J Neurosci* 23: 1013–1018, 2003.

Butovas S and Schwarz C. Spatiotemporal effects of microstimulation in rat neocortex: a parametric study using multielectrode recordings. *J Neurophysiol* 90: 3024–3039, 2003.

Connors BW and Long MA. Electrical synapses in the mammalian brain. *Annu Rev Neurosci* 27: 393–418, 2004.

Connors BW, Malenka RC, and Silva LR. Two inhibitory postsynaptic potentials, and GABAA and GABAB receptor-mediated responses in neocortex of rat and cat. *J Physiol* 406: 443–468, 1988.

Curtis DR and Lacey G. GABA-B receptor-mediated spinal inhibition. *Neuroreport* 5: 540–542, 1994.

Deans MR, Gibson JR, Sellitto C, Connors BW, and Paul DL. Synchronous activity of inhibitory networks in neocortex requires electrical synapses containing connexin36. *Neuron* 31: 477–485, 2001.

Deisz RA and Prince DA. Frequency-dependent depression of inhibition in guinea pig neocortex in vitro by GABAB receptor feed-back on GABA release. *J Physiol* 412: 513–542, 1989.

Drexler B, Roether CL, Jurd R, Rudolph U, and Antkowiak B. Opposing actions of etomidate on cortical theta oscillations are mediated by different gamma-aminobutyric acid type A receptor subtypes. *Anesthesiology* 102: 346–352, 2005.

Egert U, Knott T, Schwarz C, Nawrot M, Brandt A, Rotter S, and Diesmann M. MEA-Tools: an open source toolbox for the analysis of multi-electrode data with MATLAB. *J Neurosci Methods*. 117:33–42, 2002.

Foeller E, Vater M, and Kossl M. Laminar analysis of inhibition in the gerbil primary auditory cortex. *J Assoc Res Otolaryngol* 2: 279–296, 2001.

Fritschy JM and Brünig I. Formation and plasticity of GABAergic synapses: physiological mechanisms and pathophysiological implications. *Pharmacol Ther* 98: 299–323, 2003.

Froestl W, Mickel SJ, Von Sprecher G, Bittiger H, and Olpe HR. *Pharmacol Commun* 2: 52–56, 1992.

Galarreta M and Hestrin S. A network of fast-spiking cells in the neocortex connected by electrical synapses. *Nature* 402: 72–75, 1999.

Galarreta M and Hestrin S. Electrical synapses between GABA-releasing interneurons. *Nat Rev Neurosci* 2: 425–433, 2001a.

Galarreta M and Hestrin S. Spike transmission and synchrony detection in networks of GABAergic interneurons. *Science* 292: 2295–2299, 2001b.

Gibson JR, Beierlein M, and Connors BW. Two networks of electrically coupled inhibitory neurons in neocortex. *Nature* 402: 75–79, 1999.

Hentschke H, Schwarz C, and Antkowiak B. Neocortex is the major target of sedative concentrations of volatile anaesthetics: strong depression of firing rates and increase of GABA receptor-mediated inhibition. *Eur J Neurosci* 21: 93–102, 2005.

Hershman KM, Freedman R, and Bickford PC. GABAB antagonists diminish the inhibitory gating of auditory response in the rat hippocampus. *Neurosci Lett* 190: 133–136, 1995.

Hormuzdi SG, Pais I, LeBeau FE, Towers SK, Rozov A, Buhl EH, Whittington MA, and Monyer H. Impaired electrical signaling disrupts gamma frequency oscillations in connexin 36-deficient mice. *Neuron* 31: 487–495, 2001.

Howe JR, Sutor B, and Zieglgansberger W. Baclofen reduces post-synaptic potentials of rat cortical neurones by an action other than its hyperpolarizing action. *J Physiol* 384: 539–569, 1987.

Huntsman MM, Porcello DM, Homanics GE, DeLorey TM, and Huguenard JR. Reciprocal inhibitory connections and network synchrony in the mammalian thalamus. *Science* 283: 541–543, 1999.

Isaacson JS, Solis JM, and Nicoll RA. Local and diffuse synaptic actions of GABA in the hippocampus. *Neuron* 10: 165–175, 1993.

Jones MS, Macdonald KD, Choi B, Dudek FE, and Barth DS. Intracellular correlates of fast (>200 Hz) electrical oscillations in rat somatosensory cortex. *J Neurophysiol* 84: 1505–1518, 2000.

Jones RS and Woodhall GL. Background synaptic activity in rat entorhinal cortical neurons: differential control of transmitter release by presynaptic receptors. *J Physiol* 562: 107–120, 2005.

Kawaguchi Y and Kondo S. Parvalbumin, somatostatin and cholecystokinin as chemical markers for specific GABAergic interneuron types in the rat frontal cortex. *J Neurocytol* 31: 277–287, 2002.

Kawaguchi Y and Kubota Y. GABAergic cell subtypes and their synaptic connections in rat frontal cortex. *Cereb Cortex* 7: 476–486, 1997.

Kisvárday ZF. GABAergic networks of basket cells in the visual cortex. In: *Progress in Brain Research: Mechanisms of GABA in the Visual System*, edited by Mize RR, Marc RE, and Sillito AM. Amsterdam: Elsevier Science, 1992, vol. 90, p. 385–405.

Lingenhoehl K and Olpe HR. *Pharmacol Commun* 3: 49–54, 1993.

Markram H, Toledo-Rodriguez M, Wang Y, Gupta A, Silberberg G, and Wu C. Interneurons of the neocortical inhibitory system. *Nat Rev Neurosci* 5: 793–807, 2004.

McGuire BA, Gilbert CD, Rivlin PK, and Wiesel TN. Targets of horizontal connections in macaque primary visual cortex. *J Comp Neurol* 305: 370–392, 1991.

Mody I, De Koninck Y, Otis TS, and Soltesz I. Bridging the cleft at GABA synapses in the brain. *Trends Neurosci* 17: 517–525, 1994.

Moore CI and Nelson SB. Spatio-temporal subthreshold receptive fields in the vibrissa representation of rat primary somatosensory cortex. *J Neurophysiol* 80: 2882–2892, 1998.

Mott DD and Lewis DV. The pharmacology and function of central GABAB receptors. *Int Rev Neurobiol* 36: 97–223, 1994.

Nicolelis MA. Actions from thoughts. *Nature Suppl* 409: 403–407, 2001.

Olpe HR, Steinmann MW, Ferrat T, Pozza MF, Greiner K, Brugger F, Froestl W, Mickel SJ, and Bittiger H. The actions of orally active GABAB receptor antagonists on GABAergic transmission in vivo and in vitro. *Eur J Pharmacol* 233: 179–186, 1993.

Otis TS and Mody I. Modulation of decay kinetics and frequency of GABAA receptor-mediated spontaneous inhibitory postsynaptic currents in hippocampal neurons. *Neuroscience* 49: 13–32, 1992.

Peters A. Synaptic specifity in the cerebral cortex. In: *Synaptic Function*, edited by Edelman GM, Gall WE, and Cowan WM. New York: Wiley, 1987, p. 373–397.

Rauschecker JP and Shannon RV. Sending sound to the brain. *Science* 295: 1025–1029, 2002.

Salin PA and Prince DA. Electrophysiological mapping of $GABA_A$ receptor-mediated inhibition in adult rat somatosensory cortex. *J Neurophysiol* 75: 1589–1600, 1996a.

Salin PA and Prince DA. Spontaneous $GABA_A$ receptor-mediated inhibitory currents in adult rat somatosensory cortex. *J Neurophysiol* 75: 1573–1588, 1996b.

Solis JM and Nicoll RA. Pharmacological characterization of GABAB-mediated responses in the CA1 region of the rat hippocampal slice. *J Neurosci* 12: 3466–3472, 1992.

Staba RJ, Brett-Green B, Paulsen M, and Barth DS. Effects of ventrobasal lesion and cortical cooling on fast oscillations (>200 Hz) in rat somatosensory cortex. *J Neurophysiol* 89: 2380–2388, 2003.

Szentágothai J. The neuron network of the cerebral cortex: a functional interpretation. *Proc R Soc Lond B Biol Sci* 201: 219–248, 1978.

Tehovnik EJ. Electrical stimulation of neural tissue to evoke behavioral responses. *J Neurosci Methods* 65: 1–17, 1996.

Thompson SM and Gähwiler BH. Effects of the GABA uptake inhibitor tiagabine on inhibitory synaptic potentials in rat hippocampal slice cultures. *J Neurophysiol* 67: 1698–1701, 1992.

Thomson AM and Destexhe A. Dual intracellular recordings and computational models of slow inhibitory postsynaptic potentials in rat neocortical and hippocampal slices. *Neuroscience* 92: 1193–1215, 1999.

Thomson AM, West DC, Hahn J, and Deuchars J. Single axon IPSPs elicited in pyramidal cells by three classes of interneurons in slices of rat neocortex. *J Physiol* 496: 81–102, 1996.

Watts J and Thomson AM. Excitatory and inhibitory connections show selectivity in the neocortex. *J Physiol* 562: 89–97, 2005.

Whittington MA, Traub RD, and Jefferys JG. Synchronized oscillations in interneuron networks driven by metabotropic glutamate receptor activation. *Nature* 373: 612–615, 1995.

Zrenner E. Will retinal implants restore vision? *Science* 295: 1022–1025, 2002.

J Neurophysiol 95: 3414–3425, 2006;
doi:10.1152/jn.01060.2005.

Functional Unity of the Ponto-Cerebellum: Evidence That Intrapontine Communication Is Mediated by a Reciprocal Loop With the Cerebellar Nuclei

Martin Möck,[1,2,*] Sergejus Butovas,[1,*] and Cornelius Schwarz[1]

[1] *Abteilung für Kognitive Neurologie, Hertie-Institut für Klinische Hirnforschung; and* [2]*Abteilung Zelluläre Neurobiologie, Anatomisches Institut, Universität Tübingen, Tubingen, Germany*

Submitted 7 October 2005; accepted in final form 22 February 2006

Möck, Martin, Sergejus Butovas, and Cornelius Schwarz. Functional unity of the ponto-cerebellum: evidence that intrapontine communication is mediated by a reciprocal loop with the cerebellar nuclei. *J Neurophysiol* 95: 3414–3425, 2006; doi:10.1152/jn.01060.2005. The majority of cerebral signals destined for the cerebellum are handed over by the pontine nuclei (PN), which thoroughly reorganize the neocortical topography. The PN maps neocortical signals of wide-spread origins into adjacent compartments delineated by spatially precise distribution of cortical terminals and postsynaptic dendrites. We asked whether and how signals interact on the level of the PN. Intracellular fillings of rat PN cells in vitro did not reveal any intrinsic axonal branching neither within the range of the cells' dendrites nor farther away. Furthermore, double whole cell patch recordings did not show any signs of interaction between neighboring pontine cells. Using simultaneous unit recording in the PN and cerebellar nuclei (CN) in rats in vivo, we investigated whether PN compartments interact via extrinsic reciprocal connections with the CN. Repetitive electrical stimulation of the cerebral peduncle of ≤40 Hz readily evoked rapid sequential activation of PN and CN, demonstrating a direct connection between the structures. Stimulation of the PN gray matter led to responses in neurons ≤600 μm away from the stimulation site at latencies compatible with di- or polysynaptic pathways via the CN. Importantly, these interactions were spatially discontinuous around the stimulation electrode suggesting that reciprocal PN-CN loops in addition reflect the compartmentalized organization of the PN. These findings are in line with the idea that the cerebellum makes use of the compartmentalized map in the PN to orchestrate the composition of its own neocortical input.

INTRODUCTION

The cerebro-cerebellar projection consists of massive fiber bundles connecting neocortex and the cerebellum via an intercalated structure in the brain stem, the pontine nuclei (PN). A particular feature of this circuit is that the mapping of signals represented on the surface of the neocortex is reorganized on the level of the PN (Schwarz and Möck 2001; Schwarz and Thier 1995, 1999). Each neocortical site is mapped onto several separate compartments in three-dimensional (3D) pontine space one to several hundreds of micrometers wide. The total volume of pontine compartments subserving one spot in the neocortex has been estimated to cover a volume of 0.011 mm^3 (Schwarz and Möck 2001). The compartments do not overlap with neighboring ones receiving terminals from different sites, a characteristic which we called "nonoverlapping distribution" (Schwarz and Möck 2001). There are notable exceptions from this rule as has been demonstrated for related sites in somatotopic maps of primary and secondary somatosensory cortices (Leergaard et al. 2004), and it has been shown that somatotopy is a principle that still governs distribution of compartments in 3D space, albeit on a larger spatial scale than compartmentalization (Brodal 1968a,b; Leergaard et al. 2000; Schwarz and Möck 2001). Nevertheless, the intriguing feature of compartmentalization in the PN is that it anticipates characteristic features of the representation found in one main target structure, the granular layer in the cerebellum (called there "fractured map,") (Joseph et al. 1978; Shambes et al. 1978a,b). It has been shown that tactile signals on the two-dimensional (2D) map found in the granular layer are mapped according to rules reminiscent to the ones described in the preceding text for the PN. Signals are represented by nonoverlapping patches with sharp borders, and spatial relationship of patches cannot be predicted by the somatotopic map as found in the afferent neocortical areas (Bower et al. 1981). Presumably then the spatial reorganization of neocortical signals in the PN qualitatively reflects the specific topographical organization of signals adequate for cerebellar processing (Nelson and Bower 1990; Schwarz and Thier 1999). However, topographical reorganization by itself lends a poor raison d'être for a nucleus holding complexly organized neuronal elements and inputs from varied sources (Brodal and Bjaalie 1992; Mihailoff et al. 1989, 1992; Schwarz and Thier 1999). Pure topographical reorganization is achieved without an intervening synaptic relay in many central pathways. As an instructive example the reshuffling of retinal ganglion fibers from an organization dictated by retinal organization (macula representation on the nasal side) to one demanded by thalamo-cortical processing (macula representation in the center) within millimeters of the ocular nerve's course may be mentioned. To elucidate the PN's computational role beyond remapping of neocortical signals, it must be demonstrated if and how signals on the pontine map interact. Basically, two possibilities are to be considered: intrinsic versus extrinsic interaction. Morphological evidence in favor of intrinsic interaction is the finding that retrograde degeneration of pontine axons affected terminals and synaptic structures within the PN (Mihailoff 1978). Furthermore, communication via dendro-dendritic chemical synapses has been suggested from electron microscopic studies (Mihailoff and Border 1990; Mihailoff and McArdle 1981). Functional evidence has been more indirect. First, compound excitatory postsynaptic potentials (EPSPs) evoked from the cerebral pe-

* These authors contributed equally to this study).

Address for reprint requests and other correspondence: C. Schwarz, Hertie Institut für Klinische Hirnforschung, Universität Tübingen, Abteilung für Kognitive Neurologie, Otfried Müller Str. 27, 72076 Tübingen, Germany (E-mail: cornelius.schwarz@uni-tuebingen.de).

The costs of publication of this article were defrayed in part by the payment of page charges. The article must therefore be hereby marked "*advertisement*" in accordance with 18 U.S.C. Section 1734 solely to indicate this fact.

duncle have been elicited in vivo (Allen et al. 1975) and in vitro (Möck et al. 1997). Second, antidromic stimulation of pontine axons from the cerebellum evoked repetitive firing in PN neurons (Sasaki et al. 1970). Both findings have been interpreted as evidence for intrinsic pontine connections. On the other hand, intrinsic axonal branching of projecting fibers has not been detected in seven cases of successful, retrograde axonal fillings from the middle cerebellar peduncle (Shinoda et al. 1992). Notwithstanding the rather unsettled question whether intrinsic processing exists, the alternative possibility of extrinsic processing has been clearly elucidated using morphological methods. All pontine signals flow to the cerebellar nuclei (CN), either directly (Mihailoff 1993; Shinoda et al. 1992) or via the cerebellar cortex. In turn, the CN send an excitatory feedback projection that shows a patchy divergence (Brodal and Szikla 1972; Brodal et al. 1972b; Kitai et al. 1976; Schwarz and Schmitz 1997; Tsukahara et al. 1971; Verveer et al. 1997; Watt and Mihailoff 1983), and thus seems optimally suited to modulate subsets of pontine compartments in conjunction.

The answer to the problem whether and how intrinsic and/or extrinsic interaction of pontine signals modulate PN activity offers important clues to pontine function. The present study therefore revisited the question of intrinsic pontine circuitry with intracellular fillings and extended it to functional investigation using double patch-clamp recordings in vitro. The extrinsic pathway via the CN was studied using multielectrode recording and stimulation in vivo. While no supporting evidence for intrinsic pontine circuitry was found, we elucidate functional properties of a reciprocal ponto-nuclear connection.

METHODS

All experimental procedures were performed in accordance with the policy on the use of animals in neuroscience research of the Society for Neuroscience and German national law.

Preparation of slices and intracellular staining

The intrapontine course of axons of ponto-cerebellar projection neurons was studied in PN neurons stained by intracellular dye injection via conventional sharp microelectrodes. The neurons were either filled with Lucifer yellow (Aldrich, Milwaukee, WI) in slices of slightly fixed tissue or with neurobiotin (Sigma, St. Louis, MO) in acute slices.

The staining procedure and analysis of PN neurons filled with Lucifer yellow has been reported in detail elsewhere (Schwarz and Thier 1995, 1996). Briefly, deeply anesthetized adult Lister hooded rats in which ponto-cerebellar projection neurons were prelabeled by injection of retrograde tracers (Fluorogold, Fluorochrome, Englewood, CO; rhodamine labeled latex microspheres, Lumafluor) into the brachium pontis were transcardially perfused with phosphate buffer (PB, 0.1 M) followed by 2% paraformaldehyde in PB. The pontine brain stem of their brains was cut into coronal slices of 300-μm thickness using a vibrating microtome (Campden, London, UK). The slices were stored in cold PB until they were transferred to a modified epifluorescence microscope (Leica, Stuttgart, Germany). The somata of identified ponto-cerebellar projection neurons were impaled by glass microelectrodes with bended tips that were filled with 5% Lucifer yellow in LiCl (resistance: 150–300 MΩ). Under visual control, the dye was iontophoretically applied (negative square wave currents pulses, 3–10 nA at 2 Hz) until the dye began to leak out of the soma. The slices were then cut on a freezing microtome (80- μm thickness), mounted onto subbed slides, dried, and coverslipped with alkylacrylate. Finally, the sections were examined under an epifluorescence microscope (filters: Leica E3, A, and N1.2), and the cells were reconstructed using camera lucida drawings.

The preparation and maintenance procedures of acute slices for neurobiotin fillings were similar to those used for intracellular recordings of PN neurons (Möck et al. 1997; Schwarz et al. 1997). Deeply anesthetized Lister hooded rats (18- 24 days old) were decapitated, and their brains were carefully removed and immediately cooled in artificial cerebrospinal fluid [ACSF, containing (in mM) 124 NaCl, 5 KCl, 1.2 KH_2PO_4, 1.3 $MgSO_4$, 26 $NaHCO_3$, 2.4 $CaCl_2$, and 10 D-glucose bubbled with 95% O_2-5% CO_2, 4°C]. After isolating the pontine brain stem parasagittal slices were cut on a vibrating microtome (Leica, Wetzlar, Germany) to a thickness of 400 μm. For recovery, the slices were stored in ACSF at room temperature for 2 h. Subsequently, they were transferred to a submerged recording chamber and superfused with carbogenated ACSF at 35°C. Standard intracellular current clamp recordings were performed with glass microelectrodes filled with 2% neurobiotin in 3 M potassium acetate (50–100 MΩ) using an Axoclamp 2A amplifier (Axon Instruments, Foster City, CA) in the bridge mode. Once a cell was successfully penetrated and had developed a stable somatic membrane potential, neurobiotin was iontophoretically applied by positive square wave current pulses (0.5–0.8 nA, 0.5-s duration at 1.5 Hz) for two periods of 15 min. Thereafter the slices were kept in the recording chamber for 30 min to allow dispersion of the dye, subsequently fixed by immersion in 4% paraformaldehyde in PB overnight, cryoprotected in 30% sucrose in PB, and cut on a freezing microtome to a thickness of 60 μm. Only one cell was filled per slice. To visualize filled cells, the sections were first treated with 3% H_2O_2 for 30 min to block endogenous peroxidases. After several rinses in PB, the sections were processed through an ascending series of dimethylsulfoxide (5–40% in PB) and 0.5% Triton X-100 in PB (30 min each) to facilitate the penetration of the detection system (Lübke et al. 1996). For detection of neurobiotin, the sections were incubated with an avidin-biotin-peroxidase complex (Vectastain, Vector Laboratories, Burlingame, CA) overnight at 4°C. Next, they were incubated in 0.05% diaminobenzidine (Sigma) for 10 min and then stained with 0.05% diaminobenzidine and 0.005% H_2O_2 in PB under visual control (2–3 min). The reaction was stopped by several rinses in PB (4°C), and the sections were mounted on subbed slide, dried and dehydrated, and coverslipped with Entellan (Merck, Darmstadt, Germany). Stained PN neurons were examined with a light microscope (Leica Diaplan, Wetzlar, Germany), and those cases in which an axon was unequivocally discernable were reconstructed from camera lucida drawings.

In vitro electrophysiological procedures

For double patch recording in vitro, parasagittal slices of the pontine brain stem were prepared and maintained as described in the preceding text. The thickness of the slices, however, was reduced to 275 μm. Somatic whole cell patch-clamp recordings of pairs of PN neurons were performed with glass microelectrodes (resistance: 5–7 MΩ) filled with a solution containing (in mM) 131 K-gluconate, 5 NaCl, 5 K^+ HEPES, 5 EGTA, 4 K^+ -ATP, 0.3 Na^+ -GTP, and 0.5 $CaCl_2$ adjusted to pH 7.3 with KOH. The patch procedure was visualized using a motorized (Luigs and Neumann, Ratingen, Germany) microscope (Axioscope, Zeiss, Göttingen, Germany) with a water-immersion objective (×40, Zeiss numerical aperture: 0.75), infrared illumination, Normarski optics, and an infrared-sensitive CCD camera (Newvicon C2400-07-C, Hamamatsu, Japan). Current-clamp recordings were done at room temperature using two NPI BA-1S amplifiers (NPI electronic, Tamm, Germany) in the bridge mode. Voltage recordings were digitized at a sampling rate of 20 kHz using a PC with a 1401plus interface and Spike2 software (Cambridge Electronic Design, Cambridge, UK). For simultaneous recordings from two PN neurons, pairs of cells were selected that laid in close proximity (both somas visible on the monitor screen, i.e., located

within an area of 72 × 56 μm). To test whether these cells were interconnected by chemical or electrical synapses, we alternately applied clearly suprathreshold depolarizing current pulses (300 ms) to these cells while recording the membrane potential of both of them permanently for a period of 2.5 s. In 5 of 20 cases, we added 10 mM trimethylamine (Sigma) to the bath solution to facilitate the detection of possibly existing intercellular connections via gap junctions (Lee et al. 1996; Spray et al. 1981).

Surgery and in vivo electrophysiological procedures

Experiments were performed on 12 Sprague-Dawley albino rats (Charles River, Sulzfeld, Germany). The rats were anesthetized with a mixture of ketamine (175 mg/kg) and atropine (1 mg/kg) administered intraperitoneally. Anesthesia depth was maintained to ensure the absence of limb withdrawal and corneal reflexes. Additional injections of 25 mg/kg ketamine were given when needed. After mounting the head in a stereotaxic frame, the scalp was incised and small holes were drilled in the skull at B-7.5, L1 on the left side and at B-11.5, L3.2 (coordinates as given by Paxinos and Watson 1986) on the right side ~1 mm^2 to allow insertion of two multielectrode arrays into the PN (left hemisphere) and CN (right hemisphere). In some experiments, a third trepanation at B-5.5, L2.4 was performed to allow the insertion of a single etched and insulated tungsten microelectrode into the cerebral peduncle for electrical stimulation. While moving the electrode dorsoventrally into the brain, bursts of negative current pulses (100 μA at 300 Hz for 100 ms, 300-μs pulse duration, burst frequency: 1 Hz) were delivered to different sites of the electrode track until contralateral movements of the whole body were elicited. Typically, such a site was found at a depth of ca. 7–8 mm. The electrode was then fixed to the skull with dental acrylic. For the recording session, the cerebral peduncle was stimulated with single, 300-μs current pulses at a frequency <0.5 Hz. Stimulation amplitude was varied between the minimum current to evoke cerebellar neuronal responses and 100 μA. In the experiments using intra-pontine stimulation and recording, a ventral approach was used. The skin was cut at the neck and the trachea prepared, incised and intubated for artificial ventilation with oxygen (1 Hz, 1.2 ml; Small Animal Ventilator; Harvard Instruments, Kent, UK). The neck muscles were dissected and moved laterally together with the trachea to lay open the base of the scull overlying the pontine brain stem. After trepanation above the brain stem, the PN were accessed directly from the ventral surface of the brain stem.

Multielectrode arrays were custom made from electrolytically etched (tip angle: 8°), 100-μm-diam tungsten rod (7190, A-M Systems) as reported previously (Butovas and Schwarz 2003). Electrodes were loaded into polyimide tubing and assembled into arrays consisting in two rows of four microelectrodes (tip distance: 250 μm) for simultaneous recordings in PN and CN and one row of seven electrodes (tip distance: 200 μm) for intra-pontine stimulation and recordings. The impedance of the electrically insulated electrodes was >2 MΩ. The connection to the head stage of the amplifiers was realized by a standard micro connector (pin to plug, Bürklin, München, Germany) that was modified by computer-aided drilling of small holes (200-μm diam, 1.5 mm depth) into the gold pins for insertion of the tungsten rods. The electrical connection between electrodes and connector was made by conductive glue (E-Solder 3021, Epoxy Produkte, Fürth/Odw, Germany).

Recording was performed by a multichannel extracellular amplifier (MultiChannelSystems, Reutlingen, Germany). The extracellular potentials were AC-coupled, amplified by a magnitude of 5,000, and band-pass filtered between 200 Hz and 5 kHz. For each channel, a threshold for spike detection was adjusted. Data were digitized at 20-kHz sampling rate and stored on a PC's disk as spike cutouts (length: 2 ms, 1 ms before and 1 ms after the potential crossed the threshold) or continuous raw data. Multielectrode recordings were performed while the electrode arrays were lowered into the brain using a microdrive. For PN recordings, the electrode array was lowered through visual cortex, superior colliculus and pontine reticular formation. Characteristic 1-Hz bursts of PN action potentials were typically encountered at a depth ~8 mm and could be easily discriminated from the continuous spontaneous firing of reticular cells dorsal to the PN. In many cases, penetration of the cerebral peduncle was recognized by small amplitude neuronal noise which was modulated at 1 Hz as well, most probably reflecting the activity of peduncular fibers. All pontine recordings were carried out in ventral portions of the PN. The long axis of the array was oriented in laterolateral direction. For CN recordings, the electrode was lowered through the cerebellar cortex. Spike trains of Purkinje cells recorded were checked for the occurrence of complex spikes. The CN was reached at about 4 mm depth after a silent period of different length while the electrode passed through the cerebellar white matter. A distinctive feature of CN was the 1-Hz activity within its spike trains and the lack of complex spikes encountered. CN recordings were done in the lateral and interposed nucleus. The long axis of the array was oriented in laterolateral direction.

For intra-pontine stimulation and recording, the one-dimensional electrode array was introduced into the pontine nuclei from the ventral surface at an angle of 45° such that the electrodes penetrated the ventral PN in caudorostral direction. The first electrode in the row (located close to the ventral surface i.e., the brachium pontis) was then used for electrical stimulation while the others recorded the stimulus effects on neuronal firing rates (they spanned the dorsoventral extend of the ventral PN such that the 1 farthest away from the stimulus electrode was close to the cerebral peduncle). Very small stimulus intensities covering the threshold to evoke responses were used (8 μA, pulse durations from 100 to 600 μs resulting in charge transfer of 0.8–4.8 nC). All electrode positions for recording and stimulation were confirmed by locating electrolytic lesions (25 μA cathodal, 5 s) in Nissl-stained sections.

Analysis of spike trains

Spike sorting of single units was performed using a principal component clustering algorithm (Egert et al. 2002). Units were classified as single units if the interval between 2 SD from the mean voltage before the spike (1st bin of the cutout) and 2 SD from the mean voltage at the peak of the spike was ≥2 SD (as determined from the 1st bin); the spike train showed an absolute refractory period of 1 ms; and the SD of the latency of the peak of the spike after passing the threshold was <0.3 ms. All others were classified as multiunit data. The present sample comprises a total of 106 single units and 124 multiunits. Because results were comparable with the two classes of spikes, they were pooled for the analyses presented in this study.

Firing rate of neurons with respect to an event (i.e., electrical stimulation) was computed as spike renewal function (abbreviated here as perievent time histogram, PETH) at a resolution of 0.1 ms (bin width) and a moving window of 1 ms duration as described by (Abeles 1982b). This algorithm yields a measure of firing rate over time and allows the assignment of lower and upper confidence limits (in this study $P = 0.05$ and 0.95, respectively) to assess statistical significant deviation of firing rate as compared with a reference period. In the present study, fast trains of electrical stimuli (≤40 Hz) were delivered to the brain, thus conditions within the perievent time of subsequent PETHs in a train of stimuli cannot be considered as independent. Therefore firing rates in response to successive electrical stimuli were related to a common point of reference. To this end, the algorithm applied here deviated from that of (Abeles 1982b) in taking the reference firing rate for all PETHs in one stimulus train from a 1-s period of spontaneous firing immediately before the *first* stimuli within trains were delivered. The confidence limits offered by the renewal function were used to extract three parameters from the PETHs (see Fig. 4). First, the excess spikes were defined as the integral of the firing rate above/below the confidence limits. It signi-

fies the significant part of the average additional (excess of the upper limit, positive sign) or missing spikes (excess of the lower limit, negative sign) in response to a stimulus. Second, the latency after the stimulus event to reach the confidence limit for the response in question was computed. Finally, the response width was computed as the duration for which the firing rate exceeded the respective confidence limit.

Statistics

Population data are depicted in median [5% percentile, 95% percentile] or if normally distributed in means ± SD. As nonparametric test for nonnormally distributed variables, the Mann-Whitney *U* test was used.

RESULTS

We approached the question of possible communication between pontine compartments in three different ways. We first sought to find evidence for direct intrinsic connectivity between PN neurons. Toward this goal we searched axons of intracellularly filled cells in vitro for intrinsic branching. In a second step, we searched for electrical and/or chemical synapses between PN neurons using double patch recordings in vitro. In a final section, we report results gained from stimulation of activity in PN and CN using stimulation in the cerebral peduncle or from within the PN.

Do ponto-cerebellar axons give off intrapontine axon collaterals?

In the present study, a total of 218 pontine projection neurons filled with either Lucifer yellow ($n = 155$) in fixed slices or with neurobiotin ($n = 63$) in living slices where used to analyze whether their axons branch inside the PN. Within this sample, 59 axons were clearly distinguishable from dendrites by means of a small and constant caliber and the lack of any kind of appendages (Schwarz and Thier 1996). As projection neurons were cut during the slicing of the tissue, the axons were contained to varying lengths inside the slice (apparent length). This apparent length varied between 11 and 738 μm (median: 150 μm). Often the course of the axon was found to be meandering within the PN at seemingly arbitrary paths before approaching the brachium pontis. The actual entry into the brachium was observed in two cases. Many axons, however, could be followed for a considerable stretch within the PN outside the range of the parent cell's dendritic tree (52 of 59). A previous study indicated that the mean volume of a pontine compartment in rats is about 0.011 mm^3 (Schwarz and Möck 2001). It, therefore appears that about half of the axons studied here displayed an apparent length that extended the radius of a typical compartment assuming a radial shape and therefore have high probability to show axonal parts that passed neighboring compartments (the median apparent length of axons: 150 μm; radius of a sphere with a volume of 0.011 mm^3: 139 μm; indicated in Fig. 1*A*). Figure 1*B* shows the distribution of apparent axonal length within our sample. Gray columns are axons that display lengths under 150 μm and thus may be included within their parent compartment; black columns represent axonal length that had a high chance to display parts outside the parent compartment. However, the search for branching points on all stained axons using close microscopic inspection did not reveal a single collateral branching. Based on this material, we conclude that 59 axons do not branch within the parent compartment and roughly half of them do not do so in the neighboring compartment. Therefore we can exclude at a fairly high certainty that intra-compartment connections and inter-compartment connections between neighboring compartments exist. Our data set provides a less reassuring base to judge possible branching at remote sites and within the brachium pontis.

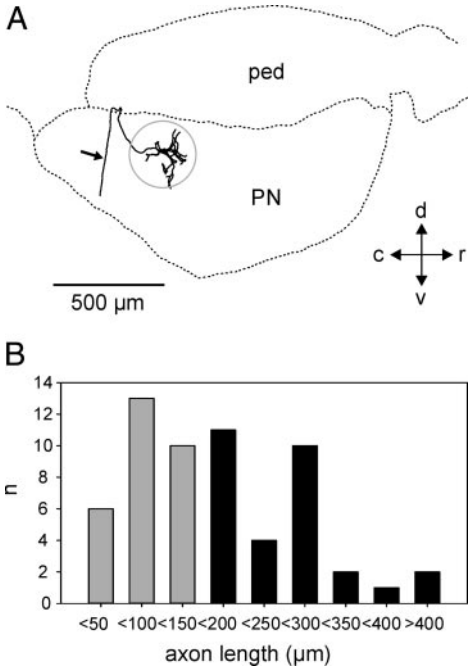

FIG. 1. Absence of intra-pontine axonal branching of pontine nuclei (PN) neurons. *A*: camera lucida drawing of a neurobiotin-filled PN neuron in a parasagittal slice of the PN. In this example, the detectable part of the axon (arrow) had a length of 738 μm almost reaching the ventral edge of the PN. The dashed circle surrounding soma and dendrites indicates the average diameter of a pontine compartment as defined by its afferent terminations (for details see text). *B*: distribution of the length of axons of PN neurons filled with either Lucifer yellow or neurobiotin ($n = 59$). The axon length was measured from camera lucida drawings. The median of the distribution was 150 μm, i.e., the gray bars represent those cases below the median ($n = 28$). c, caudal; d, dorsal; ped, cerebral peduncle; r, rostral; v, ventral.

Paired whole cell patch-clamp recordings of pontine nuclei neurons in vitro

To approach the question of intrapontine connections on a functional level, we performed double patch-clamp recordings of neighboring neurons. This method, in addition to unveil axonic synaptic interconnections missed by the morphological analysis, would in addition allow us to detect dendro-dendritic connections via electrical or chemical synapses. The possibility of dendro-dendritic connections is suggested by the membrane specializations and dendritic appendages of atypical (non-spinous) morphology (Schwarz and Thier 1996). Although there is no evidence for gap junctions in rat PN so far, serial chemical synapses have been suggested based on electron microscopic observations (Mihailoff and McArdle 1981). To test whether one or more of these types of connections exist, we performed simultaneous whole cell patch-clamp recordings from proximate PN neurons. Twenty pairs of neurons were accepted for this test according to the following criteria: they

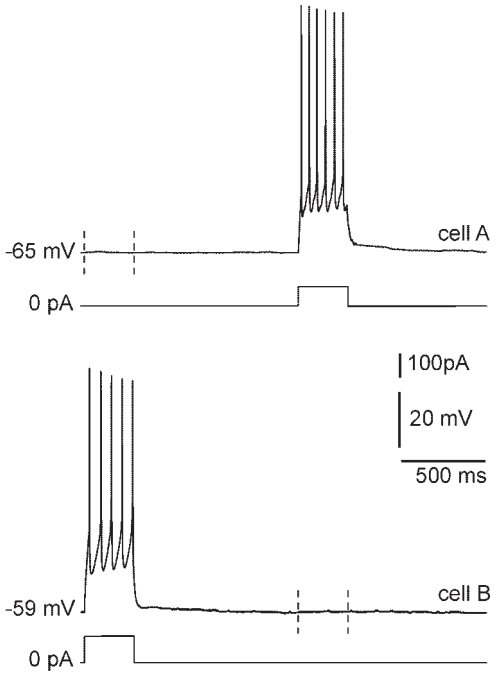

FIG. 2. Lack of synaptic interactions between proximate PN neurons. The example shows the membrane potential traces from 2 PN neurons recorded simultaneously for 2.5 s. The DC current commands are shown directly below the corresponding voltage traces. Note that the voltage traces in cell A as well as in cell B show neither postsynaptic potentials nor spikelets during the periods (bordered by vertical dashed lines) in which cell B or cell A, respectively, were driven above firing threshold by intracellular current application.

developed a stable somatic membrane potential without spontaneous firing, had ≥150 MΩ apparent steady-state input resistance, and clearly overshooting action potentials in response to suprathreshold depolarizing current pulses. On average, these cells had a somatic membrane potential of −60.8 ± 4.9 mV, a firing threshold of −38.4 ± 5.5 mV, and an apparent steady-state input resistance of 357 ± 133.6 MΩ (when tested with −10 pA pulses). Furthermore, these cells displayed a marked firing rate adaptation when depolarized across threshold and a rapid inward rectification in response to negative current pulses (−10 to −100 pA). Therefore their membrane properties were comparable to those observed with sharp electrode recordings at physiological temperature (Schwarz et al. 1997).

A typical observation made during simultaneous recordings of two neighboring PN neurons is shown in Fig. 2. Both cells were alternatingly stimulated by intracellular current application. Suprathreshold depolarizing current pulses evoked a spike train in the cell receiving the current pulse. However, during the time period in which one of the cells was activated, we did not detect any corresponding changes in the membrane potential of the other cell: neither postsynaptic potentials evoked via chemical synapses nor spikelets transmitted via gap junctions. The same negative result was obtained in the remaining 19 pairs of cells. Because the junctional conductance of electrical synapses is controlled by the internal pH, i.e., acidification reduces the conductance and vice versa (Spray et al. 1981), we applied 10 mM trimethylamine to the bath solution in five cases to increase the chance to detect electrical coupling. Alkalinization of the internal pH, however, did not result in the disclosure of electrical coupling. Therefore we conclude that synaptic communication between proximate neurons is not a prevailing feature in rat PN.

Responses of PN and CN units to stimulation of cerebral peduncle

An alternative way how communication between pontine compartments could be established is via extrinsic pathways—in particular the reciprocal connection to the CN. We therefore extended our investigations to in vivo firing of PN and CN neurons using simultaneous recordings in the two structures with multielectrode arrays. Electrical stimulation in the cerebral peduncle, the afferents to the PN, evoked PN excitation at a mean latency of 4.0 ms and CN excitation at a latency of around 5.6 ms (single cathodal pulse, duration: 0.3 ms, amplitude: 100 μA, statistics given in the following text; Figs. 3 and 4). This pattern is consistent with a direct route of activation via excitatory synapses between PN and CN (Mihailoff 1993) but is not compatible with a route of activation via the cerebellar cortex. The reason is that Purkinje cells—the only output of the cerebellar cortex—would be expected to evoke an early inhibitory response in CN neurons (Ito et al. 1970). Following the fast excitatory response, CN firing was strongly suppressed for a period of time. Considering the activation latency of Purkinje cells found earlier (Schwarz and Welsh 2001), this phenomenon could in principle be based on Purkinje cell inhibition. Figure 3 plots examples of Purkinje cell responses of the earlier study together with the CN recordings of the present study. Purkinje cell activation evoked from deep layers of motor cortex displays a latency of

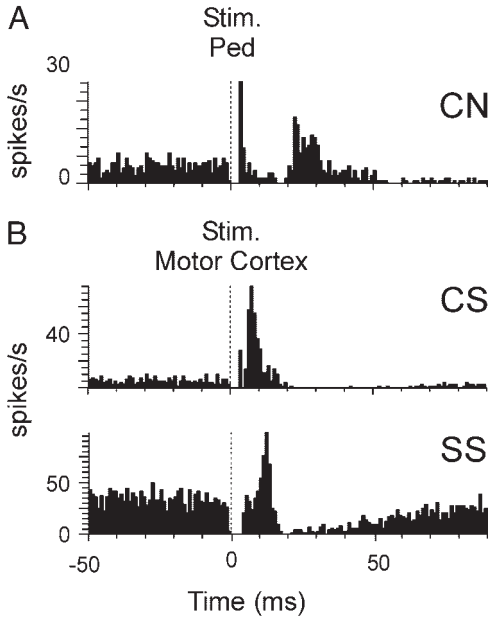

FIG. 3. Fast cerebellar nuclei responses evoked by electrical stimulation in the cerebral peduncle are not compatible with conveyance via the cerebellar cortex. *A*: typical evoked cerebellar nuclei (CN) response. The short-latency excitation arrives at a latency of ~5 ms and is followed by an inhibitory period and a 2nd activation at ~20 ms. *B*: Purkinje cell response evoked from motor cortex for comparison (data from Schwarz and Welsh 2001). Response of simple spikes (SS) and complex spikes (CS) are evoked at a considerably later point in time as compared with the CN response (~11 ms; see DISCUSSION for details). Histogram bin width: 1 ms.

10–11 ms (Schwarz and Welsh 2001), fitting well with the suppression of CN neurons observed after peduncular stimulation (even taking account of some extra run time of action potentials from motor cortex to the site in the peduncle where the stimulation was performed in the present study—the latency difference is not expected to exceed 2 ms). In view of the restriction of targets of the PN to the cerebellar cortex and the CN, we conclude that the fast CN excitation reflects direct activation via collaterals of excitatory mossy or climbing fibers originating in the PN and inferior olive and possibly other precerebellar nuclei. Finally the period of suppressed firing rate was then interrupted by a rebound excitation that was without counterpart in PC firing and therefore was possibly based on intrinsic properties of CN neurons (Jahnsen 1986; Kitai et al. 1977; Llinás and Mühlethaler 1988; McCrea et al. 1977).

Figure 4 demonstrates the responses of four PN and four CN units recorded simultaneously to the same stimulation in the cerebral peduncle. After the sharp early excitation (★; 80 of 125 PETHs exceeded the confidence interval of 95%), PN neurons typically showed a weaker second excitatory response at a latency of ~15 ms which reached significance in 76 of 125 cases (Fig. 4, ●). In addition, all PN trains showed a very long

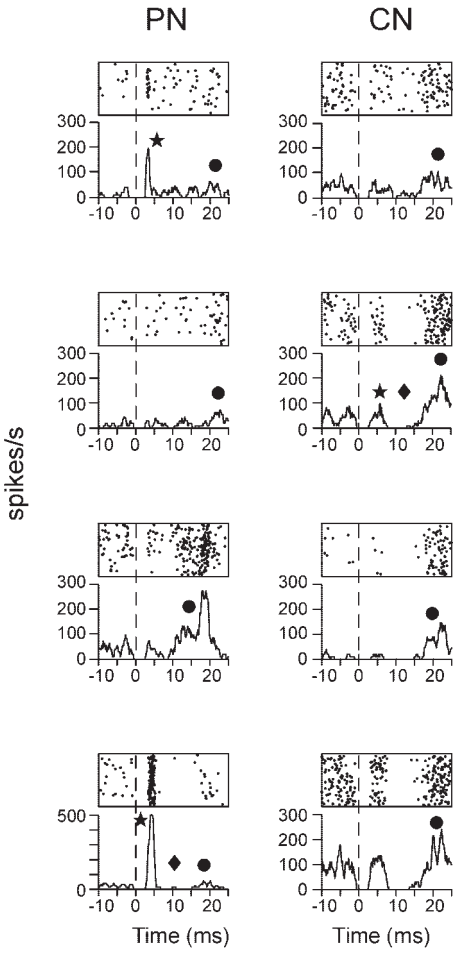

FIG. 4. Fast succession of responses to stimulation in the cerebral peduncle in PN and CN. Example of 8 PETHs and raster plots (top) recorded simultaneously on 2 2×4 electrode arrays in PN and CN. Similar response elements can be seen in both structures. The typical response is a fast excitation at successive latencies (PN: ~4 ms; CN: ~5.6 ms; ★) followed by an inhibition (◆) and a 2nd activation at 15 –to 20 ms (●). Histogram bin width: 0.1 ms; - - -, time of stimulation.

suppression of firing rate lasting well beyond the two excitatory peaks just described (duration ≤300 ms in some cases, see for an example Fig. 7*A*) that was not present when stimulating from within the PN. Consistent with a diverging projection pattern of PN efferents, the fast excitation of CN neurons reached only half the strength as the one in the PN and was observed with lower probability (Fig. 4, ★; 28 of 64 PETHs). The mean latency difference between PN and CN responses of 1.6 ms is well consistent with a monosynaptic conveyance of activation (PN: 4.0 ± 1.0 ms, $n = 80$; CN: mean 5.6 ± 1.6 ms, $n = 28$, Student's t-test, $P < 0.01$). The short-latency CN response was typically followed by two more robust features of neuronal response: a suppression of firing rate (50 of 64 at an average latency of 6.6 ± 1.0 ms, Fig. 4, ◆) and a second excitation at a latency of 17.1 ± 2.1 ms (53 of 64, Fig. 4, ●).

In a next step, we investigated whether the neuronal responses of PN and CN just described were able to follow repetitive inputs from neocortical fibers by analyzing responses to bursts of five stimulation pulses at frequencies of 5, 10, 20, and 40 Hz applied to the cerebral peduncle (Fig. 5*A*). The general finding was that the short-latency excitatory peak in PN and CN survived repetitive stimulation at all frequencies. In some neurons, even an increment in the short-latency response could be observed (Fig. 5, *B* and *C*). The late excitation, however, was highly sensitive to repetitive stimulation. It was visible with burst stimuli delivered at the lowest frequency tested (5 Hz) but was significantly suppressed applying higher stimulus frequencies, particularly so in the CN.

For the quantification of responses to repetitive stimulation, only stronger responses (minimum 0.1 excess spikes) were selected. The rational for this selection was that artifacts introduced by the detection of a response using a threshold are minimal if responses far exceeding the threshold are considered. Forty-six PN units showed short-latency responses exceeding 0.1 excess spikes. These units generated an average of 0.41 excess spikes at a latency of 4.1 ms. The duration of significant elevation of firing rate was 2.1 ms. The population data of excess spikes, latency, and response duration showed a robust—yet on average unchanged—excitatory response to pulses in bursts from 5 to 40 Hz (Fig. 6*B*). Statistical testing was performed by grouping the responses as follows. Group 1 included all responses to the first pulses in a stimulus train irrespective of stimulation frequency. Groups 2–5 included the responses to the remaining stimuli ordered with respect to frequency. Applying a one-way ANOVA, it was then tested if the responses to repetitive stimuli differed significantly from the responses to the first stimulus in a train. For the short-latency response of PN trains, the null hypothesis had to be accepted ($P > 0.05$) that responses to different stimulus frequencies were indistinguishable to the response after the first pulse testing three variables (excess spikes, latency, and response width). The PN response observed at longer latencies (14 ± 2.5 ms) exceeded in only 10 of 125 cases the criterion of 0.1 excess spikes. This response was sensitive to repetitive stimulation in a frequency-dependent fashion such that higher frequencies tended to evoke smaller late responses. Statistical testing reached significance in the strength of the response (1-way ANOVA, $P = 0.03$). The multiple comparisons (Scheffé), however, did not reach significant results. The closest to significance was the difference between the first

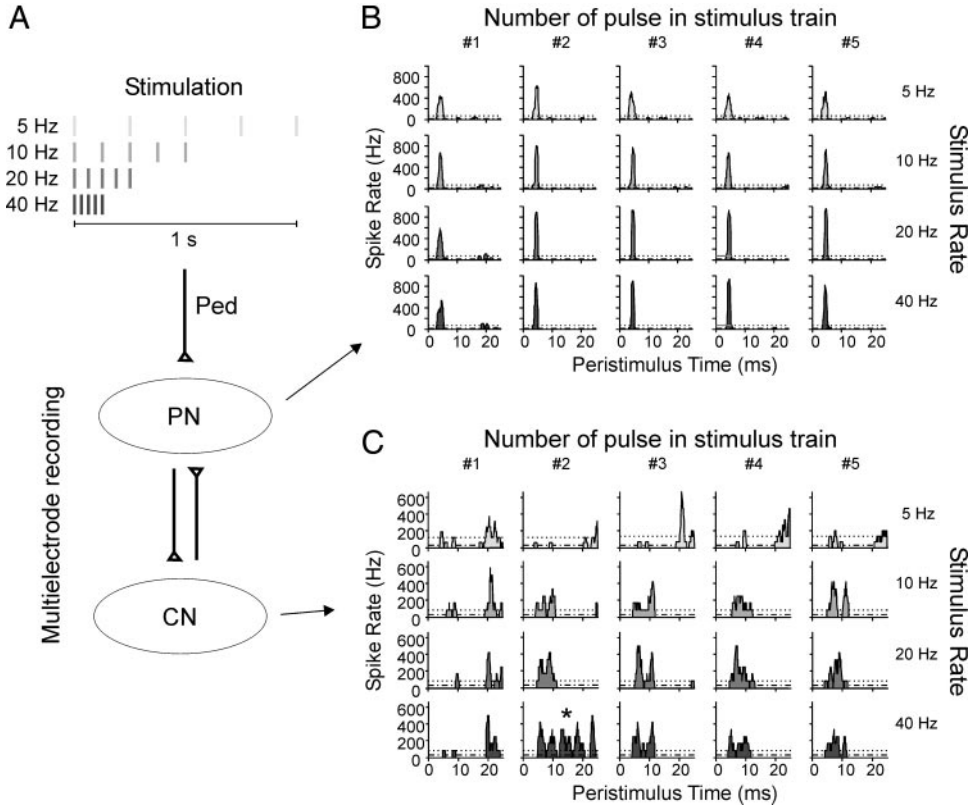

FIG. 5. PN and CN evoked activity follows rapid repetitive stimulation in the cerebral peduncle. *A*: experimental situation. Bursts of 5 electrical stimulation pulses in the cerebral peduncle (marked as ticks, gray code indicates frequency) were given at different frequencies in pseudorandom order. Evoked activity was recorded along the disynaptic pathway in the PN and the CN. *B*: example of a single unit recording in the PN. Gray levels mark stimulation frequency. Each PETH is triggered by a pulse in the train (columns) at different frequency (rows). The stimulus pulse occurred at *time 0*. Horizontal broken lines depict mean firing rate and 95% confidence interval. Histogram bin size 0.1 ms. *C*: same format as in *B* but CN single unit. Note in both recordings the stability of the fast excitatory peak with respect to stimulus repetitions. Note also the vanishing of the second excitation with repetitive stimulation at higher frequencies. The star denotes a special situation that occurred frequently after the 2nd pulse at 40 Hz in the CN. Here the late excitation evoked by the 1st pulse interacted with the fast response to the 2nd pulse. Because the late excitation adapts with high frequencies, such response interaction was not observed with further repetitions of the stimulation.

pulses and the group of 40-Hz pulses ($P = 0.06$, marked with a white circle in Fig. 6). The latency and precision (response width) of the responses during repetitive stimulation were not significantly different (1-way ANOVA, $P > 0.05$).

Similar results were obtained for the CN units. Statistical testing of neuronal responses to the first pulse in a spike train and the ones evoked by the following pulses delivered at different frequencies were performed as has been described before for the PN. Again only trains were selected for the analysis if the response to be tested was stronger than 0.1 excess spikes following single pulses (short-latency response: 9 of 64; long-latency response: 28 of 64). For the short-latency excitatory response and the ensuing suppression, one-way ANOVA indicated no difference between the groups ($P > 0.05$). However, a highly significant difference was found for the late excitatory response (1-way ANOVA, $P < 10^{-5}$). The post hoc test (Scheffé) revealed that the excess spikes and the response width of the late response were significantly lower during repetitive stimulation as compared with the first pulse (marked with asterisks for $P < 0.05$ and double asterisks for $P < 0.01$ in Fig. 6*E*). The latency showed a certain tendency to be longer with increasing stimulus frequency a trend that reached significance with 40-Hz trains.

In summary, PN and CN neurons are well able to respond and follow fast repetitive activation in the activity of the peduncular fibers for up to five periods without attenuation of the short-latency excitatory response. On the other hand, excitatory responses at latencies >10 ms in both structures are sensitive to repetitive stimulation. Higher stimulus frequencies are most effective to reduce these responses.

Responses to intra-pontine stimulation

To directly assess intra-pontine interaction, we used a dense linear seven-electrode array (tip distance: 200 μm) inserted into the PN using a ventral approach. The first electrode in the row (located close to the ventral surface i.e., the brachium pontis) was then used for electrical stimulation while the others recorded the stimulus effects on neuronal firing rates (they spanned the dorsoventral extend of the ventral PN such that the one farthest away from the stimulus electrode was close to the cerebral peduncle). Stimulus intensities covered the threshold to evoke responses (0.8–4.8 nC). We performed recordings at 30 locations of the array within the PN in four animals. In 10 of these locations, the electrical stimulus evoked responses on one of the recording electrodes. In the remaining locations, no responses were obtained using this stimulus intensity. Surprisingly, the effects of intra-pontine stimulation differed from that of peduncular stimulation reported above in a markedly qualitative way. First of all, responses to intra-pontine stimulation occurred at a longer latency than those to stimulation in the cerebral peduncle (Fig. 7, *A* and *B*). Whereas the latter arrived on average at 4 ms, the ones obtained after intra-pontine stimulation showed a mean latency of 8.5 ± 1.4 ms. Second, responses after peduncular stimulation always showed a long-lasting inhibitory period (≤300 ms), whereas those evoked by intra-pontine stimulation did not. Importantly, assessment of threshold activation by varying the stimulus intensities revealed that this qualitative difference was not due to the difference in absolute stimulus intensities used. Compared with intrapontine stimulation, threshold intensities were much higher and variable from site to site for peduncular stimulation (7.5–30 nC)—most

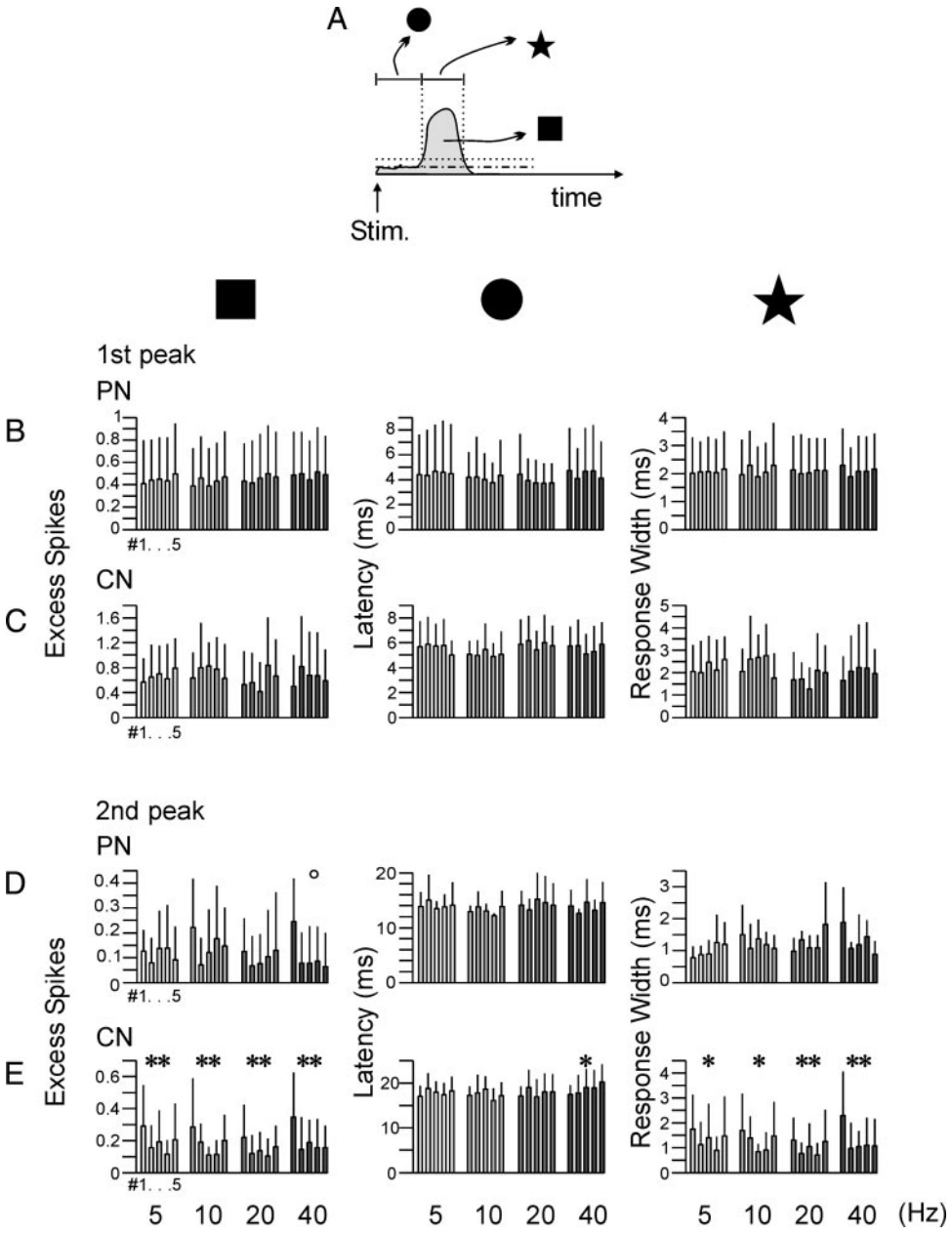

FIG. 6. Quantitative analysis of responses to repetitive stimulation in the cerebral peduncle in PN and CN (gray color in *B–E* denotes stimulation frequency identical to Fig. 5). *A*: schematic PETH depicting the measurements. The broken lines indicate mean and 95% confidence interval of firing rate. Response latency was measured as the time from stimulation until the spike rate crossed the confidence interval (circle). Response duration was measured as the time the spike rate stayed above the confidence interval (star). Response strength ("excess spikes") was measured as the integral of the rate function above the confidence interval (square). *B* and *C*: bar plot of means and SD of these parameters for the fast excitation. Each bar indicates the parameters of the responses to 1 single pulse (number indicated on the abscissa) at different frequencies (gray coded as in Fig. 5) *D* and *E*: same format for the 2nd excitatory response. The asterisks and hollow circle mark significance values obtained from the post hoc Scheffé test (double asterisk: $P < 0.01$; 1 asterisk: $P < 0.05$; white circle: $P = 0.06$) in case a 1-way ANOVA indicated significant differences at a level of $P < 0.05$.

probably due to varying spatial relationships of the stimulation site to the location of fibers that targeted the recorded units in the PN. However, using threshold activation as reference point rather than absolute intensities, the qualitative difference held. The inhibitory pattern evoked by peduncular stimulation appeared as soon as threshold activation was reached for all stimulation sites and all neurons studied (Fig. 7*A*), whereas such a pattern was never seen after intra-pontine stimulation (Fig. 7*C*). These observations allow the conclusion that the responses seen after intrapontine stimulation were not mediated by peduncular fibers (or their branches) within the pontine gray matter (Fig. 7*B*).

Spatially, responses evoked from intra-pontine sites were seen exclusively on the first three electrodes along the array (<600 μm). Interestingly though, responding neurons were distributed unevenly along the electrode array. Figure 7*C* exemplifies this observation. PETHs based on single-unit recordings from three electrodes neighboring the stimulus site are shown. The neuron recorded from the electrode 400 μm away from the stimulation site responded to a 1.6-nC charge transfer, whereas the neurons at a distance of 200 and 600 μm did not. The nonresponsive neurons kept inactive even after application of the maximum intensity (4.8 nC). In fact, at only half of the recording sites we obtained responses in a continuous fashion. In these cases, either the first electrode or the two first electrodes (directly neighboring the stimulation site) picked up responding neurons (Fig. 8, rows 1–5). In the remaining five cases, there was always a gap (i.e., a nonresponding neuron) in the row of neurons recorded between the stimulation site and a responsive one further away (Fig. 8, rows 6–10). In other words, a response at a distant electrode did not predict that neurons located closer to the stimulation electrode would respond as well.

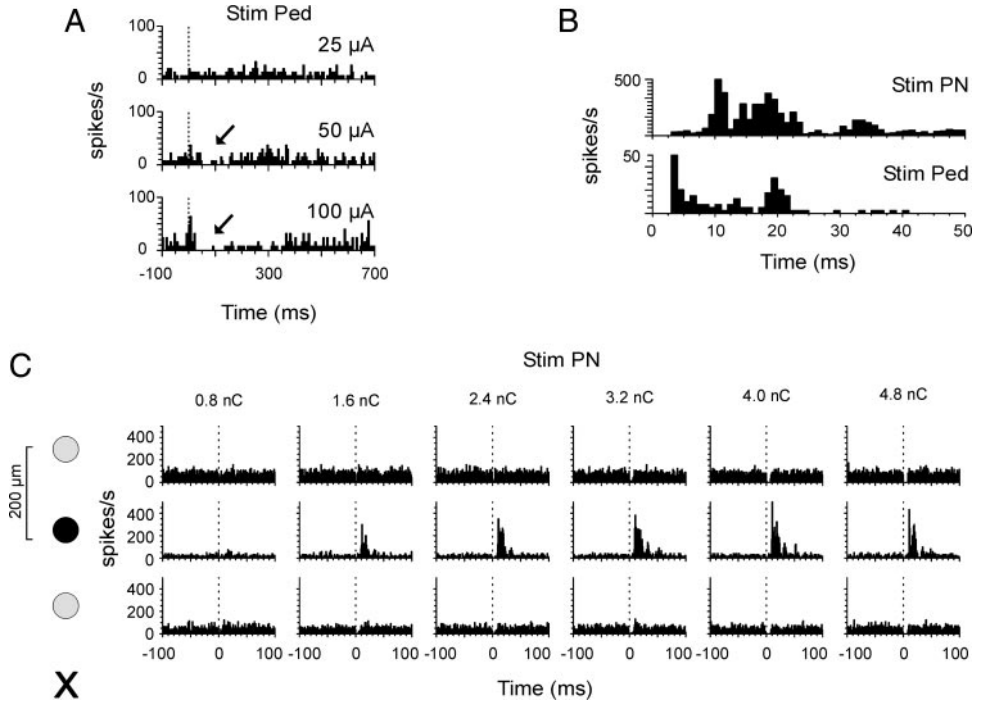

FIG. 7. Intra-pontine stimulation close to threshold discloses long-latency responses in PN cells. *A*: representative response of a PN unit (multiunit) after stimulation of the cerebral peduncle (compare Figs. 4–6). Responses to pulses of different intensities are shown (7.5, 15, and 30 nC corresponding to 25, 50, and 100 μA at 300 μs). The example depicts the typical finding that the inhibition appears together with the excitatory peak at threshold intensities (denoted by arrows). *B*: comparison of effects of stimulation inside the PN (*top*) with the peduncular stimulation (*bottom,* single unit, note the 2 distinct excitatory peaks as shown before) at an expanded time scale. The fast excitatory response after peduncular stimulation occurs much earlier than that seen after intra-pontine stimulation. *C*: multielectrode recording of responses after intra-pontine stimulation. Each row depicts PETHs obtained from electrodes with distance of 200 μm (*bottom*), 400 μm (*middle*), and 600 μm (*top*) to the stimulation electrodes. The symbols on the far left indicate the location of the stimulation electrode (×, ventral PN close to the medial cerebellar peduncle) and recording electrodes (● and ◎, located dorsally from the stimulation electrode in the ventral PN, ◎: nonresponsive unit, ●: responsive unit). Along rows responses after different stimulus intensities are shown (charge transfer from 0.8 to 4.8 nC). Stimulus intensities were varied in pseudorandom way. The excitatory response recorded on the center electrode emerged at a charge transfer of 1.6 nC. Note that the units on the other 2 electrodes remained unresponsive to stimulation at all intensities. Bin width of histograms: 1 ms.

DISCUSSION

This study revealed interactions of sites within the PN that are as far apart as 600 μm using low-intensity intrapontine electrical stimulation. This interaction is most likely based on reciprocal connections between PN and CN because, first, neither axonal collaterals of PN neurons in this range nor dendro-dendritic coupling of adjacent PN neurons was found. Second, rapid direct signal transmission from PN to CN could be demonstrated. Third, the response latencies matched a possible di- or polysynaptic transmission between PN and CN. Studying the temporal characteristics of signal procession through PN and CN revealed that this circuit could follow high rate repetitive stimulation of its afferents (≤40 Hz).

Lack of intrapontine communication mediated by intrinsic connections

Evidence for or against the possibility that pontine sites interact via intrinsic collaterals has been partly contradictive and indirect. The study most to the point so far was the intra-axonal filling with horseradish peroxidase (HRP) from the medial cerebellar peduncle (Shinoda et al. 1992) (although the main goal of this study was the demonstration of collateral branches to the CN—*not* intrinsic branches in the PN). In a small subset of seven axons, Shinoda et al. were able to backfill the entire axon down to the pontine soma but did not observe any hint of intrinsic branching. However, the possible existence of dendro-dendritic interactions suggested by electron microscopic studies was left unresolved (Mihailoff and Border 1990; Mihailoff and McArdle 1981). Also the existence of possible electrical synapses remained unknown. Moreover, the existence of intrinsic connectivity was suggested by more indirect evidence—the finding of degenerating synaptic terminals after lesioning ponto-cerebellar fibers (Mihailoff 1978); repetitive firing after retrograde stimulation of PN neurons (Sasaki et al. 1970); and sequences of EPSPs evoked by stimulation of the cerebral peduncle in the pontine nuclei in cats in vivo (Allen et al. 1975) and in rats in vitro (Möck et al. 1997). We have revisited the problem by filling pontine neurons in vitro which yielded a large number of axons filled with either Lucifer yellow or neurobiotin, two intracellular tracers that have been readily used to visualize small axonal branching. Furthermore, we have intracellularly recorded from neighboring pairs of PN neurons. Neither of these approaches yielded positive evidence for the existence of short-range interactions. It has to be pointed out that our morphological and electrophysiological investigation did not resolve the issue of long range interactions (e.g., connections to the other hemisphere, etc.) which the study of Shinoda et al. readily covered. But, within the short range of up to ~0.7 mm, it confirmed and extended the finding of Shinoda et al. (1992) with large numbers of filled axons and with additional functional inves-

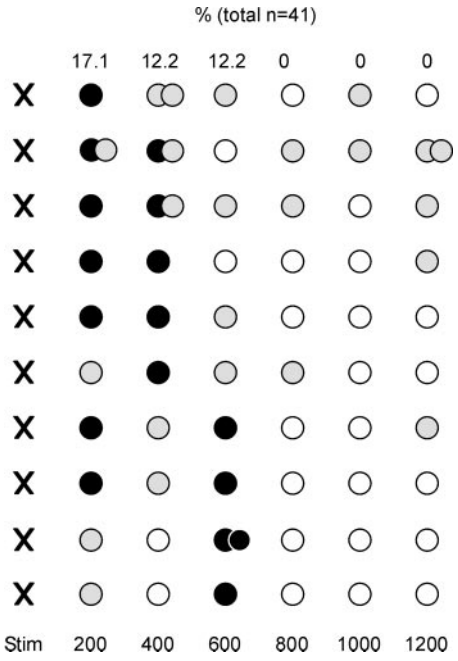

FIG. 8. Intra-pontine stimulation evokes spatially discontinuous responses. All recordings in which ≥1 electrode recorded from a responsive PN unit at 3.2 nC are shown in rows. As in Fig. 7, the stimulation electrode is denoted by × and the recording electrodes as circles (double circles denote 2 units recorded from the same electrode; electrode locations within the PN as in Fig. 7). The color code is: black, responding unit; gray, nonresponding unit; white, no unit recorded on this electrode. Responding units were limited to a distance of 600 μm from the stimulus electrode. Half of the recordings showed continuous responses across electrodes, the other half showed gaps of nonresponding units between stimulation electrode and a responding unit.

tigation that had the potential to detect also interactions mediated by neuronal elements different from axons. Most importantly, the range of ~0.7 mm, covered by our analyses based on axonal fillings and paired intracellular recordings, matches very well the extent to which the pontine interactions after intra-pontine stimulation in vivo were confined. From that we feel confident to conclude that short-range intra-pontine communication is possible in spite of the absence of intrinsic short-range interconnections.

Extrinsic interaction between sites in the PN via the CN

The search for possible extrinsic circuits that could mediate intra-pontine communication (i.e., a feedback loop) is rendered easy by the limited number of PN projection targets: only the cerebellum, cortex and nuclei, are known targets of PN efferent axons (Brodal and Bjaalie 1992; Mihailoff 1994; Shinoda et al. 1992). In turn, the PN receive a copy of the cerebellar output from the CN (Brodal et al. 1972a; Schwarz and Schmitz 1997; Watt and Mihailoff 1983). Our present finding of a fast sequence of neuronal responses evoked from PN and CN after peduncular stimulation suggests that, first, the transmission of peduncular activity to the CN without the need of cerebellocortical activation is possible. In addition, a sequence of fast excitation and long-lasting inhibition after the short-latency excitation was visible in pontine recordings even with threshold stimulation intensities. Peduncular stimulation evokes activity in neocortical fibers that runs in orthodromic as well as antidromic directions. While orthodromic activation of pontine afferents easily explains the fast excitation of PN cells, the most parsimonious explanation of the long depression of firing rates in the PN is that it is due antidromic conveyance of action potential followed by bouncing neocortical activity: undoubtedly, the volley of antidromically transmitted action potentials evoked at the peduncular stimulation site reached axonal branching of cortical layer 5 projection neurons and, thus ignited significant parts of the neocortical circuitry. There is a host of evidence that subcortical white matter stimulation or intracortical stimulation leads to a long-lasting slow depression of the cortical firing rate most possible due to intrinsic inhibitory interneurons (discussed in Butovas and Schwarz 2003). The characteristic of this cortical inhibition matches very well the pattern seen in PN neurons, and it is therefore likely that the latter is due to neocortical withdrawal of excitatory drive to the PN. Compared with this possibility, presumptive activation of inferior olive and other precerebellar nuclei in the mossy fiber pathway (lateral reticular nucleus, nucleus reticularis tegmenti pontis) is difficult to draw on for an explanation of the long inhibitory period in PN cells. First these structures activate CN cells directly by excitatory mossy and climbing fiber collaterals (Shinoda et al. 1987, 2000; Sugihara et al. 1996) and, second, the well-known 10-Hz oscillations in the inferior olive evoked by neocortical stimulation under ketamine (Schwarz and Welsh 2001) were not present in the PN activity observed here. Finally, it should be noted that monosynaptic activation of inhibitory synapses in the pontine nuclei, albeit they have been found in vitro, are not sufficient to explain the entire inhibitory response because their action is much shorter (Möck et al. 1997).

The fast excitation and slow inhibition seen with peduncular stimulation was entirely absent after intra-pontine stimulation. This strongly suggests that the stimulation strategy applied did not stimulate a significant amount of pontine afferents. The following facts seem to be important to explain this finding. The electrodes were oriented in a dorsoventral direction with the stimulation electrode close to the brachium pontis (medial cerebellar peduncle) and the recording electrodes located toward the cerebral peduncle. It is therefore conceivable that the electrical field induced (which we chose to be small and close to activation threshold to keep the activated spot of pontine tissue as small as possible and to keep stimulus artifacts in the neighboring recording electrodes manageable) predominantly reached outgoing fibers entering the brachium and to a much lesser extent incoming fibers from the cerebral peduncle. These arguments also reduce the likelihood that other afferent fiber systems which are not part of the cerebral peduncle (and thus were not activated by the experiments with peduncular stimulation) were at the basis of the responses after intrapontine stimulation because, like peduncular fibers, they commonly enter the PN along a dorsoventral trajectory often penetrating through the cerebral peduncle. One prominent example is the feedback projection of the CN to the PN (Schwarz and Schmitz 1997). In summary, we conclude that intra-pontine stimulation (as applied in this study) selectively activates the pontine efferents and leaves the afferents largely unaffected. It, thus seems to be optimal to isolate the effect of activity in PN outputs from the activity related to diverse connections of the branches of PN input fibers. Consequently, if one recalls that the only pontine projection target is the cerebellum, the delayed pontine excitation observed with this type of stimulation

must have been mediated by the cerebellum. The fact that it is a pure excitation excludes the involvement of Purkinje cells because the inhibitory action of Purkinje cells onto CN projection neurons (De Zeeuw and Berrebi 1996) would have been imposed on PN cells as a withdrawal of excitation (Schwarz and Schmitz 1997). This is not to say that Purkinje cell inhibition did not play a role in the responses observed. It only indicates that the first part of the response (which was always excitatory) was not determined by Purkinje cell activity. At a later time of the PN response, it is well conceivable that Purkinje cell inhibition overlays the excitatory response but does not impose as inhibitory response of its own.

Functional considerations

The question how sites in the pontine nuclei interact is fundamental for our understanding of pontine function. In case of pure intrinsic interconnections, the computational role of the PN would have to be considered as a feedforward adaptor of neocortical signals for the use of the cerebellum. The present study does not favor such a role (however, the existence of putative inhibitory interneurons, albeit seemingly exclusive to the PN in primates, should be mentioned at this point) (Mihailoff et al. 1992; Möck et al. 1999; Thier and Koehler 1987). Rather, our observations suggest that pontine sites uniquely communicate via a reciprocal ponto-nuclear feedback loop. In this setting, the role of the pontine nuclei appears to be situated more in the framework of a larger ponto-cerebellar signal processing unit in which the PN are set to take over the role of a feedback controlled input stage. Generally speaking, a feedback-controlled input stage performs a dynamic adaptation of incoming signals for the purposes of the receiving structure. It is an interesting fact that such dynamic adaptation seems to be distinctive for the mossy fibers originating in the pontine nuclei as other mossy fiber systems seem to be lacking cerebellar feedback (notably the classic ones originating in the vestibular nerve ganglion and spinal chord). What makes neocortical signals conveyed via the PN so different from other mossy fiber signals that they have to be adapted before they enter the cerebellum?

Two notions, one pertaining to the spatial, the other to the temporal aspects of coding of pontine signals seem worth considering and may guide future research. First, as laid out in the INTRODUCTION, the precise and complex topographical rearrangement of neocortical signals in the PN may reflect specific demands of cerebellar signal processing. Dynamic feedback control could serve as a spatial filter that dynamically selects relevant signal combinations from local sets of pontine compartments. Second, temporal coding, based on synchronous and/or rhythmic firing among neuronal assemblies, thought to be present in neocortex (Abeles 1982a; Llinás 1988; Singer and Gray 1995) may need recoding of some sort before entering the cerebellum. The reason is that an assembly code that relies on divergent, reciprocal interconnectivity (Abeles 1982a; Braitenberg and Schüz 1991) can hardly be upheld by the cerebellar cortex, which essentially is a feedforward throughput structure lacking reciprocal connections (Schwarz and Thier 1999). Indeed, oscillatory neuronal activity in the cerebellar cortex was found to be located in the molecular layer (Courtemanche and Lamarre 2005; Hartmann and Bower 1998), but little evidence has been gathered to date that cerebellar simple spikes of Purkinje cells are able to convey information using synchronous rhythmic activity (Jaeger 2003; Schwarz and Welsh 2001). The present study yielded evidence that rhythmic activity of $\leq$40 Hz readily gains access to the cerebellum via the PN-CN loop. Patterns of spontaneous activity in the CN, however, do not indicate a propensity of the CN to actively underpin and uphold such rhythmic activity (Schwarz, unpublished observation). It is therefore conceivable that the cerebellum may extract information contained in a temporal code but may be inapt to passing it on. The necessity of recoding implied by this scenario may find its structural basis in the complex arrangement of pontine compartments under reciprocal feedback control of the cerebellum as described in the present study. There is the possibility to be studied in the future that a temporal code in neocortical signals could be converted to a spatial code by the dynamically adjustable spatial filter implemented by the PN-CN loop. In this view, the cerebellum could single out neocortical signals that are bound by a temporal code for further processing on the cerebro-cerebellar loop.

ACKNOWLEDGMENTS

We thank S. Kramer and U. Grosshennig for excellent technical assistance.

GRANTS

This work was supported by Bundesministerium für Bildung und Forschung Grant 0311858 and Deutsche Forschungsgemeinschaft Grant SFB 550-B11. Additional funding was provided by the Hertie Foundation and the Hermann and Lilly Schilling Foundation.

REFERENCES

Abeles M. *Local Cortical Circuits. An electrophysiological Study.* Springer: Berlin: 1982a.

Abeles M. Quantification, smoothing, and confidence limits for single units' histograms. *J Neurosci Methods* 5: 317–325, 1982b.

Allen GI, Korn H, Oshima T, and Toyama K. The mode of synaptic linkage in the cerbro-ponto-cerebellar pathway of the cat. II. Responses of single cells in the pontine nuclei. *Exp Brain Res* 24: 15–36, 1975.

Bower JM, Beermann DH, Gibson JM, Shambes GM, and Welker W. Principles of organization of a cerebro-cerebellar circuit. *Brain Behav Evol* 18: 1–18, 1981.

Braitenberg V and Schüz A. *Anatomy of the Cortex.* Springer Verlag: Berlin Heidelberg New York: 1991.

Brodal A, Destombes J, Lacerda AM, and Angaut P. A cerebellar projection onto the pontine nuclei. An experimental anatomical study in the cat. *Exp Brain Res* 16: 115–139, 1972a.

Brodal A, Lacerda AM, Destombes J, and Angaut P. The pattern in the projection of the intracerebellar nuclei onto the nucleus reticularis tegmenti pontis in the cat. An experimental anatomical study. *Exp Brain Res* 16: 140–160, 1972b.

Brodal A and Szikla G. The termination of the brachium conjunctivum descendens in the nucleus reticularis tegmenti pontis. *Brain Res* 39: 337–351, 1972.

Brodal P. The corticopontine projection in the cat. Demonstration of a somatotopically organized projection from the second somatosensory cortex. *Arch ital Biol* 106: 310–322, 1968a.

Brodal P. The corticopontine projection in the cat. I. Demonstration of a somatotopically organized projection from the primary sensorimotor cortex. *Exp Brain Res* 5: 210–234, 1968b.

Brodal P and Bjaalie JG. Organization of the pontine nuclei. *Neurosci Res* 13: 83–118, 1992.

Butovas S and Schwarz C. Spatiotemporal effects of microstimulation in rat neocortex: a parametric study using multielectrode recordings. *J Neurophysiol* 90: 3024–3039, 2003.

Courtemanche R and Lamarre Y. Local field potential oscillations in primate cerebellar cortex: synchronization with cerebral cortex during active and passive expectancy. *J Neurophysiol* 93: 2039–2052, 2005.

De Zeeuw CI and Berrebi AS. Individual Purkinje cell axons terminate on both inhibitory and excitatory neurons in the cerebellar and vestibular nuclei. *Ann NY Acad Sci* 781: 607–610, 1996.

Egert U, Knott T, Schwarz C, Nawrot M, Brandt A, Rotter S, and Diesmann M. MEA-Tools: an open source toolbox for the analysis of multielectrode data with MATLAB. *J Neurosci Methods* 117: 33–42, 2002.

Hartmann MJ and Bower JM. Oscillatory activity in the cerebellar hemispheres of unrestrained rats. *J Neurophysiol 1998* Sep 80: 1598–1604, 1998.

Ito M, Yoshida M, Obata K, Kawai N, and Udo M. Inhibitory control of intracerebellar nuclei by the Purkinje cell axons. *Exp Brain Res* 10: 64–80, 1970.

Jaeger D. No parallel fiber volleys in the cerebellar cortex: evidence from cross-correlation analysis between Purkinje cells in a computer model and in recordings from anesthetized rats. *J Comput Neurosci* 14: 311–327, 2003.

Jahnsen H. Electrophysiological characteristics of neurones in the guinea- pig deep cerebellar nuclei in vitro. *J Physiol* 372: 129–147, 1986.

Joseph JW, Shambes GM, Gibson JM, and Welker W. Tactile projections to granule cells in caudal vermis of the rat's cerebellum. *Brain Behav Evol* 15: 141–149, 1978.

Kitai ST, Kocsis JD, and Kiyohara T. Electrophysiological properties of nucleus reticularis tegmenti pontis cells: antidromic and synaptic activation. *Exp Brain Res* 24: 295–309, 1976.

Kitai ST, McCrea RA, Preston RJ, and Bishop GA. Electrophysiological and horseradish peroxidase studies of precerebellar afferents to the nucleus interpositus anterior. I. Climbing fiber system. *Brain Res* 122: 197–214, 1977.

Lee J, Taira T, Pihlaja P, Ransom BR, and Kaila K. Effects of CO2 on excitatory transmission apparently caused by changes in intracellular pH in the rat hippocampal slice. *Brain Res* 706: 210–216, 1996.

Leergaard TB, Alloway KD, Pham TA, Bolstad I, Hoffer ZS, Pettersen C, and Bjaalie JG. Three-dimensional topography of corticopontine projections from rat sensorimotor cortex: comparisons with corticostriatal projections reveal diverse integrative organization. *J Comp Neurol* 478: 306–322, 2004.

Leergaard TB, Lyngstad KA, Thompson JH, Taeymans S, Vos BP, De Schutter E, Bower JM, and Bjaalie JG. Rat somatosensory cerebropontocerebellar pathways: spatial relationships of the somatotopic map of the primary somatosensory cortex are preserved in a three-dimensional clustered pontine map. *J Comp Neurol* 422: 246–266, 2000.

Llinás R. The intrinsic electrophysiological properties of mammalian neurons: insights into central nervous system function. *Science* 242: 1654–1664, 1988.

Llinás R and Mühlethaler M. Electrophysiology of guinea-pig cerebellar nuclear cells in the in vitro brain stem-cerebellar preparation. *J Physiol* 404: 241–258, 1988.

Lübke J, Markram H, Frotscher M, and Sakmann B. Frequency and dendritic distribution of autapses established by layer 5 pyramidal neurons in the developing rat neocortex: comparison with synaptic innervation of adjacent neurons of the same class. *J Neurosci* 16: 3209–3218, 1996.

McCrea RA, Bishop GA, and Kitai ST. Electrophysiological and horseradish peroxidase studies of precerebellar afferents to the nucleus interpositus anterior. II. Mossy fiber system. *Brain Res* 122: 215–228, 1977.

Mihailoff GA. Principal neurons of the basilar pons as the source of a recurrent collateral system. *Brain Res Bull* 3: 319–332, 1978.

Mihailoff GA. Cerebellar nuclear projections from the basilar pontine nuclei and nucleus reticularis tegmenti pontis as demonstrated with PHA- L tracing in the rat. *J Comp Neurol* 330: 130–146, 1993.

Mihailoff GA. Identification of pontocerebellar axon collateral synaptic boutons in the rat cerebellar nuclei. *Brain Res* 648: 313–318, 1994.

Mihailoff GA and Border BG. Evidence for the presence of presynaptic dendrites and GABA-immunogold labeled synaptic boutons in the monkey basilar pontine nuclei. *Brain Res* 516: 141–146, 1990.

Mihailoff GA, Kosinski RJ, Azizi SA, and Border BG. Survey of noncortical afferent projections to the basilar pontine nuclei:a retrograde tracing study in the rat. *J Comp Neurol* 282: 617–643, 1989.

Mihailoff GA, Kosinski SA, Azizi SA, Lee HS, and Border BG. The expanding role of the basilar pontine nuclei as a source of cerebellar afferents. In: The cerebellum revisited, edited by Llinás R and Sotelo C. Springer-Verlag: New York Berlin Heidelberg, 1992, p. 135–164.

Mihailoff GA and McArdle CB. The cytoarchitecture, cytology, and synaptic organization of the basilar pontine nuclei in the rat. II. Electron microscopic studies. *J Comp Neurol* 195: 203–219, 1981.

Möck M, Schwarz C, and Thier P. Electrophysiological properties of rat pontine neurons in vitro. II. Postsynaptic potentials. *J Neurophysiol* 78: 3338–3350, 1997.

Möck M, Schwarz C, Wahle P, and Thier P. GABAergic inhibition in the rat pontine nuclei is exclusively extrinsic: evidence from an in situ hybridization study for GAD67 mRNA. *Exp Brain Res* 124: 529–532, 1999.

Nelson ME and Bower JM. Brain maps and parallel computers. *Trends Neurosci* 13: 403–408, 1990.

Paxinos G and Watson C. *The Rat Brain in Stereotaxic Coordinates.* San Diego, CA: Accademic, 1986.

Sasaki K, Kawaguchi S, Shimono T, and Prelevic S. Electrophysiological studies of the pontine nuclei. *Brain Res* 20: 425–438, 1970.

Schwarz C and Möck M. Spatial arrangement of cerebro-pontine terminals. *J Comp Neurol* 435: 418–432, 2001.

Schwarz C, Möck M, and Thier P. Electrophysiological properties of rat pontine nuclei neurons in vitro. I. Membrane potentials and firing patterns. *J Neurophysiol* 78: 3323–3337, 1997.

Schwarz C and Schmitz Y. Projections from the cerebellar lateral nucleus to precerebellar nuclei in the mossy fiber pathway is glutamatergic: a study combining anterograde tracing with immunogold labeling in the rat. *J Comp Neurol* 381: 320–334, 1997.

Schwarz C and Thier P. Modular organization of the pontine nuclei: Dendritic fields of identified pontine projection neurons in the rat respect the borders of cortical afferent fields. *J Neurosci* 15: 3475–3489, 1995.

Schwarz C and Thier P. Comparison of projection neurons in the pontine nuclei and the nucleus reticularis tegmenti pontis of the rat. *J Comp Neurol* 376: 403–419, 1996.

Schwarz C and Thier P. Binding of signals relevant for action: towards a hypothesis of the functional role of the pontine nuclei. *Trends Neurosci* 22: 443–451, 1999.

Schwarz C and Welsh JP. Dynamic modulation of mossy fiber system throughput by inferior olive synchrony: a multielectrode study of cerebellar cortex activated by motor cortex. *J Neurophysiol* 86: 2489–2504, 2001.

Shambes GM, Beermann DH, and Welker WI. Multiple tactile areas in cerebellar cortex: another patchy cutaneous projection to granule cell columns in the rat. *Brain Res* 156: 123–128, 1978a.

Shambes GM, Gibson JM, and Welker WI. Fractured somatotopy in granule cell tactile areas of rat cerebellar hemispheres revealed by micromapping. *Brain Behav Evol* 15: 94–140, 1978b.

Shinoda Y, Sugihara I, Wu HS, and Sugiuchi Y. The entire trajectory of single climbing and mossy fibers in the cerebellar nuclei and cortex. *Prog Brain Res* 124: 173–186, 2000.

Shinoda Y, Sugiuchi Y, and Futami T. Excitatory inputs to cerebellar dentate nucleus neurons from the cerebral cortex in the cat. *Exp Brain Res* 67: 299–315, 1987.

Shinoda Y, Sugiuchi Y, Futami T, and Izawa R. Axon collaterals of mossy fibers from the pontine nucleus in the cerebellar dentate nucleus. *J Neurophysiol* 67: 547–560, 1992.

Singer W and Gray CM. Visual feature integration and the temporal correlation hypothesis. *Annu Rev Neurosci* 18: 555–586, 1995.

Spray DC, Harris AL, and Bennett MV. Gap junctional conductance is a simple and sensitive function of intracellular pH. *Science* 211: 712–715, 1981.

Sugihara I, Wu H, and Shinoda Y. Morphology of axon collaterals of single climbing fibers in the deep cerebellar nuclei of the rat. *Neurosci Lett* 217: 33–36, 1996.

Thier P and Koehler W. Morphology, number and distribution of putative GABA-ergic neurons in the basilar pontine gray of the monkey. *J Comp Neurol* 265: 311–322, 1987.

Tsukahara N, Bando T, Kitai ST, and Kiyohara T. Cerebello-pontine reverberating circuit. *Brain Res* 33: 233–237, 1971.

Verveer C, Hawkins RK, Ruigrok TJ, and De Zeeuw CI. Ultrastructural study of the GABAergic and cerebellar input to the nucleus reticularis tegmenti pontis. *Brain Res* 766: 289–296, 1997.

Watt CB and Mihailoff GA. The cerebellopontine system in the rat. I. Autoradiographic studies. *J Comp Neurol* 215: 312–330, 1983.

European Journal of Neuroscience, Vol. 25, pp. 2161–2169, 2007 doi:10.1111/j.1460-9568.2007.05449.x

Detection psychophysics of intracortical microstimulation in rat primary somatosensory cortex

Sergejus Butovas and Cornelius Schwarz
Hertie-Institute for Clinical Brain Research, Department of Cognitive Neurology, University Tübingen, 72076 Tübingen, Germany

Keywords: barrel cortex, brain–machine interface, electrical stimulation, head-fixed rat

Abstract

A problem of purposeful intracortical microstimulation is the long duration of neuronal integration time and the associated complex temporal interactions of effects to individual pulses in trains. Here we investigated the effects of repetitive stimuli on perception. We trained head-restraint rats to indicate the detection of cortical microstimulation in infragranular layers of barrel cortex. Three stimulus parameters: stimulus intensity, number of pulses and frequency were varied, and psychometric detection curves were assessed using the method of constant stimuli. The average psychophysical threshold of single pulses was 2.0 nC – a measure very close to what has been found earlier for the evocation of short-latency action potentials in neurons near the stimulation electrode. Detection of single-pulse stimulation always saturated at probabilities of about 0.8. In contrast, repetitive stimuli gave rise to lower thresholds (by a factor of two at 15 pulses, 320 Hz), and to saturation at probabilities close to 1. Interestingly, a large fraction of these perceptual benefits was observed already with double pulses. Moreover, the perceptual efficacy of individual pulses was higher using double pulses compared with longer sequences, i.e. double pulses were detected better than expected from the assumption of independence of single-pulse effects, while trains of 15 pulses fell well short of this expectation. The present results thus point to double-pulse stimulation as an optimal choice when trading economic stimulation against optimizing of the percept.

Introduction

An important question in systems neurobiology is how perception is related to patterns of neocortical neuronal activity. One important tool in this quest is intracortical microstimulation, which has been shown to be able to purposefully generate and/or alter percepts. When used as a surrogate of sensory input in primary sensory cortices, intracortical microstimulation is readily interpreted as a sensory event within the respective mode. Microstimulation in the primary visual cortex evokes visual percepts (Schmidt *et al*., 1996; DeYoe *et al*., 2005), and tactile flutter discrimination is maintained by substituting the mechanical stimulus by repetitive intracortical stimulation in the primary somatosensory cortex (Romo *et al*., 1998, 2000). Within a modality, cortical microstimulation displays a remarkable specificity for the point of stimulation within a cortical map (Leal-Campanario *et al*., 2006) and for feature selectivity of the neurons at the stimulation site (Salzman *et al*., 1990). Moreover, microstimulation has also been shown to be able to act as a surrogate of neuronal activity underlying subjective experience in the frontal cortex (de Lafuente & Romo, 2005, 2006). From these findings, intracortical microstimulation appears as a promising approach to imprint meaningful activity patterns onto cortical circuits to restore sensory function.

To examine the detailed effect of specific patterns of activity on the percept, the relationships between stimulus command, evoked neuronal activity and the percept have to be studied in detail. A particularly important aspect is the possible perceptual effect of interactions between neuronal responses evoked by different stimulus pulses. The present study focuses on the temporal domain (i.e. repetitive stimulation) but, interaction potentially takes place also in the spatial domain (i.e. by using dense multielectrode arrays). Cortical microstimulation has been reported to evoke a sequence of short excitation of a few milliseconds followed by long inhibition of firing rates ($\sim$ 100 ms) (Butovas & Schwarz, 2003). The characteristics of the latter were shaped by the action of γ-aminobutyric acid $(GABA)_B$ receptors and electrical synapses interconnecting inhibitory neurons (Butovas *et al*., 2006). An interesting feature of the inhibition was its virtually fixed duration that could not be extended by single or double stimulation (at interstimulus intervals <100 ms). On the other hand, repetitive stimulation using more than 2 pulses at frequencies higher than 10 Hz led to a confluence of inhibition against which the evoked spikes at short latencies stand out (Butovas & Schwarz, 2003). In contrast to this rather complex non-linear interaction, the magnitude of the fast excitatory response produced by repetitive pulses was stable or even showed a tendency to be enhanced – a counterintuitive result in view of the fact that at the time of the repeated excitation the network was massively inhibited. As a first step to relate these known patterns of neuronal activity to the percept of the individual we asked here, using psychophysical measurements in head-fixed, operantly conditioned rats, whether and how the probability of detection of electrical stimulation patterns is determined by parameters of repetitive microstimulation.

Correspondence: Dr C. Schwarz, as above.
E-mail: cornelius.schwarz@uni-tuebingen.de

Received 24 November 2006, revised 19 January 2007, accepted 29 January 2007

Materials and methods

Surgery and behavioural training

Five Long–Evans male rats (12–14 weeks old, body weight 350–450 g) were used in the present study. All experimental and surgical

procedures were performed in accordance with the policy and the use of animals in neuroscience research of the Society for Neuroscience and German Law and approved by the Reg. Prăsidium Tűbingen. Prior to surgery rats were accustomed to the experimenter and the setup for at least 2 weeks. Anaesthesia was initialized and continued to the end of the surgery with isoflurane (1–2.5%). Isoflurane concentration was adjusted to keep the hind-limb withdraw reflexes below threshold. The animals' body temperature was held at 37 °C by a feedback-controlled heating pad (Fine Science Tools, Heidelberg, Germany). To implant the electrode array the animals were placed in a stereotaxic device and craniotomy over the barrel cortex was performed. A set of stainless steel microscrews was placed in the skull. A custom-made microelectrode array was placed at a depth of $\sim$1500 μm and embedded together with the skull screws into light-curing dental cement (Flowline, Heraeus Kulzer, Hanau, Germany). The wound was cleaned and disinfected with hydrogen peroxide. The open skin was sutured and carefully attached to the implant. After surgery the animals were kept warm and treated with analgesics (Buprenophin, 0.02 mg/kg) and were allowed to recover for 14 days.

As described in detail elsewhere (Stüttgen *et al*., 2006), the behavioural training started with systematic desensitization to accommodate the rats to head-fixation followed by water restriction. The weight of the animals during periods of water restriction was monitored daily. A reduction in body weight was prevented by additional water supply. Training sessions were scheduled two–three times daily for 5 days followed by 2 days of free access to water. We conditioned the subjects to respond to electrical stimuli by emitting a lick within 0.5 s after the start of stimulation ('reinforcement period', Fig. 1A) in order to obtain a drop of water as reward for correct performance. Initially rats received a train of electrical stimuli consisting of 15 pulses (at 320 Hz) at an easily detectable intensity. The interstimulus intervals were varied by choosing them at random between 3.75 and 6.25 s (mean 5 s, flat probability distribution). Dependent on the performance of the rat, the number of stimulus pulses was reduced from session to session until the animal would respond reliably to single pulses. To prevent premature responses a 1-s period before stimulus delivery was required to be free of licks ('non-licking period', Fig. 1A). If a lick was emitted in this time window the stimulus presentation was postponed by 1 s.

After the sessions used to measure the psychophysical curve, additional sessions were added in which the horizontal movement of whiskers was assessed (see Hentschke *et al*., 2006 for details). All experiments were performed in complete darkness and sound-isolated environment.

Microstimulation and electrophysiology

Microelectrode arrays were custom-made in our laboratory. Sixteen pulled glass-coated platinum tungsten electrodes (80 μm shank diameter, 23 μm diameter of the metal core, free tip length $\sim$10 μm, impedance > 1 MΩ; Thomas Recording, Giessen, Germany) were placed inside a 4 × 4 array of polyimide tubing, with distance between tips of about 300 μm (HV Technologies, Trenton, GA, USA). The electrodes were soldered to Teflon-insulated silver wires (Science Products, Hofheim, Germany), which in turn were connected to a microplug (Bürklin, Munich, Germany). The electrode array was inserted into the posteriomedial barrel subfield (barrel cortex) at a depth of 1500 μm below the pia corresponding to infragranular layers. Only one electrode per animal was chosen for stimulation, and remained the same throughout training and psychophysical testing. To stimulate the cortex we used rectangular biphasic (cathodal first) trains of 1, 2, 5 and 15 pulses at varying frequency (5, 10, 40 and 320 Hz). Stimulus intensity expressed as charge transfer (measured in nC) was varied by combining pulse durations from 100 to 600 μs in steps of 100 μs, and amplitudes from 4 to 25 μA in the following way: [0.8, 1.6, 2.4, 3.2, 4.0, 4.8] nC → [100, 200, …, 600] μs * 8 μA; [1.8, 2.7] nC → [200, 300] μs * 9 μA; [0.4] nC → 100 μs * 4 μA; [1.2] nC → 200 μs * 6 μA; [6.0] nC → 600 μs * 10 μA; [7.5] nC → 300 μs * 25 μA; [10] nC → 500 μs * 20 μA. Electrical stimuli covering this parametric space were presented in a pseudorandom fashion by a programmable stimulator (STG 1008, MultiChannelSystems, Reutlingen, Germany).

Behavioural data analysis

Psychophysical performance is expressed here as the ratio between the number of presented and the number of detected stimuli as a function of stimulation intensity (Fig. 1C). In order to determine the detection threshold, the psychometric function was fit by a logistic model of the following form:

$$N(t) = c + (1 - c) \times k/(1 + \mathrm{e}^{-\alpha t - \beta}) \quad (1)$$

where c and k set the range of values assumed, α sets the maximum slope, and β sets the position of the inflection point on the abscissa. The inflection point of the resulting S-shaped curve was taken as the detection threshold (see Fig. 3A). To assess the effects of pulse number and frequency on detection we used the non-parametric Kruskal–Wallace test. Detection thresholds and behavioural performance are expressed as mean ± SD.

Results

The present data set was obtained from five well-trained animals that emitted licks after presentations of clearly suprathreshold repetitive stimuli in almost 100% of the trials. Active whisker movement was only rarely encountered in the present experimental conditions. Only a very small minority (1.64 ± 0.48% of all trials, $n = 3$ animals) contained whisker velocities above 0.03 m/s in an interval 75 ms before the stimulus, confirming earlier reports of absence of whisking in head-fixed rats under experimental conditions as used here (Gao *et al*., 2003; Stüttgen *et al*., 2006). Thus, the present experimental conditions assured that stimuli were presented while the barrel cortex was in the 'passive state' characterized by low background firing and high sensory responses (Hentschke *et al*., 2006). After reaching optimal performance in the initial training with suprathreshold stimuli, the animals were subjected to daily sessions (typically three per day) in which the whole stimulus set was presented in a pseudorandom sequence. Each session lasted maximally 15 min and contained on average 130 stimulus presentations. If the animal showed signs of non-responsiveness the session was interrupted and the stimulus sequence was continued next session. This regime was possible because the conditions from session to session were held identical (the electrodes were not moved) and had the advantage that the motivation of the rats was high throughout the entire period of measurement, unhampered by tapering of response during longer sessions due to satiation. Accordingly, the probability of all animals to respond to the two strongest stimuli in the set (4 and 2.7 nC, 15 pulses at 320 Hz) was 1 in 90 of the 96 sessions that went into the present data set [in the other six the best response was 97% ($n = 2$), 80% ($n = 2$) and 60% ($n = 2$)] and response latencies (first lick after stimulation) were about 200 ms for all well-detectable stimuli. In summary, the detection

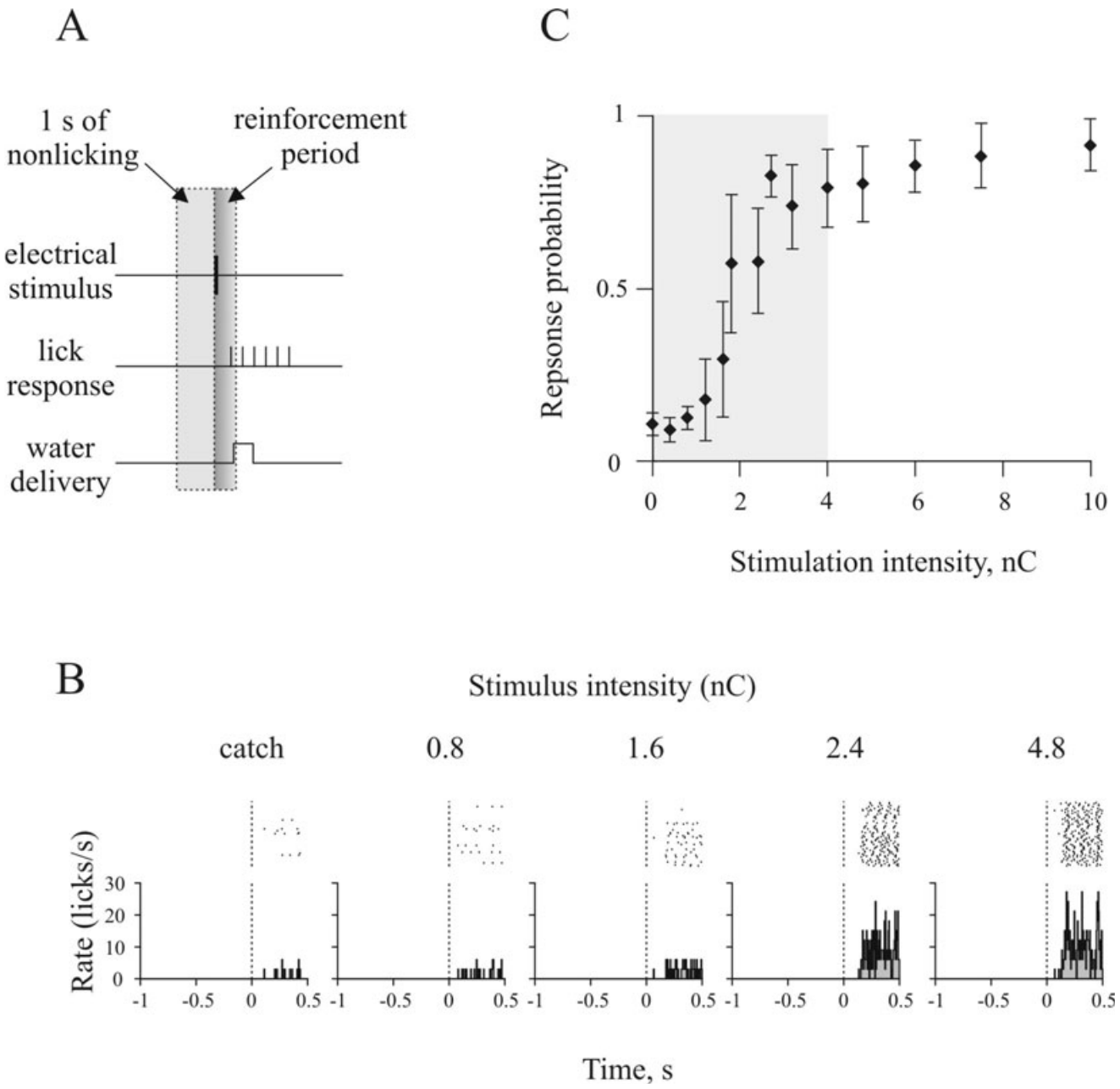

FIG. 1. Assessment of detection curves. (A) Schematic of experimental design. Licking in the 'non-licking interval' 1 s before the stimulus postponed the stimulus by 1 s. The animals were required to respond during 500 ms after stimulus onset ('reinforcement period') to obtain a reward. (B) Typical example of performance to single-pulse stimulation as a function of charge transfer. Shown are licks with respect to stimulation time as raster plots and peri-time histograms. Note the typical rhythmic licking pattern at ~7 Hz. The number of emitted licks increased with stimulation intensity. This example is representative in that stimulation intensity had no gross effect on first lick latency. (C) Detection probability of single pulses plotted against charge transfer taken from five animals. Error bars depict standard deviation.

curves shown in this report originate from many sessions in the course of which a minimum of 188 repetitions of each stimulus (including catch trials) were presented. Some stimuli were presented up to 300 times to the same animal. The set of stimuli comprised 62 stimuli combining 14 intensities, four pulses, four frequencies and catch trials. The stimulus set does not exhaust the combinatorial possibilities offered by these parameter arrays nor was the whole data set presented to each animal. The structure of the data set is detailed in Table 1.

In our analysis we first focus on the responses to single pulses. With higher pulse intensity all animals emitted increasing numbers of licks (in a periodic fashion at a frequency of ~7 Hz, Fig. 1B) and probability of response (lick within the reinforcement period, Fig. 1C). The typical detection curve was S-shaped, and could well be approximated by a logistic fit (see Materials and methods). The fitted curve had its inflection point (defined as detection threshold) at ~2 nC (2.07 ± 0.4 nC) and asymptotically approached 0.8 probability at 4 nC (0.80 ± 0.12, $n = 5$ animals, grey area in Fig. 1C). Stronger stimuli (up to 10 nC) were detected somewhat better, but performance never reached levels close to 1. This is noteworthy because, in contrast, repetitive stimulation was consistently detected at probabilities close to 1 at about 4 nC.

TABLE 1. Combination of stimulus parameters tested in each animal

		2 pulses				5 pulses		15 pulses		
	1 pulse	5 Hz	10 Hz	40 Hz	320 Hz	40 Hz	320 Hz	40 Hz	320 Hz	Total
Rat 1	8[a]	–	–	–	–	–	–	–	–	8
Rat 2	8[a]	–	–	–	–	–	–	–	–	8
Rat 3	8[b]	–	–	–	–	7	7	7	7	34
Rat 4	14	6	6	6	6	6	6	6	6	62
Rat 5	14	6	6	6	6	6	6	6	6	62

The numbers plotted depict the numbers of intensities used for the parameter combination (in nC) as follows: 8^a = [0, 0.8, 1.6, 2.4, 3.2, 4.0, 4.8, 7.5]; 8^b = [0, 0.8, 1.6, 2.4, 3.2, 4.0, 4.8, 6.0]; 7 = [0, 0.8, 1.6, 2.4, 3.2, 4.0, 4.8]; 14 = [0, 0.4, 0.8, 1.2, 1.6, 1.8, 2.4, 2.7, 3.2, 4.0, 4.8, 6.0, 7.5, 10.0]; 6 = [0, 0.4, 0.8, 1.2, 1.8, 2.7, 4.0].

Next we compare detectability of single pulses and repetitive stimulation. Three variables were varied in the stimulus set: stimulus intensity (0–4.0 nC, in steps of 0.8 nC), the number of pulses in the train (2, 5 and 15 pulses) and their frequency (5, 10, 40 and 320 Hz). Together with single pulses and catch stimuli, the repetitive stimuli were presented in a pseudorandom fashion. In comparison to single pulses, repetitive stimuli had two effects. First, they resulted in a leftward shift of the psychometric curve, i.e. to a lowering of the threshold. This effect was visible already when comparing a single pulse with double pulses (Fig. 2A and B), most conspicuously so at small interpulse intervals (Fig. 2B), and was most prominent with 5 and 15 pulses (Fig. 2C and D). The second effect was surprising:

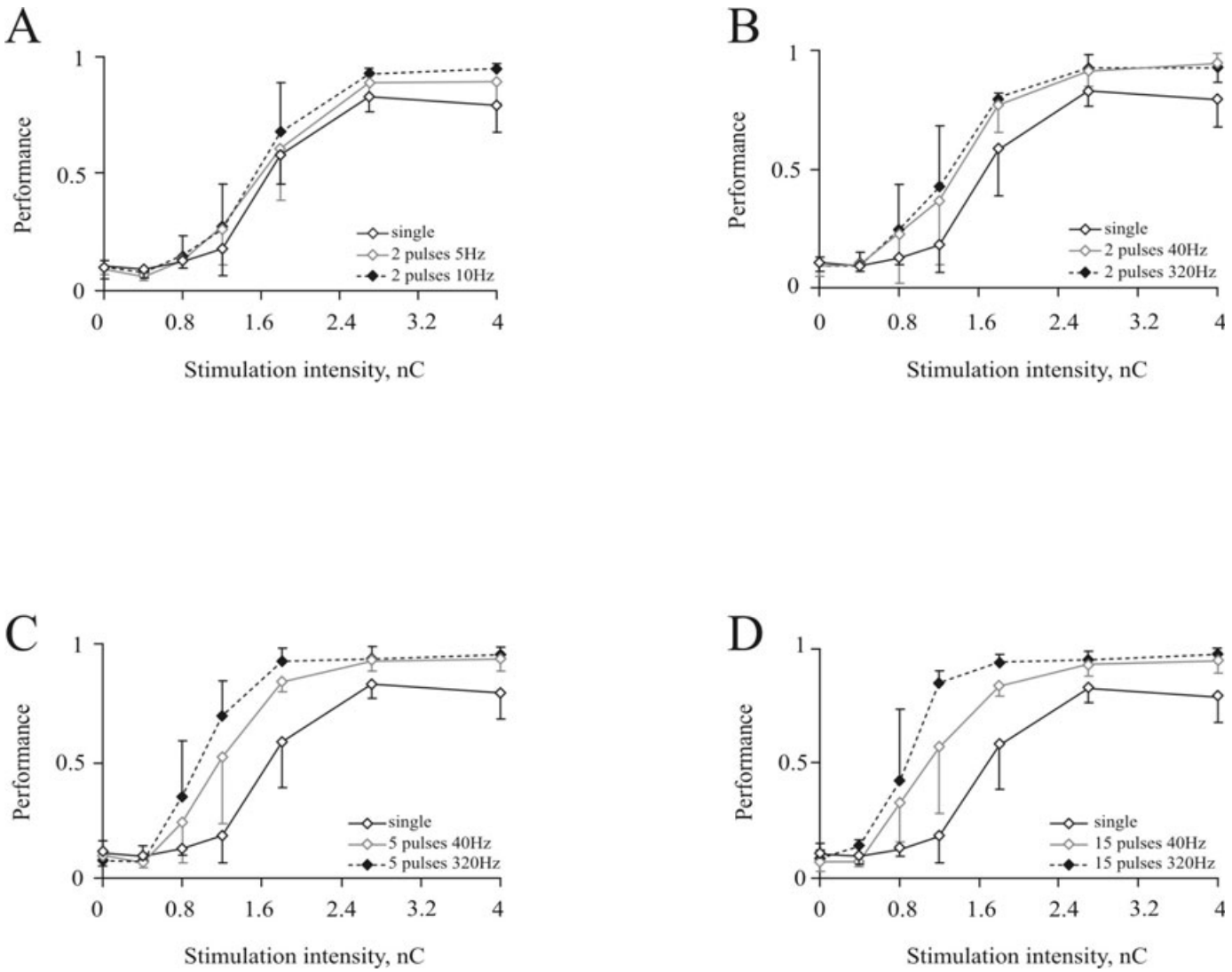

FIG. 2. Psychometric detection curves averaged across animals. (A) Detection of pulse duplets at 5 and 10 Hz. (B) Detection of pulse duplets at 40 and 320 Hz. (C) Detection of trains of 5 pulses at 40 and 320 Hz. (D) Detection of trains of 15 pulses at 40 and 320 Hz. For comparison the single-pulse detection curve is shown as a black line in all subpanels. Error bars depict standard deviation.

as mentioned above, repetitive stimulation allowed the animals to respond to stimuli of strong intensity with probabilities approaching 1, a level that seemed to be unattainable for the animals in response to single pulses. The difference in saturation level was present in the detection curves of single animals (not shown), was readily observed in detection curves from double-pulse stimulations (Fig. 2B), and was fully pronounced using 5 and 15 pulses (Fig. 2C and D), [d_m signifies the maximum detection probability reached, single-pulse $d_m = 0.80 \pm 0.12$; double-pulse (5, 10, 40, 320 Hz) $d_m = 0.91 \pm 0.09$, 0.96 ± 0.02, 0.93 ± 0.04, 0.92 ± 0.06; 5 pulses (40, 320 Hz) $d_m = 0.92 \pm 0.04$, 0.92 ± 0.04; 15 pulses (40, 320 Hz) $d_m = 0.94 \pm 0.04$, 0.93 ± 0.05]. Statistical significance was confirmed by Kruskal–Wallace test, taking frequency ($P = 0.03$, $n = 25$) and number of pulses as the independent variables ($P = 0.02$, $n = 21$).

We quantified the effect on the threshold detectability by fitting logistic curves to the psychometric data. As exemplified in Fig. 3A, we took the abscissa value at the inflection point as the intensity threshold (I_t). Plotting these thresholds against the number of pulses showed a clear trend of lowering the threshold with increasing number of pulses and frequency (Fig. 3B). The threshold of single pulse was 2.07 ± 0.4 nC, and was consistently lowered with increasing number of pulses [2 pulses at 5, 10, 40 and 320 Hz ($I_t = 1.45 \pm 0.26$, 1.56 ± 0.33, 1.33 ± 0.46 and 1.22 ± 0.39 nC), 5 pulses at 40 and 320 Hz ($I_t = 1.25 \pm 0.34$ and 1.02 ± 0.21), and 15 pulses at 40 and 320 Hz ($I_t = 1.21 \pm 0.31$ and 0.92 ± 0.11)]. As above for the saturation level, the difference in thresholds was statistically significant, taking frequency ($P = 0.02$, $n = 25$) and number of pulses as the independent variables ($P = 0.01$, $n = 21$, Kruskal–Wallace test). Figure 3C plots the relationship between threshold and stimulus frequency using exclusively the data obtained with 2 pulses stimulation (because here two additional frequencies 5 and 10 Hz were presented, see Table 1).

In a final analysis we asked how improvement of detection assuming independent effects of individual pulses in a series relates to the one actually measured. The estimation of the combined independent effects corresponds to the combinatorial probability of detecting at least one pulse in a series of pulses

$$p_n = 1 - (1 - p)^n \quad (2)$$

where n is the number of pulses, p the response probability to a single pulse and p_n the probability to detect one pulse in a series of n pulses. Applied to raw data, this estimation procedure greatly amplified chance performance (as given by the response to catch trials). In order to avoid this problem, the estimation was done using 'catch-corrected data' calculated by

$$p_c = (p - p_{catch})/(1 - p_{catch}) \quad (3)$$

where p_c is the catch-corrected performance, p is the measured performance and p_{catch} is the performance at catch trials. This procedure remaps the detection probability from the interval $[p_{catch}, 1]$ onto $[0, 1]$. From the catch-corrected data, we estimated the detection probability of a series of independent multiple pulses according to

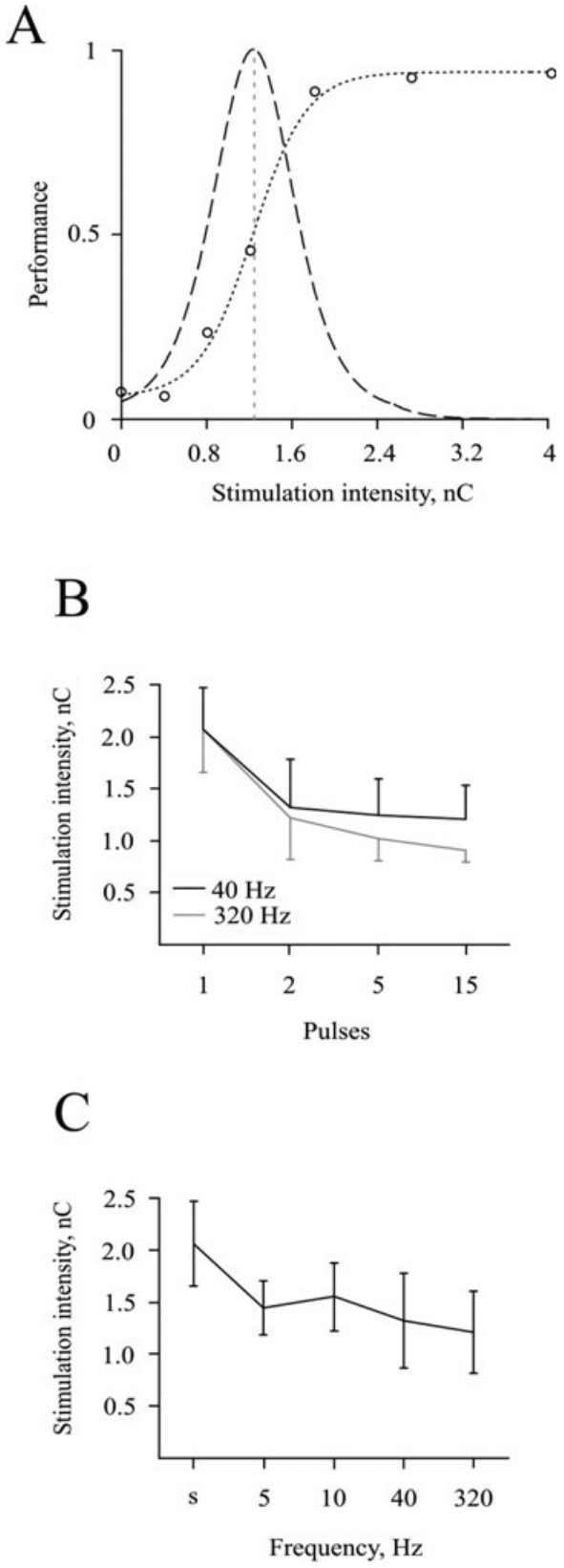

FIG. 3. Detection of electrical stimulus improved with number of pulses and interpulse frequency. (A) Example of detection threshold estimation. Each psychometric S-shaped curve (open circles, data from one animal) was fit by a logistic model (dotted S-shaped curve). The inflection point of the logistic curve was defined as the detection threshold (grey vertical dotted line). The bell-shaped broken line shows the first derivative of the logistic fit. (B) Compared with single pulses, detection thresholds of repetitive stimuli were lower, but levelled off at 2, 5 and 15 pulses. (C) Detection thresholds of pulse duplets are plotted against frequencies. Detection thresholds of single pulses are plotted for comparison (labelled 's' on the abscissa). Error bars depict standard deviation.

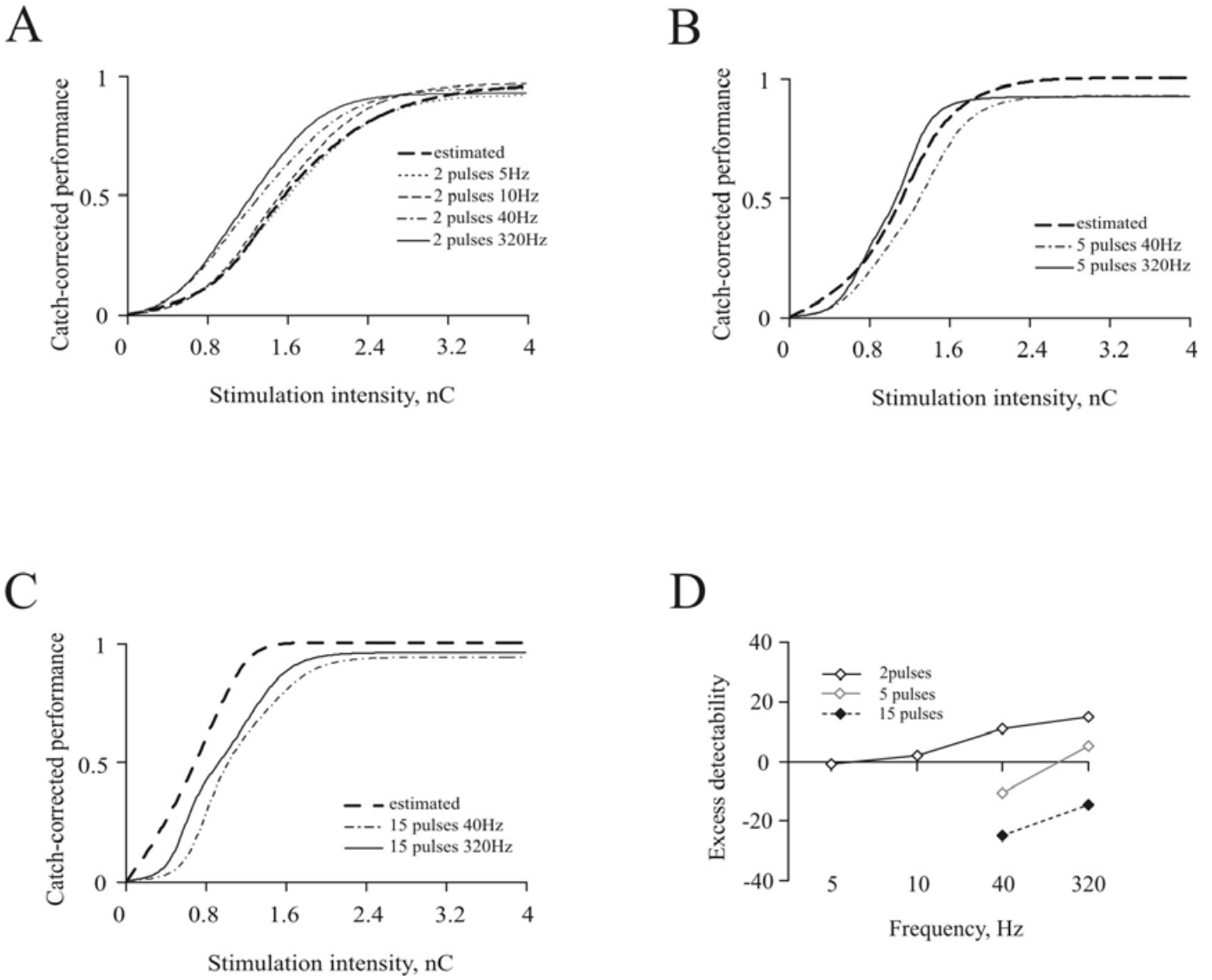

FIG. 4. Estimated detection probability of repetitive stimulation assuming independent effects of individual pulses compared with actually measured curves using repetitive stimuli. Logistic fits averaged across animals are plotted in colour. The thick black broken line depicts the estimate calculated from single-pulse data. Detection probability of (A) pulse duplets, (B) 5 pulses and (C) 15 pulses. (D) The difference of detectability of actual data and estimated data (measured at the steepest point of the estimated curves, tagged 'excess detectability') plotted against the number of pulses. Two pulses show excess detectability for 40 and 320 Hz (but not for 5 and 10 Hz). Five pulses at high frequencies fail to show consistent excess detectability, while detection of 15 pulses falls short of the expected probability, and thus shows negative excess.

Eq. (2) (thick broken black lines in Fig. 4) and compared them with the curves actually observed (thin line types in Fig. 4). As logistic curves showed an excellent goodness of fit to the data (the coefficient of determination r^2 was always higher than 0.96), we plot the fitted curves averaged across animals for clarity. The first impression from this analysis is that the assumption of statistically independent effects of individual pulses did not give rise to a gross deviation from the measured data. Nevertheless, comparing results carefully across the number of pulses (compare subpanels Fig. 4A–C) and across frequencies (compare thin line types within a subpanel), a clear and consistent trend was observed: Compared with the estimated performance the actual performance got worse the more pulses and the higher frequencies were used. This fact is highlighted by Fig. 4D, which plots the difference in response probability of the logistic fits for all repetitive stimuli to the respective estimated curve (measured at the intensity corresponding to the steepest point of the estimation curve). For pulse trains at frequencies of 40 and 320 Hz, performance exceeded the combinatorial probability for 2 pulses stimuli, was about the level of the estimate using 5 pulses stimuli, and clearly stayed below the expected value for 15 pulses stimuli. For double-pulse stimuli at lower frequencies (5 and 10 Hz), the difference between estimated and measured detectability was negligible.

Discussion

The present report shows a peculiar non-continuity of detection performance between detection of single pulses to detection of repetitive-pulse stimulation. Compared with single pulses, double pulses led to a decrease in threshold and a higher performance at suprathreshold intensities. Adding more pulses to the stimulus improved the performance. However, compared with the expected

TABLE 2. Perceptual efficacy

Frequency and number of pulses	Threshold pulse intensity (nC) I_t	Threshold total charge transfer (nC) $I_{tot} = n * I_t$	Change of threshold compared with single pulse (nC) ΔI_t	Change of threshold per additional pulse (nC) $\Delta I_t/(n-1)$	Change of charge transfer compared with single pulse (nC) ΔI_{tot}	Change of charge transfer per additional pulse (nC) $\Delta I_{tot}/(n-1)$	Change of threshold relative to total charge transfer $\Delta I_t/I_{tot}$
320 Hz							
1	2.07	2.07	0.00	–	0.00	–	–
2	1.22	2.44	0.85	0.85	0.37	0.37	2.30
5	1.02	5.10	1.05	0.26	3.03	0.76	0.35
15	0.92	13.80	1.15	0.08	11.73	0.84	0.10
40 Hz							
1	2.07	2.07	0.00	–	0.00	–	–
2	1.33	2.66	0.74	0.74	0.59	0.59	1.25
5	1.34	6.70	0.73	0.18	4.63	1.16	0.16
15	1.21	18.15	0.86	0.06	16.08	1.15	0.05

performance estimated from the combinatorial probability of independent multiple pulses, double-pulse stimulation showed a favourable utilization of individual pulses for detection.

Small intensity threshold for perception – comparison to previous work

Despite some variation, the studies that have explicitly measured psychometric curves based on systematic variation of stimulus intensities so far yield accumulating evidence that very low charge transfers (about 0.4–2 nC) in primary visual and auditory cortices in rats, cats, monkeys and humans can suffice to modulate behaviour (Schmidt *et al*., 1996; Rousche & Normann, 1999; Rousche *et al*., 2003; DeYoe *et al*., 2005). The present study extends these findings to the primary somatosensory cortex in rats. Additional evidence for the notion that stimuli <2 nC are behaviourally relevant comes from studies that did not aim to establish intensity thresholds but nevertheless observed stimulation-dependent modulation of behaviour using intensities lower than 2 nC (Salzman *et al*., 1990; Tehovnik *et al*., 2002). It is difficult to compare absolute psychophysical thresholds between studies because they depend on the characteristics of electrodes, species, cortical area and subpial depth of stimulation site, but also on the specific behavioural task and the motivational state of the animals. For example high impedance–small surface microelectrodes that give rise to high charge densities tend to give rise to thresholds below 1 nC (DeYoe *et al*., 2005), while lower impedance electrodes with large surface area (e.g. the ones of the 'Utah array') tend to generate higher thresholds (Rousche *et al*., 1999, 2003). Layer-specific variation of threshold has been found for psychophysical thresholds in humans and monkeys (Bak *et al*., 1990; DeYoe *et al*., 2005), and for the generation of saccades in the primary visual cortex (Tehovnik *et al*., 2003b). The three studies report that infragranular layers, the site stimulated in the present study, display amongst the lowest thresholds for the modulation of behaviour. The latter researchers also have provided striking evidence for the relevance of the behavioural state of the animal for stimulation results (Tehovnik *et al*., 2003a). Despite these sources of variance that were not the subject of the present study, we believe that the thresholds assessed here come close to the minimal ones – at least for the depth of stimulation used here. Our experiments were performed using highly over-trained, immobilized animals in an environment that was void of visual and auditory distracters (darkness and sound-attenuated chamber). Moreover, only sessions in which the animals were highly motivated were included into the analysis (reflected by the routine observation of close to 100% performance with repetitive suprathreshold stimuli). In summary, the low threshold values obtained in this and the previous studies suggest that the usage of charge transfers near 2 nC per pulse is feasible to generate a percept and, thus, we propose to adopt it as a target figure for future application in cortical prostheses. The low threshold compares favourably with stimulus intensities commonly used in neurobiological experiments that are up to three orders of magnitude higher (reviewed in Tehovnik, 1996).

Consequences for future application in stimulating neuroprostheses

One characteristic problem of stimulating neuroprostheses is the trade-off between potential deleterious effects of chronic stimulation and the quality of the evoked percept. Therefore, two possible strategies to minimize charge transfer must be considered. First, the reduction of intensity per pulse and, second, the reduction of pulse number needed to generate a certain percept. It is difficult at present to judge which strategy is the more important one, because the exact relation of total charge transfer (or total number of pulses) to tissue damage is not known for low stimulus intensities applied over the long time periods as needed for neuroprosthetic applications. Despite this uncertainty, it is reasonable that both optimization strategies should be pursued, and the present data bear relevance for both of them. It is the first study, to our knowledge, that systematically compares psychophysical performance to single vs. repetitive pulses using microstimulation via penetrating electrodes (but, see Bartlett *et al*., 2005 who reported data on single-pulse detection using much higher intensities via subpial macroelectrodes). Table 2 breaks down average pulse intensities and total charge transfer at threshold for trains using different numbers of pulses and frequencies. With respect to intensity reduction, it is an important result that, in order to achieve the same detection performance, pulse intensity can be reduced by about half when using repetitive stimuli at 320 Hz instead of single pulses. However, the reduced pulse intensity by a factor 0.44 comes at the cost of transferring about 6.6 times more total charge per perceptual event (1 pulse at 2.07 nC vs. 15 pulses at 0.92 nC, Table 2, column 2). Compared with this, 2 pulses at 320 Hz already reduced the pulse intensity by a factor of 0.58 (1 pulse at 2.07 nC vs. 2 pulses at 1.22 nC, Table 2, column 2), while only slightly increasing the total charge transfer by a factor of 1.18. Perceptual efficacy can be expressed as the reduction of threshold per additional pulse or as the reduction of threshold per total charge transfer. Both expressions of perceptual efficacy (Table 2, columns 5 and 8) show highest values for

doublets and, thus, indicate that neither single pulses nor stimulation with long pulse trains will provide an optimal solution under these counteracting constraints. Rather, from the present results we predict that it will be useful to attempt the application of high-frequency doublets at near-threshold intensities as an elementary pattern of stimulation in future cortical neuroprosthetic devices.

Relationship of neuronal activity and perception

The following discussion is focused on possible neuronal mechanisms that may participate in determining the found optimum of perceptual efficacy at a low number of pulses. For this purpose, we first need to compare the present findings with the known neuronal correlates of single- and multi-pulse stimulation worked out earlier (Butovas & Schwarz, 2003; Butovas *et al*., 2006). These studies reported that the standard response to a single pulse (first visible at a threshold of 1.6 nC) is a short-latency spike followed by $\sim$100 ms of reduced firing rate partly based on $GABA_B$ receptor activation. Thus, the intensity threshold for short-latency excitation and inhibition is similar to the threshold for single-pulse detection measured here. At a stimulus intensity of 1.6 nC about 80% of neocortical neurons close to the stimulation site (distance 450 μm) increase their firing rate by more than 25% and generate an average of 0.52–0.56 excess spikes, while those at a distance of 1350 μm still respond in about 30% of cases and generate about 0.2 excess spikes (see Table 1 in Butovas & Schwarz, 2003; excess spikes are defined as significant deviation of observed spike numbers in a certain time window under the assumption that spiking is governed by a Poisson process at background firing rate). It should be noted that a third response element, 'rebound activity' following the inhibitory response is not yet present at this pulse intensity. It starts to become relevant only at 2.4 nC (in a subset of 10–20% of the recorded units), an intensity that in the present psychophysical experiments was detected already at near-maximum probability (see Fig. 1C). In summary, the psychophysical performance to single pulses as measured here matches the neurometric threshold for short-latency excitation and ensuing long-lasting inhibition very well. Two possibilities must be therefore considered: either perception of microstimulation close to threshold is based on detecting the short-latency excitatory spikes or the relative lack of activity during the $\sim$100-ms inhibitory period. In our present data the first lick in response to single-pulse stimulation was observed at an average latency of as low as 200 ms, which − taking first a reaction time of $\sim$100 ms and a movement time of $\sim$70 ms to reach the spout with the tongue (assuming rhythmic movement at $\sim$7 Hz) into account, and second discount a certain advantage in latency using microstimulation vs. peripheral stimulation (Otto *et al*., 2005) − renders the monitoring of the long inhibitory response as the basis for behaviour unlikely and clearly favours the alternative possibility that the fast excess spikes are the basis for detection of single-pulse stimulation.

The present psychophysical data show a lowering of the detection threshold and a higher saturation level of response probability when adding a second pulse at different interpulse intervals. Double pulses are known to lead to a complex interaction pattern on the neuronal level (Butovas & Schwarz, 2003). In case the interpulse interval is shorter than $\sim$100 ms, the second pulse hits the neuronal tissue in the middle of the inhibitory response evoked by the first pulse. Somewhat counterintuitively, the second pulse elicits the same number of excess spikes as the first pulse but virtually fails to elicit an inhibitory response of ordinary length by its own. Furthermore, longer pulse trains at frequencies higher than 10 Hz yield a similar number of excess spikes per pulse, but lead to a fusion of the inhibitory periods into a constant inhibitory background (see also Chung & Ferster, 1998). Thus, in contrast to single pulses (and the first pulse in a series), repetitive pulses at frequencies $>$10 Hz are characterized by the interaction of individual neuronal responses that results in excess spikes standing out against a virtual lack of background activity due to strong continuous inhibition. It is conceivable that this qualitative difference may be exploited for the improved detectability of repetitive stimulation. It is not unrealistic to assume that there exist neuronal mechanisms that are specifically tuned to inputs that occur amidst paucity of neuronal background activity. For instance it has been shown that neurons in the rat somatosensory cortex show a propensity for higher responses if synaptic inputs arrive during quiescent, hyperpolarized periods ('down state') as compared with inputs arriving during high ongoing activity (depolarized, 'up state') (Petersen *et al*., 2003; Sachdev *et al*., 2004).

From this we can formulate the hypothesis that the step-like improvement of detection performance between single pulses and pulse trains may be based on the excellent signal-to-noise ratio of spikes evoked by the second pulse due to low background firing during the long-lasting inhibitory responses. This hypothesis predicts that the detectability of repetitive stimulation should exceed the detectability of the same number of pulses with independent effects in case the frequency is high enough to allow for interaction of the neuronal responses. Indeed this is what we found: excess detectability of pulse doublets was close to zero at frequencies of 5 and 10 Hz, which do not allow for neuronal interaction and showed a consistent increment with higher frequencies (40 and 320 Hz, i.e. interpulse intervals 25 and 3.1 ms). With repetitive stimulation using 5 and 15 pulses, excess detectability also consistently rose with higher frequencies; however, the absolute level of excess detectability decreased and even became negative with 15 pulses (Fig. 4D). We speculate that additional adaptive phenomena play a role for the decrement of excess detectability using long pulse series. Clearly, mechanisms that fit the needed characteristics exist in the neocortex. Frequency adaptation is ubiquitous and is believed to be based on short-term depression of thalamocortical synapses (Chung & Ferster, 1998) and intrinsic synapses, amongst them excitatory synapses interconnecting pyramidal neurons (Thomson, 2003). In view of the fact that the short-latency response in the vicinity of the stimulation site did not diminish with repetitive stimulation (Butovas & Schwarz, 2003), these presumed mechanisms most likely come into play along polysynaptic pathways that lead to the activity that directly underlies the subjective experience of the individual. In monkeys such activity is located in cortical areas downstream from the primary somatosensory cortex (de Lafuente & Romo, 2005, 2006). Albeit it must be emphasized that under the present conditions (using maximal 15 pulses) the absolute detectability was still high, we hold it possible that the decrement of excess detectability may be related to the well-known phenomenon of perceptual fading with long repetitive stimulation of the sensory periphery (Ditchburn & Ginsborg, 1952) as well as after neocortical microstimulation (Schmidt *et al*., 1996).

In summary, the present results point to a dependency of perception on the network dynamics in the primary somatosensory cortex. Short repetitive activity embedded in potent inhibition seems to be advantageous to gain access to downstream neuronal structures generating the percept. It is clear that the prototypic highly synchronous activity accompanied by widespread inhibition in space and time evoked by cortical microstimulation (Butovas & Schwarz, 2003) is highly unlikely to occur with natural sensory stimulation. Notwithstanding this qualification, the effects of microstimulation may serve as a model system in which a peculiar balance of excitation and inhibition

can be evoked and its effects on perception be studied. It is now commonly believed that sensory inputs to primary sensory areas evoke a subtly balanced activity in the inhibitory and excitatory system through feedforward mechanisms (Swadlow & Gusev, 2000) and lateral dispersion of inhibition (Moore *et al*., 1999). Thus, the network response to sensory inputs may be, at least partly, carried by the variance of firing (fluctuations) rather than by the modulation of the mean firing rate (Kuhn *et al*., 2004; Silberberg *et al*., 2004). Therefore, the search is on for the particular space–time combination of excitatory and inhibitory activity that would best influence downstream centres of perception. Our present results motivate the search for spatio-temporally local episodes of sensory-evoked cortical activity that are characterized by a large fluctuation in sensory inputs evoking highly reliable cortical activity (cf. Mainen & Sejnowski, 1995; Hunter *et al*., 1998) combined with potent inhibition.

Acknowledgements

This work was supported by the German Federal Ministry of Education and Research (BMBF 311858), and grants from the German Research Council (DFG SFB 550-B11, DFG SCHW 577/7-1). We thank Maik Stüttgen for helpful comments on a preliminary version of the manuscript and Ursula Pascht for excellent technical assistance.

Abbreviation

GABA, γ-aminobutyric acid.

References

Bak, M., Girvin, J.P., Hambrecht, F.T., Kufta, C.V., Loeb, G.E. & Schmidt, E.M. (1990) Visual sensations produced by intracortical microstimulation of the human occipital cortex. *Med. Biol. Engng Comput.*, **28**, 257–259.

Bartlett, J.R., DeYoe, E.A., Doty, R.W., Lee, B.B., Lewine, J.D., Negrao, N. & Overman, W.H. Jr (2005) Psychophysics of electrical stimulation of striate cortex in macaques. *J. Neurophysiol.*, **94**, 3430–3442.

Butovas, S., Hormuzdi, S.G., Monyer, H. & Schwarz, C. (2006) Effects of electrically coupled inhibitory networks on local neuronal responses to intracortical microstimulation. *J. Neurophysiol.*, **96**, 1227–1236.

Butovas, S. & Schwarz, C. (2003) Spatiotemporal effects of microstimulation in rat neocortex: a parametric study using multielectrode recordings. *J. Neurophysiol.*, **90**, 3024–3039.

Chung, S. & Ferster, D. (1998) Strength and orientation tuning of the thalamic input to simple cells revealed by electrically evoked cortical suppression. *Neuron*, **20**, 1177–1189.

DeYoe, E.A., Lewine, J.D. & Doty, R.W. (2005) Laminar variation in threshold for detection of electrical excitation of striate cortex by macaques. *J. Neurophysiol.*, **94**, 3443–3450.

Ditchburn, R.W. & Ginsborg, B.L. (1952) Vision with a stabilized retinal image. *Nature*, **170**, 36–37.

Gao, P., Hattox, A.M., Jones, L.M., Keller, A. & Zeigler, H.P. (2003) Whisker motor cortex ablation and whisker movement patterns. *Somatosens. Mot. Res.*, **20**, 191–198.

Hentschke, H., Haiss, F. & Schwarz, C. (2006) Central signals rapidly switch tactile processing in rat barrel cortex during whisker movements. *Cereb. Cortex*, **16**, 1142–1156.

Hunter, J.D., Milton, J.G., Thomas, P.J. & Cowan, J.D. (1998) Resonance effect for neural spike time reliability. *J. Neurophysiol.*, **80**, 1427–1438.

Kuhn, A., Aertsen, A. & Rotter, S. (2004) Neuronal integration of synaptic input in the fluctuation-driven regime. *J. Neurosci.*, **24**, 2345–2356.

de Lafuente, V. & Romo, R. (2005) Neuronal correlates of subjective sensory experience. *Nat. Neurosci.*, **8**, 1698–1703.

de Lafuente, V. & Romo, R. (2006) Neural correlate of subjective sensory experience gradually builds up across cortical areas. *Proc. Natl Acad. Sci. USA*, **103**, 14266–14271.

Leal-Campanario, R., Delgado-Garcia, J.M. & Gruart, A. (2006) Microstimulation of the somatosensory cortex can substitute for vibrissa stimulation during Pavlovian conditioning. *Proc. Natl Acad. Sci. USA*, **103**, 10052–10057.

Mainen, Z.F. & Sejnowski, T.J. (1995) Reliability of spike timing in neocortical neurons. *Science*, **268**, 1503–1506.

Moore, C.I., Nelson, S.B. & Sur, M. (1999) Dynamics of neuronal processing in rat somatosensory cortex. *Trends Neurosci.*, **22**, 513–520.

Otto, K.J., Rousche, P.J. & Kipke, D.R. (2005) Microstimulation in auditory cortex provides a substrate for detailed behaviors. *Hear. Res.*, **210**, 112–117.

Petersen, C.C., Hahn, T.T., Mehta, M., Grinvald, A. & Sakmann, B. (2003) Interaction of sensory responses with spontaneous depolarization in layer 2/3 barrel cortex. *Proc. Natl Acad. Sci. USA*, **100**, 13638–13643.

Romo, R., Hernandez, A., Zainos, A., Brody, C.D. & Lemus, L. (2000) Sensing without touching: psychophysical performance based on cortical microstimulation [In Process Citation]. *Neuron*, **26**, 273–278.

Romo, R., Hernandez, A., Zainos, A. & Salinas, E. (1998) Somatosensory discrimination based on cortical microstimulation. *Nature*, **392**, 387–390.

Rousche, P.J. & Normann, R.A. (1999) Chronic intracortical microstimulation (ICMS) of cat sensory cortex using the Utah Intracortical Electrode Array. *IEEE Trans. Rehabil. Engng*, **7**, 56–68.

Rousche, P.J., Otto, K.J., Reilly, M.P. & Kipke, D.R. (2003) Single electrode micro-stimulation of rat auditory cortex: an evaluation of behavioral performance. *Hear. Res.*, **179**, 62–71.

Rousche, P.J., Petersen, R.S., Battiston, S., Giannotta, S. & Diamond, M.E. (1999) Examination of the spatial and temporal distribution of sensory cortical activity using a 100-electrode array. *J. Neurosci. Meth.*, **90**, 57–66.

Sachdev, R.N., Ebner, F.F. & Wilson, C.J. (2004) Effect of subthreshold up and down states on the whisker-evoked response in somatosensory cortex. *J. Neurophysiol.*, **92**, 3511–3521.

Salzman, C.D., Britten, K.H. & Newsome, W.T. (1990) Cortical microstimulation influences perceptual judgements of motion direction. *Nature*, **346**, 174–177.

Schmidt, E.M., Bak, M.J., Hambrecht, F.T., Kufta, C.V., O'Rourke, D.K. & Vallabhanath, P. (1996) Feasibility of a visual prosthesis for the blind based on intracortical microstimulation of the visual cortex. *Brain*, **119**, 507–522.

Silberberg, G., Bethge, M., Markram, H., Pawelzik, K. & Tsodyks, M. (2004) Dynamics of population rate codes in ensembles of neocortical neurons. *J. Neurophysiol.*, **91**, 704–709.

Stüttgen, M.C., Rüter, J. & Schwarz, C. (2006) Two psychophysical channels of Whisker deflection in rats align with two neuronal classes of primary afferents. *J. Neurosci.*, **26**, 7933–7941.

Swadlow, H.A. & Gusev, A.G. (2000) The influence of single VB thalamocortical impulses on barrel columns of rabbit somatosensory cortex. *J. Neurophysiol.*, **83**, 2802–2813.

Tehovnik, E.J. (1996) Electrical stimulation of neural tissue to evoke behavioral responses. *J. Neurosci. Meth.*, **65**, 1–17.

Tehovnik, E.J., Slocum, W.M. & Carvey, C.E. (2003a) Behavioural state affects saccadic eye movements evoked by microstimulation of striate cortex. *Eur. J. Neurosci.*, **18**, 969–979.

Tehovnik, E.J., Slocum, W.M. & Schiller, P.H. (2002) Differential effects of laminar stimulation of V1 cortex on target selection by macaque monkeys. *Eur. J. Neurosci.*, **16**, 751–760.

Tehovnik, E.J., Slocum, W.M. & Schiller, P.H. (2003b) Saccadic eye movements evoked by microstimulation of striate cortex. *Eur. J. Neurosci.*, **17**, 870–878.

Thomson, A.M. (2003) Presynaptic frequency- and pattern-dependent filtering. *J. Comput. Neurosci.*, **15**, 159–202.